

**TECHNICAL SERVICES FOR MINE  
COMMUNICATIONS RESEARCH**

**TRANSMIT ANTENNAS FOR PORTABLE  
VLF TO MF WIRELESS MINE COMMUNICATIONS**

Robert L. Lagace -- Task Leader  
David A. Curtis, John D. Foulkes, John L. Rothery

UNITED STATES  
DEPARTMENT OF THE INTERIOR  
BUREAU OF MINES

USBM CONTRACT FINAL REPORT (HO346045)  
Task C, Task Order No. 1  
May 1977

ARTHUR D. LITTLE, INC.  
Cambridge, Massachusetts



Arthur D. Little, Inc.

1. Report No.	2.	3. Recipient's Accession No.	
4. Title and Subtitle Technical Services for Mine Communications Research TASK C(T.O.1) TRANSMIT ANTENNAS FOR PORTABLE VLF TO MF WIRELESS MINE COMMUNICATIONS		5. Report Date May 1977	6.
7. Author(s) Robert L. Lagace, David A. Curtis, John D. Foulkes, John L. Rothery		8. Performing Organization Report No. ADL-77229-Task C	
9. Performing Organization Name and Address Arthur D. Little, Inc. Acorn Park Cambridge, Massachusetts 02140		10. Project/Task/Work Unit No.	11. Contract or Grant No. HO346045-Task Order No. 1
12. Sponsoring Organization Name and Address Office of the Assistant Director-Mining Bureau of Mines Department of the Interior Washington, D. C. 20241		13. Type of Report Final (Task C) May 1974 - May 1977	
15. Supplementary Notes		14.	
16. Abstract An investigation is made of the feasibility of developing compact transmit antennas and/or other means to efficiently couple VLF to MF band radio energy between portable wireless communication units in coal mines. The completely wireless communication ranges between two portable radios equipped with practically-sized reference loop antennas in representative coal mine environments are estimated. Antenna technology is assessed with respect to transmit moment, range, intrinsic safety, battery and wearability requirements to determine the most suitable antenna types for use by miners. It is concluded that air-core bandolier loop antennas, and perhaps ferrite-loaded loop antennas, having peak transmit moments of about 2.5 ampere-m <sup>2</sup> will be the most effective antenna choices for portable units. This choice, however, will not allow the range goal of 1350 feet to be attained in mines having unfavorable signal attenuation and noise environments. Rectangular air-core loops are compared with grounded horizontal-wire and vertical-wire mode exciters for fixed station applications. The potential for significantly increasing the wireless communication range by inductively coupling to communications and power lines in a mine is evaluated and found to be considerable based on theoretical coupling equations. Lastly, the theoretical performance of a hybrid noise cancelling diversity receiving technique that utilizes both the electric and magnetic field components of the ambient noise to improve the receiver output signal-to-noise ratio under certain adverse conditions is estimated and shown to be favorable when the magnetic and electric field noise components are highly correlated.			
17. Originator's Key Words Mines - Radio Communication Antennas - VLF to MF Radio Propagation - Conducting Media Noise-Diversity Cancelling Coal Mine Communications		18. Availability Statement	
19. U.S. Security Classif. of the Report	20. U.S. Security Classif. of This Page	21. No. of Pages 157	22. Price

USBM H0346045

TECHNICAL SERVICES FOR MINE  
COMMUNICATIONS RESEARCH

TRANSMIT ANTENNAS  
FOR PORTABLE VLF TO MF WIRELESS MINE COMMUNICATIONS

Robert L. Lagace -- Task Leader  
David A. Curtis, John D. Foulkes, John L. Rothery

ARTHUR D. LITTLE, INC.  
Cambridge, Massachusetts 02140  
C-77229

The views and conclusions contained in this document are those of the authors and should not be interpreted as necessarily representing the official policies or recommendations of the Interior Department's Bureau of Mines or of the U. S. Government.

USBM CONTRACT FINAL REPORT (H0346045)  
Task C, Task Order No. 1

MAY 1977

UNITED STATES  
DEPARTMENT OF THE INTERIOR  
BUREAU OF MINES

## FOREWORD

This report was prepared by Arthur D. Little, Inc., Cambridge, Massachusetts under USBM Contract No. H0346045. The contract was initiated under the Coal Mine Health and Safety Program. It was administered under the technical direction of the Pittsburgh Mining and Safety Research Center with Mr. Howard E. Parkinson acting as the technical project officer. Mr. Michael W. College was the contract administrator for the Bureau of Mines.

This report is a summary of the work recently completed as part of this contract during the period May 1974 to May 1977. This report was submitted by the authors in May 1977.

No inventions or patents were developed and no applications for inventions or patents are pending.

## TABLE OF CONTENTS

	Page
List of Tables	viii
List of Figures	ix
I. EXECUTIVE SUMMARY	1
A. OBJECTIVE	1
B. APPROACH	1
C. FINDINGS AND CONCLUSIONS	2
1. Wireless Range Estimates	2
2. Antenna Technology	3
3. Coupling to Mine Conductors	4
4. Noise Cancelling Diversity Reception	4
II. MINE WIRELESS RADIO RANGE ESTIMATES	7
A. SUMMARY	7
B. INTRODUCTION	7
C. THE HOMOGENEOUS MEDIUM MODEL	8
1. Signal Field Strengths	8
2. Range Estimates	12
a. Single Sideband Voice	12
b. Narrowband Paging	16
D. THE THREE-LAYER MODEL	18
1. Signal Field Strengths	19
2. Range Estimates for FM Voice	22
3. Discussion of Implications	27
III. ANTENNA TECHNOLOGY	29
A. SUMMARY	29

TABLE OF CONTENTS (Continued)

	Page
B. ELECTRICALLY SMALL ANTENNAS	31
1. Electrical Smallness	31
2. Radiation Resistance	32
3. Efficiency	33
4. Quality Factor-Q	34
5. Power Factor	34
6. Effective Volume	36
7. Application Implications	41
8. Impact of Conducting Media	45
C. PORTABLE MANPACK ANTENNAS	49
1. Conventional Whip Antennas	49
2. Active Whip Antennas	51
3. Conventional Loop Antennas	54
4. Ferrite-Loaded Loops	63
5. Special Multi-Turn Loop (MTL) Antennas	68
D. FIXED STATION ANTENNAS	72
1. Vertical Plane Loops	72
2. Alternative Mode Exciters	75
a. Horizontal Grounded Long Wires	75
b. Vertical Grounded Wires	81
3. Other Loop Antennas	85
E. REFERENCES	87
IV. COUPLING TO EXISTING CONDUCTORS IN MINES	95
A. SUMMARY	95
B. INTRODUCTION	95
C. REPRESENTATIVE GEOMETRIES	96

TABLE OF CONTENTS (Continued)

	Page
D. COUPLING TO SIMPLE TWO-WIRE LINES	101
1. Case 1a - Coplanar Geometry	101
a. Electric Field Method	101
b. Magnetic Field Method	106
2. Case 1b - Aligned Geometry, Magnetic Field Method	109
3. Unfavorable Geometries	111
E. COUPLING TO TWISTED PAIR CABLE	113
F. LOOP-TO-LOOP COUPLING VIA THE LINE	113
G. SIGNAL-TO-NOISE RATIO ESTIMATES	115
V. HYBRID NOISE CANCELLING DIVERSITY RECEIVING TECHNIQUE	123
A. SUMMARY	123
B. INTRODUCTION	123
C. SIGNAL-TO-NOISE RATIO IMPROVEMENT ANALYSIS	128
1. Nomenclature	128
2. Signal-to-Noise Ratio	128
3. Circle Diagram Interpretations	132
4. Expected Values	137
5. Boundary Plots and Performance	141
D. RECOMMENDED FIELD MEASUREMENTS	143

LIST OF TABLES

Table No.		Page
2-1	Range Estimates for Wireless Communication with Personal Portable FM Radios in a High-Coal Seam	26
4-1	Typical Dimensions for Structures of Interest in a Mine	96
4-2	Regions of Validity for Using $\beta R \ll 1$ Criterion, the Inductive-Field Approximation (In Air)	101
4-3	Values of $E_\phi$ in the Plane of a Loop at a Distance R Away in Air	107
4-4	Currents in $\mu$ amperes Induced in Conductors for the Situation of Figure 4-1a (In Air)	108
4-5	Voltages Induced in Cable Conductors in the Situation of Figure 4-1b (In Air)	112



## LIST OF FIGURES

Figure No.		Page
2-1	Magnetic Field Strength $/H_z/$ from a Loop Antenna in an Air Medium	10
2-2	Magnetic Field Strength $/H_z/$ from a Loop Antenna in a Conducting Medium and $z^2$ RMS Magnetic Field Noise in Mines (Normalized to 2.5kHz Bandwidth)	11
2-3	Comparison of Loop Signal in Conducting Medium (from Figure 2-2) and Mine Noise Near Operating Machinery (Normalized to 2.5kHz Bandwidth)	13
2-4	Comparison of Loop Signal in Conducting Medium (from Figure 2-2) and Mine Noise in Haulageway (Normalized to 2.5kHz Bandwidth)	14
2-5	Magnetic Field Strength $/H_z/$ from a Loop Antenna in a Conducting Medium and $z^2$ RMS Magnetic Field Noise in Mines (Normalized to a 10Hz Bandwidth)	15
2-6	Three Layer Model Geometry for Low and Medium Frequency Radio Wave Propagation	20
2-7	Theoretical Magnetic Field Strength Plots Versus Distance and Frequency for Three Layer Model for Two Values of Coal Conductivity $\sigma_c = 1.4 \times 10^{-4}$ Mho/m and $\sigma_c = 10^{-2}$ Mho/m	20
2-8	Representative RMS Magnetic Field Noise Levels Measured in the McElroy Coal Mine	23
2-9	Representative RMS Magnetic Field Noise Levels Measured in the Robena and Itmann Coal Mines	24
3-1	Behavior of Antenna Intrinsic Q (Based on Chu <sup>(1)</sup> )	35
3-2	Effective Volumes and Radiation Power Factors for Electrically Small Antennas	37
3-3	Illustration of Radiation Power Factor Limitations Imposed by Antenna Effective Volume Relative to Volume of a Radian Sphere	39
3-4	Comparative Examples of the Effective Volumes of Several Common Antenna Types	40

LIST OF FIGURES (Continued)

Figure No.		Page
3-5	Example of an LF Band T-Antenna	43
3-6	Example of State-of-the Art Large VLF Antenna in Northwest Cape Australia	44
3-7	Active Transmit Antenna FEBL Configuration	53
3-8	FEBL Configuration for Maximizing Antenna Current Moment	53
3-9	Equivalent Circuits	53
3-10	Sketches of Several Bandolier Loop Antenna Configurations	56
3-11	Minimum Igniting Current as a Function of an Inductive Circuit for an 8.3% Methane/Air Mixture	59
3-12	Minimum Ignition Voltage as a Function of Capacitance for Ignition of an 8.3% Methane/ Air Mixture	61
3-13	Typical Configuration for Loops Loaded with Ferromagnetic Cores	64
3-14	Sketch of Flux Concentration Caused by High Permeability Rod	64
3-15	Apparent Permeability, $\mu_{rod}$ , as a Function of Rod $\ell/d$ and Rod Intrinsic Permeability, $\mu$	64
3-16	MTL Antenna Diagram and Impedance Characteristics	70
3-17	Wall-Mounted Fixed Station Loop in Coal Mine Tunnel	73
3-18	Fixed-Station Turnstyle Loop Antenna Configu- ration	73
3-19	Turnstyle Antenna Installation Possibilities in a Coal Mine Environment	73
3-20	Propagation at ELF in the Earth-Ionosphere Waveguide	77

LIST OF FIGURES (Continued)

Figure No.		Page
3-21	Sketch of a Grounded Long Wire Antenna Installed in a Coal Mine Tunnel	77
3-22	Long Wire Turnstyle Configuration in an Entry/ Crosscut Intersection	79
3-23	Long Wire Array Configurations in a Mine Entry and a Crosscut	79
3-24	Sketch of a Grounded Vertical Wire Antenna Installed in a Coal Mine Tunnel	82
3-25	Conceptual Sketches of Vertical Wire Mode Exciter Configurations	82
4-1	Different Geometries for a Horizontal Loop Antenna and a Twin-Lead Cable	97
4-2	Different Geometries for a Horizontal Loop Antenna and a Twisted-Pair Cable	99
4-3	Ranges of Validity of Coplanarity Assumptions	100
4-4	Geometry of the Transmitting Loop and Trans- mission Line for the Case of Figure 4-1(a)	103
4-5	Equivalent Transmission Line Circuit for Induced Voltage and Current (Case of $Z_1 = Z_2 =$ $Z_0$ )	111
4-6	Comparison of Loop-to-Loop-via-the-Line Signal Levels in Air with Equivalent Receiver Noise and Representative RMS Magnetic Field Noise Levels Measured in the McElroy Coal Mine	116
4-7	Comparison of Loop-to-Loop-via-the-Line Signal Levels in Air with Equivalent Receiver Noise and Representative RMS Magnetic Field Noise Levels Measured in the Robena and Itmann Coal Mines	117
5-1	Hybrid Noise Cancelling Diversity Receiving Technique (Simplified Basic Operation)	127
5-2	Correlated Noise Vector Diagram	130
5-3	Signal Factor Circle Diagram	133

LIST OF FIGURES (Continued)

Figure No.		Page
5-4	Signal Factor of I versus Phase Angle $\theta$ in the Presence of an E-Field Signal $S_E$	134
5-5	Circle Diagram for Signal and Noise Factors of I	136
5-6	Circle Diagram Indicating Region where $I \leq 1$	136
5-7	Expected Value of the Improvement Factor $\langle I \rangle$ in dB versus $1/\alpha$ and $(R_{EC}/R_{HC})$ for Two Values of $\beta/\alpha$ (0.1, 1.0) and $\langle \theta \rangle = \pi/2$	139
5-8	Correction Term Q to $\langle I \rangle$ versus Phase Angle $\theta$ and Ratio $R_{EC}/R_{HC}$	140
5-9	Boundary Plot of $R_{EC}/R_{HC}$ versus $1/\alpha$ for Specified Improvement Factors $\langle I \rangle$ with $\beta/\alpha = 1$	142

## I. EXECUTIVE SUMMARY

### A. OBJECTIVE

The objective of this task was to study and evaluate the feasibility of developing compact transmit antennas and/or other means for efficiently coupling VLF to MF radio energy between portable wireless communication units in coal mines. The Bureau of Mines would like to achieve a portable-to-portable range of about 1350 ft., especially in conductor-free areas of typical U. S. room and pillar coal mines, namely areas where electrical conductors such as power cables, trolley lines, and communication lines are absent. In the presence of these conductors, achieving the desired communication range is usually not a problem. The 1350 ft. conductor-free range corresponds to that required for two miners to communicate between the leftmost and rightmost entries (spaced about 600 ft. apart) of a seven-entry mine development while also being separated by a longitudinal distance of about 1000 ft. along the entries. This requires an area-coverage capability that is not adversely affected by the presence of the largely rectilinear grid of tunnels in the coal seam. Thus, the frequency band from 30 kHz to 1 MHz was selected as the band of primary interest for this investigation.

### B. APPROACH

First, the ranges for completely wireless communication between two portable radios using practically-sized loop antennas in representative coal mine environments were estimated. Antenna technology in the VLF to MF band was then assessed in light of the range, intrinsic safety, and wearability requirements, to determine the most suitable antenna types for the application, and whether any of them could significantly improve upon the overall performance predicted for the reference loop antenna used in making the range estimates. Effort was also directed in two related areas. The first was a study to determine whether inductive coupling to cables and other conducting structures in the mine could substantially increase the communications range, since such cables, etc., are usually present where men are working underground.

The second was a study to assess the potential benefits of using a diversity reception noise cancelling technique, that utilizes both the electric and magnetic field components of the ambient noise, to substantially improve the output signal-to-noise ratio of the receiver when a portable unit must be operated in the vicinity of a strong source of electrical noise.

## C. FINDINGS AND CONCLUSIONS

### 1. Wireless Range Estimates

Estimates were made of the wireless communication range attainable in an underground coal mine in the presence of mine generated electromagnetic noise, for man-carried radios of practical size and source strength operating in the frequency band from 10 kHz to 1 MHz. A conventional air-core bandolier-type loop antenna of strength  $M = 0.5$  to  $0.7 \text{ ampere-m}^2$  was used as a reference source to gage the amount of improvement in antenna performance required, if any deficiency in range, and therefore signal strength, must be overcome solely through improved antenna design.

It is shown that for mines having an effective conductivity of  $10^{-2} \text{ Mho/m}$  (near the upper limit for coal), the deficiency in signal-to-noise ratio, and thus range, is insuperable with man-carried equipment at any frequency in the band of interest. In mines for which a three-layer propagation model is applicable and the effective conductivity of the coal is about  $10^{-4} \text{ Mho/m}$  (near the lower limit for coal), the deficiencies become much more manageable, particularly at frequencies between about 300 kHz and 1 MHz. Here, moderate improvements in antenna/transmitter design and/or reception techniques may be able to provide modest increases in communication range, and reductions in battery size and therefore weight of the portable units. However, the most likely value or range of values for the in-situ conductivity of U. S. bituminous coal must still be determined before a general conclusion can be drawn on the percentage of mines in which the desired range goal in completely conductor-free areas is likely to be achievable.

## 2. Antenna Technology

Transmit antenna technology available in the VLF through MF bands was examined for its utility in portable mine wireless radio applications. In particular, an assessment was made of the feasibility of developing compact, portable transmit antennas that will efficiently generate radio waves in coal mines. The size of such antennas relative to wavelength classifies them as electrically small antennas which, by their very nature, are poor radiators. No major breakthroughs have occurred, or are likely to occur, to change this fact. Thus, the VLF-MF mine wireless communication problem is one of optimizing the near field and induction field coupling between two loosely coupled portable electromagnetic field transducers (antennas) in the physical and noise environment of a mine. The problem is made more difficult by the mine's lossy conducting medium which introduces considerable signal attenuation.

As a result, the choice of a specific antenna should not be based on its radiation efficiency. Instead it should be based on the overall power efficiency and practicality achievable by the complete transmitter-antenna system in producing the largest usable signal at the desired range within the practical constraints of system overall size, weight, convenience of use, intrinsic safety, and ruggedness for roving miners. **Thus, it is concluded that conventional air-core bandolier loop antennas, and perhaps small ferrite-loaded loop antennas, will be the most suitable and reasonable choices for roving miner portable radio applications at frequencies below about 1 MHz.** Furthermore, a transmit moment of about  $2.5 \text{ amp-m}^2$  (peak) appears to be a practical upper bound for intrinsically safe portable units for use by miners. Therefore, the completely wireless range goal of 1350 feet will probably be achievable only in the most favorable coal mine propagation and noise environments, and range capabilities will not be significantly better than those predicted for units having a transmit moment of  $0.7 \text{ amp-m}^2$ . For fixed station applications, horizontal-wire and vertical-rod mode excitors may also offer comparable or better performance than planar air-core loops, but in-mine measurements will be needed to resolve this matter.

### 3. Coupling to Mine Conductors

To evaluate the potential advantages and practicality of extending mine wireless ranges by coupling to existing conducting structures in mines, theoretical coupling equations were developed. The equations relate loop antenna strength, frequency, and its distance from two-wire cables and structures, to the current and voltage induced in that structure by the loop antenna. These equations allow one to compute not only the loop-to-structure coupling but also loop-to-loop coupling via the two-wire structure. Results computed for three frequencies (3, 100, and 1000 kHz) indicate that:

- performance improves with closeness to the two-wire structure, increased separation of the wires, and increasing frequency up to about 0.5 - 1 MHz in a mine tunnel;
- loop-to-loop communications along a haulageway appear practical in the presence of a trolley wire system and may also be usable in the presence of untwisted cables and single wires attached to the ribs;
- ranges of several kilometers are predicted for the 200 kHz - 1 MHz band when the loops are within about 2 meters of unloaded trolley wire/rails;
- coupling to twisted pair cables is severely reduced over that for untwisted pairs;
- performance should be significantly reduced for loops located in tunnels adjacent to the one in which the conductors are located.

### 4. Noise Cancelling Diversity Reception

A hybrid noise cancelling diversity receiving technique was examined that would try to capitalize on the high levels of both electric and magnetic field noise components present in many parts of a mine at the frequencies of interest below 1 MHz. It is shown that if the instantaneous correlation is high enough between the noise E and H field components, it should be possible to improve the output signal-to-noise performance of a mine wireless system by cancelling a major portion of the H-field noise picked up in a loop antenna by properly



combining it (manually or automatically) with the E-field noise picked up by a small dipole or whip antenna that would be insensitive to H-field signals and the ambient H-field noise. This selectivity between signal and noise is likely for portable units using loop antennas that generate primarily H fields which couple to the receiver of other portables primarily through magnetic induction.

Calculations to date indicate that potential signal-to-noise improvements between 10-15 dB may be possible when the E and H noise components are 80% to 90% correlated, a condition which may prevail in the vicinity of severe noise sources. Such a S/N increase could then result in extending the range of a wireless communications system, or reducing the power required to attain a given range in the presence of high ambient electrical noise near one of the receiving units. Some basic field measurements are required to determine whether the degree of correlation between the E and H noise field components is high enough to warrant a more rigorous analysis and further development effort.

(This page intentionally left blank)

## II. MINE WIRELESS RADIO RANGE ESTIMATES

### A. SUMMARY

The feasibility of achieving a wireless communication range of 1,350 ft (412 m) in an underground coal mine, in the presence of mine generated electromagnetic noise, with man-carried radios of practical size and source strength in the frequency band from 10 kHz to 1 MHz is assessed. A conventional air-core bandolier-type loop antenna of strength  $M = 0.5$  to  $0.7$  ampere-m<sup>2</sup> is used as a reference source, to gage the amount of improvement required if any deficiency in range, and therefore signal strength, must be overcome solely through improved antenna design. It is shown that for mines having an effective conductivity of  $10^{-2}$  Mho/m (**near the upper limit for coal**), the deficiency in signal-to-noise ratio, and thus range, is insuperable (by a vast margin) with man-carried equipment at any frequency in the band of interest. In mines for which a three-layer propagation model is applicable and the effective conductivity of **the coal is about  $10^{-4}$  Mho/m (near the lower limit for coal)**, the deficiencies become much more manageable, particularly at frequencies between about 300 kHz and 1 MHz. Here, moderate improvements in antenna/transmitter design and/or reception techniques may be able to provide practical solutions. However, the most likely value or range of values for the in-situ conductivity of U.S. bituminous coal must still be determined before a generally applicable system can be developed for achieving the desired range goal in completely conductor-free areas of mines.

### B. INTRODUCTION

The objective of this chapter is to establish some reference levels of performance that can be expected in a mine environment. A well-defined, practical sized antenna that can be conveniently worn on the body of a mobile miner, namely an air-core, multi-turn bandolier-type loop having a transmit magnetic moment in the range of 0.5 to 2 ampere-meter<sup>2</sup>, is used as a reference signal source. The theoretical field strength generated by this source over the 1,350 ft range of interest is calculated for two electromagnetic wave propagation models for the underground coal mine. These signal levels are then compared with

expected electromagnetic noise levels under mine operating conditions to estimate corresponding ranges of communication. From these calculations, deficiencies in transmitter strength become apparent, together with the amount of improvement required at each frequency to achieve the 1,350 ft range goal. The potential for overcoming these deficiencies through new developments in antenna technology in this frequency band is discussed in Chapter III.

In the following sections of this chapter, performance estimates are made for two propagation models for the mine environment; an infinite homogeneous medium model, and a three-layer model consisting of a horizontal layer of coal surrounded by rock which extends to infinity above and below the coal.

### C. THE HOMOGENEOUS MEDIUM MODEL

This section treats the case where the coal seam and the surrounding rock are considered to act as one continuous, homogeneous, conducting medium of infinite extent and conductivity  $\sigma$ , in which an infinitesimal loop antenna of ~~magnetic~~ dipole moment  $M$  is immersed. It is a model in which the presence of air spaces represented by the rectilinear grid of tunnels in the coal seam and the air-earth interface above the mine is ignored, reasonable simplifying assumptions for the frequencies, mine tunnel cross-sections, and mine depths of interest. In each instance we compute the value of the magnitude of the component of magnetic field perpendicular to the plane of the loop, for observation points which lie on a radial line in the plane of the loop. We designate this component as  $|H_z|$  in the following equations. For convenient reference and comparison with this conducting medium case, we have also computed values for the same magnetic field component produced by the same loop when placed in an air medium.

#### 1. Signal Field Strengths

If  $r$  is the distance of the observation point from the loop,  $f$  is the frequency of operation, and  $M$  is the magnetic dipole moment, then the magnitude of the field component  $|H_z|$  as a function of distance and frequency is given for both the air and conducting medium cases by the conventional field equations below (with terms grouped as shown for convenience).

### Air Medium

$$|H_z| = \frac{M}{4\pi r^3} (1 + X^4 - X^2)^{1/2} \quad (1)$$

where  $X = \frac{\omega r}{c}$  (2)

and  $c = (\epsilon_0 \mu_0)^{-1/2}$  is the velocity of light in free space (3)

### Conducting Medium

$$|H_z| = \frac{M}{4\pi r^3} e^{-G/\sqrt{2}} (G^4 + \sqrt{2}G^3 + G^2 + \sqrt{2}G + 1)^{1/2} \quad (4)$$

where  $G = r(\omega \mu_0 \sigma)^{1/2} = \sqrt{2} r/\delta$  (5)

and  $\sigma$  is the electrical conductivity of the medium

$\delta$  is the skin depth

The conducting medium equations are those that apply when displacement currents are negligible, a reasonable approximation in a coal/rock medium of assumed conductivity  $\sigma = 10^{-2}$  Mho/m at operating frequencies below a few MHz.

Graphs of the field strength magnitudes are plotted versus frequency, with range from the loop as a parameter, in Figures 2-1 and 2-2 for air and conducting media respectively. A nominal value of  $\sigma = 10^{-2}$  Mho/m was used for the conducting medium (near the upper limit for coal). In both cases a source magnetic dipole moment  $M=NIA$  of value 0.5 ampere-meter<sup>2</sup> was used, a conservative practical value for a man-carried radio. The plotted field strengths may be interpreted as peak or rms amplitudes accordingly as  $M$  is either the peak or rms dipole moment. Note that for the air medium, Figure 2-1 shows that at given distance the magnetic field  $|H_z|$  eventually increases with increasing frequency. This occurs as the radiation field term exceeds the induction field terms, thereby leading to higher field strengths at higher frequencies. Figure 2-2 shows that the converse is true in a conducting medium. Namely for the  $\sigma = 10^{-2}$  Mho/m case, as the frequency is increased, the increasing radiation field term is more than overpowered by an exponential attenuation factor caused by the resistive losses in the medium. Thus, the maximum achievable ranges are severely reduced in the conducting medium over that possible in air, and it is seen that in this conducting medium higher field strengths are obtained by reducing the operating frequency instead of raising it.

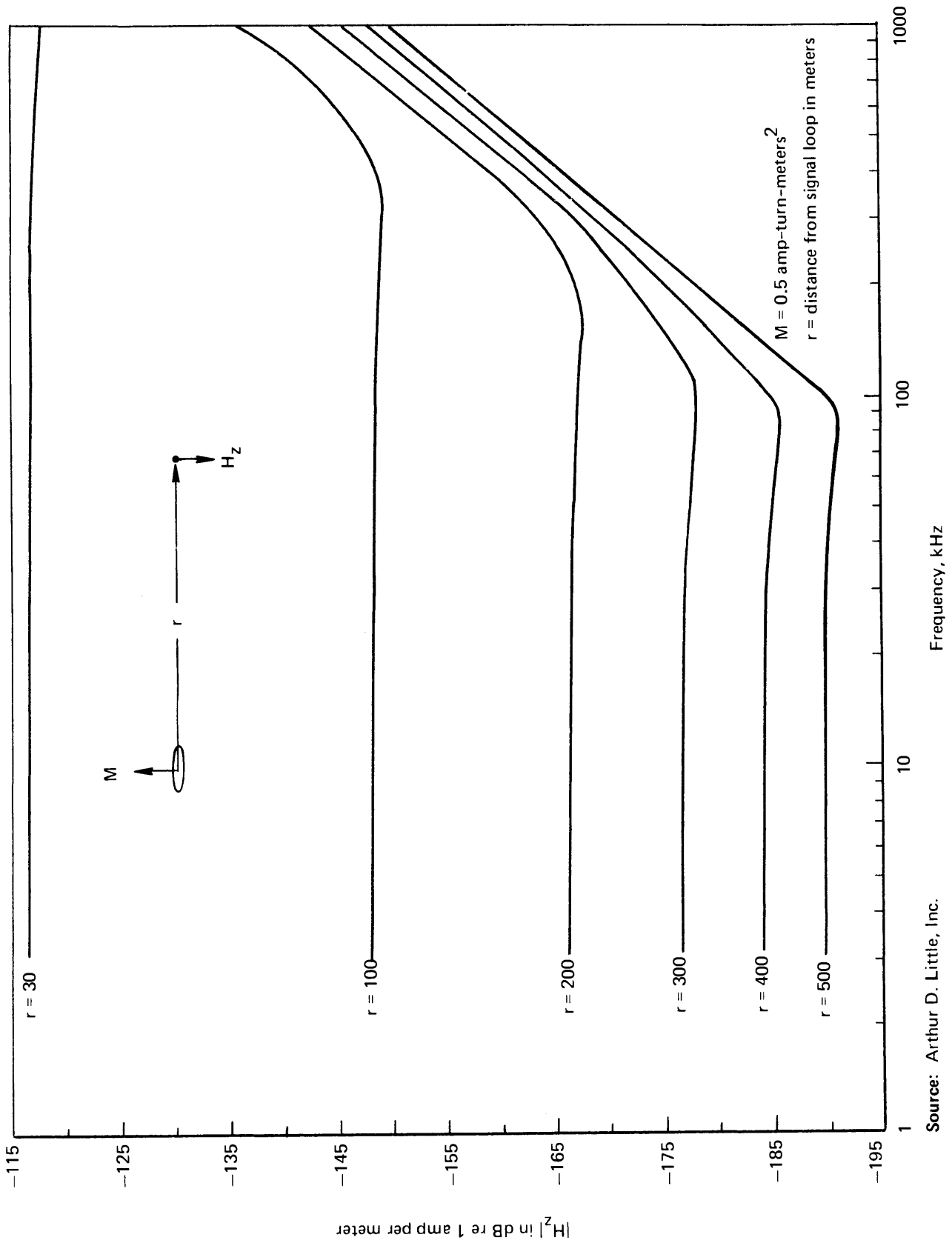
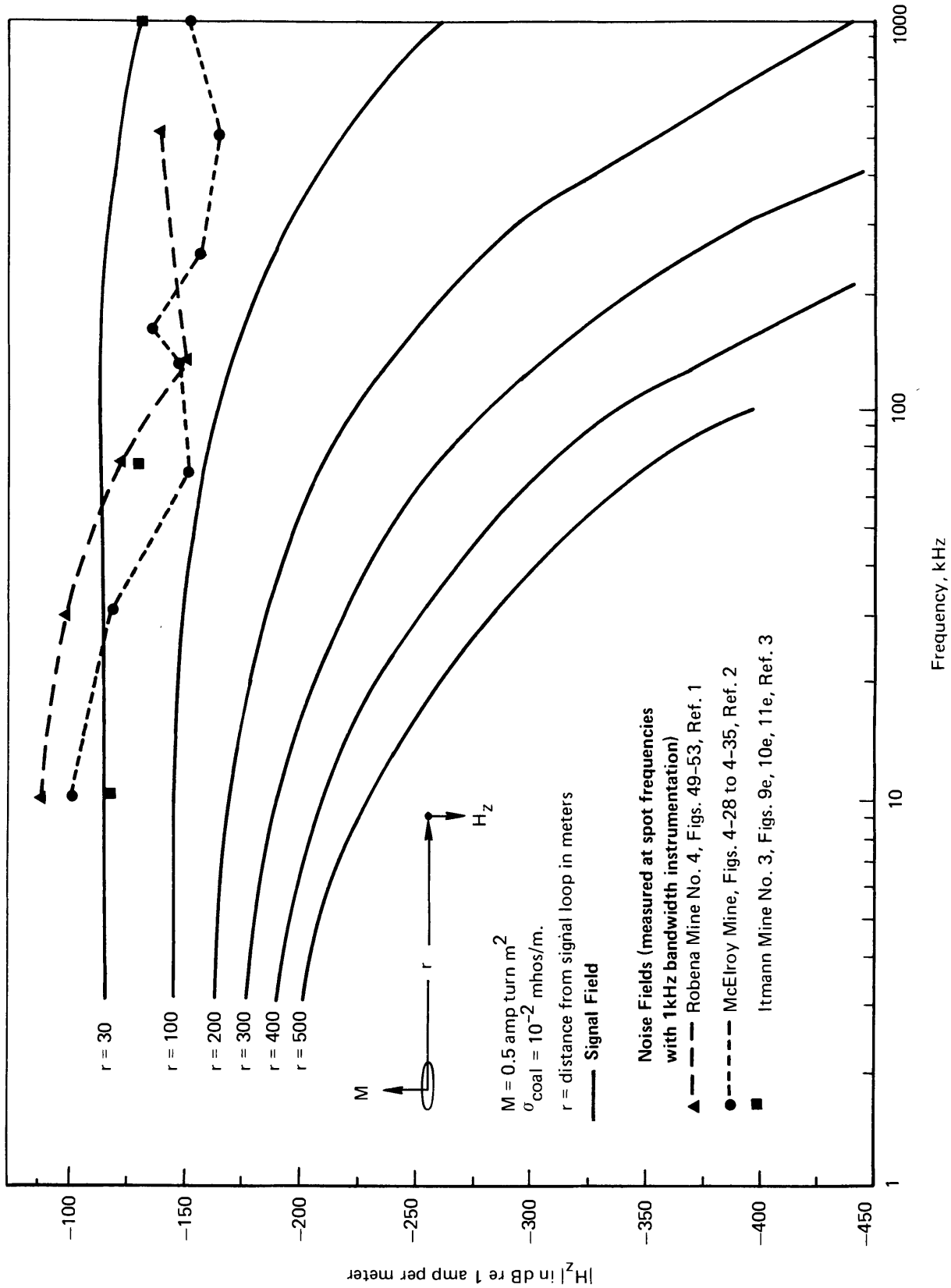


FIGURE 2-1 MAGNETIC FIELD STRENGTH  $|H_z|$  FROM A LOOP ANTENNA IN AN AIR MEDIUM

Source: Arthur D. Little, Inc.



Source: Arthur D. Little, Inc. and National Bureau of Standards.

FIGURE 2-2 MAGNETIC FIELD STRENGTH  $H_z$  FROM A LOOP ANTENNA IN A CONDUCTING MEDIUM AND RMS MAGNETIC FIELD NOISE IN MINES (NORMALIZED TO 2.5kHz BANDWIDTH)

## 2. Range Estimates

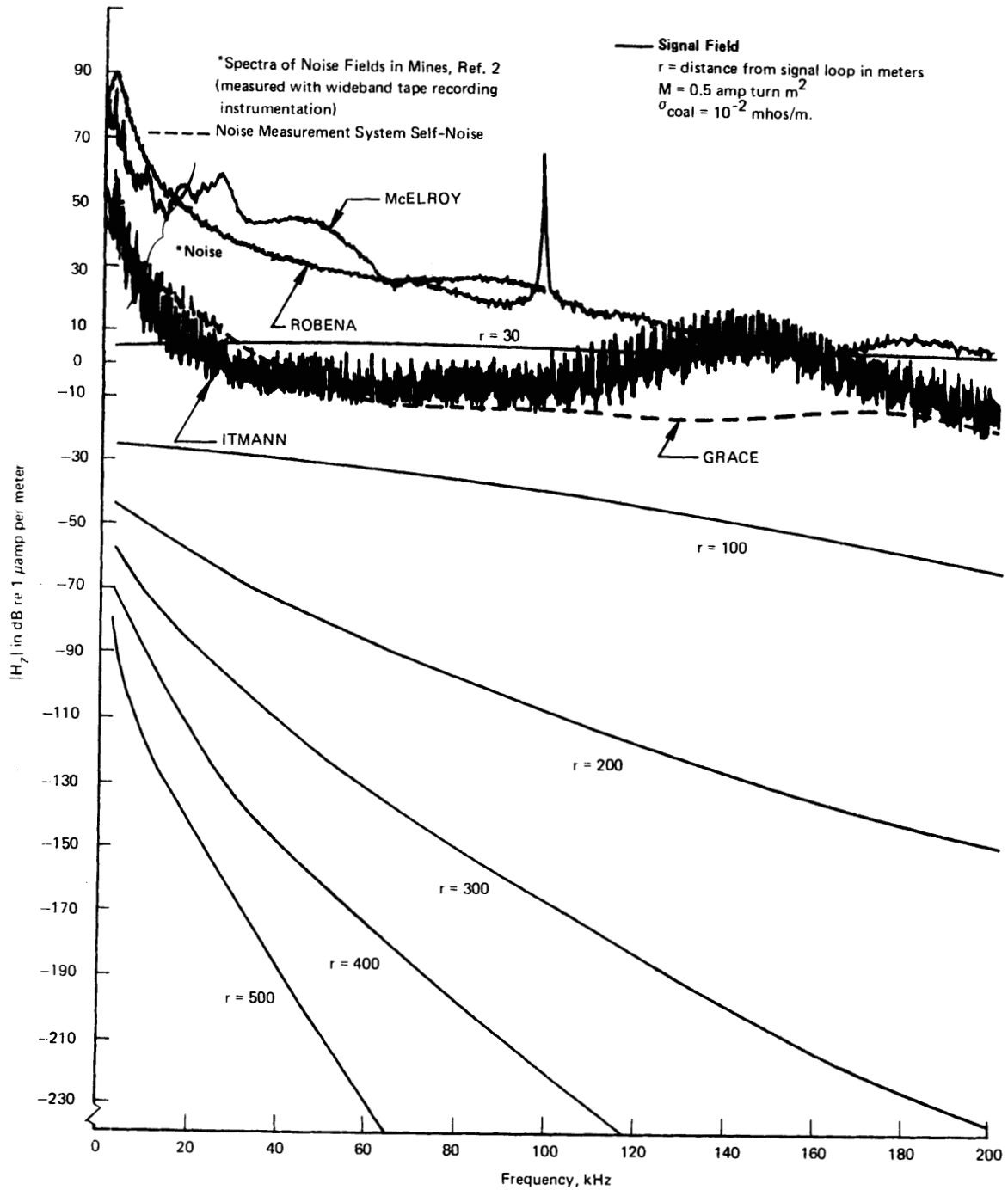
### a. Single Sideband Voice

Plotted in Figure 2-2 are magnetic field rms noise levels measured in three coal mines<sup>(1, 2, 3)</sup> for comparison with the signal strength curves. The noise levels have been normalized for a single sideband AM voice system effective bandwidth of 2.5 kHz. These noise data were all taken in mine working sections with instrumentation having an effective bandwidth of 1 kHz at spot frequencies. At the Robena and McElroy mines the data were taken about 100 meters from working faces. The dip in noise level around 130 kHz at Robena was concluded to be atypically low and should not be considered representative. Both Robena and McElroy mines employ room and pillar continuous mining techniques. At the Itmann No. 3 mine, data were taken near the face area of a longwall working section.

In Figure 2-3, the signal levels of Figure 2-2 have been replotted for comparison with samples of wideband tape recordings of magnetic field noise levels measured near operating machinery in four mines<sup>(2)</sup>. The noise levels have again been normalized to a bandwidth of 2.5 kHz. Figure 2-5 contains a similar comparison of signal and noise levels, but for noise level samples measured in rail haulageways. The noise levels in Figures 2-3 and 2-4 were obtained by narrowband FFT spectrum analysis of wideband tape recordings having upper cut off frequencies of 100 kHz (Robena) and 200 kHz (other mines).

- 
1. W. D. Bensema, M. Kanda and J. W. Adams, "Electromagnetic Noise in Robena No. 4 Coal Mine", NBS Technical Note 654, April, 1974.
  2. M. Kanda, J. W. Adams and W. D. Bensema, "Electromagnetic Noise in McElroy Mine", NBSIR 74-389, June, 1974.
  3. M. Kanda, "Time and Amplitude Statistics for Electromagnetic Noise in Mines", NBSIR 74-378, June, 1974.





Source: Arthur D. Little, Inc. and National Bureau of Standards.

**FIGURE 2-3 COMPARISON OF LOOP SIGNAL IN CONDUCTING MEDIUM (FROM FIGURE 2-2) AND MINE NOISE NEAR OPERATING MACHINERY (NORMALIZED TO 2.5kHz BANDWIDTH)**

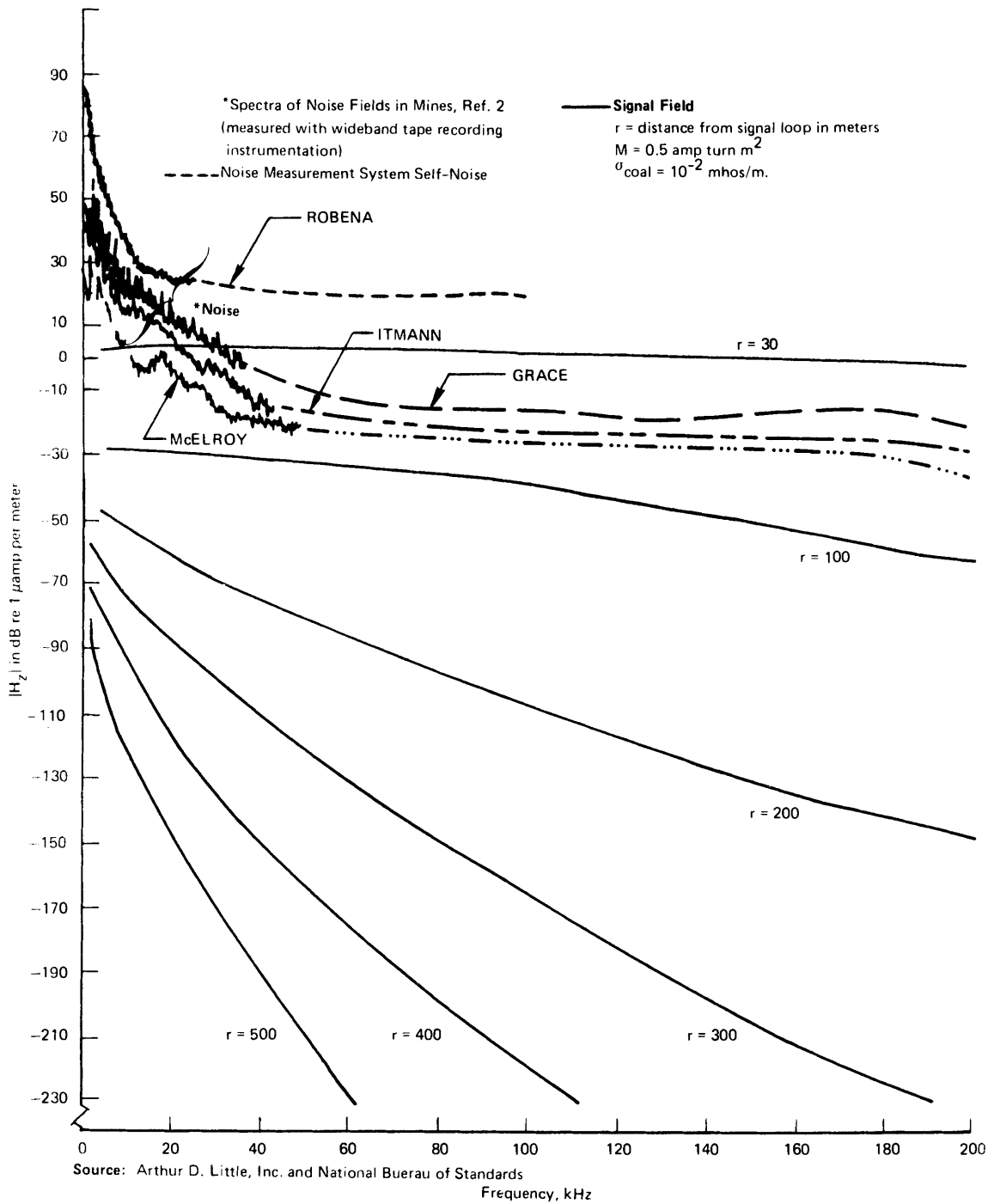
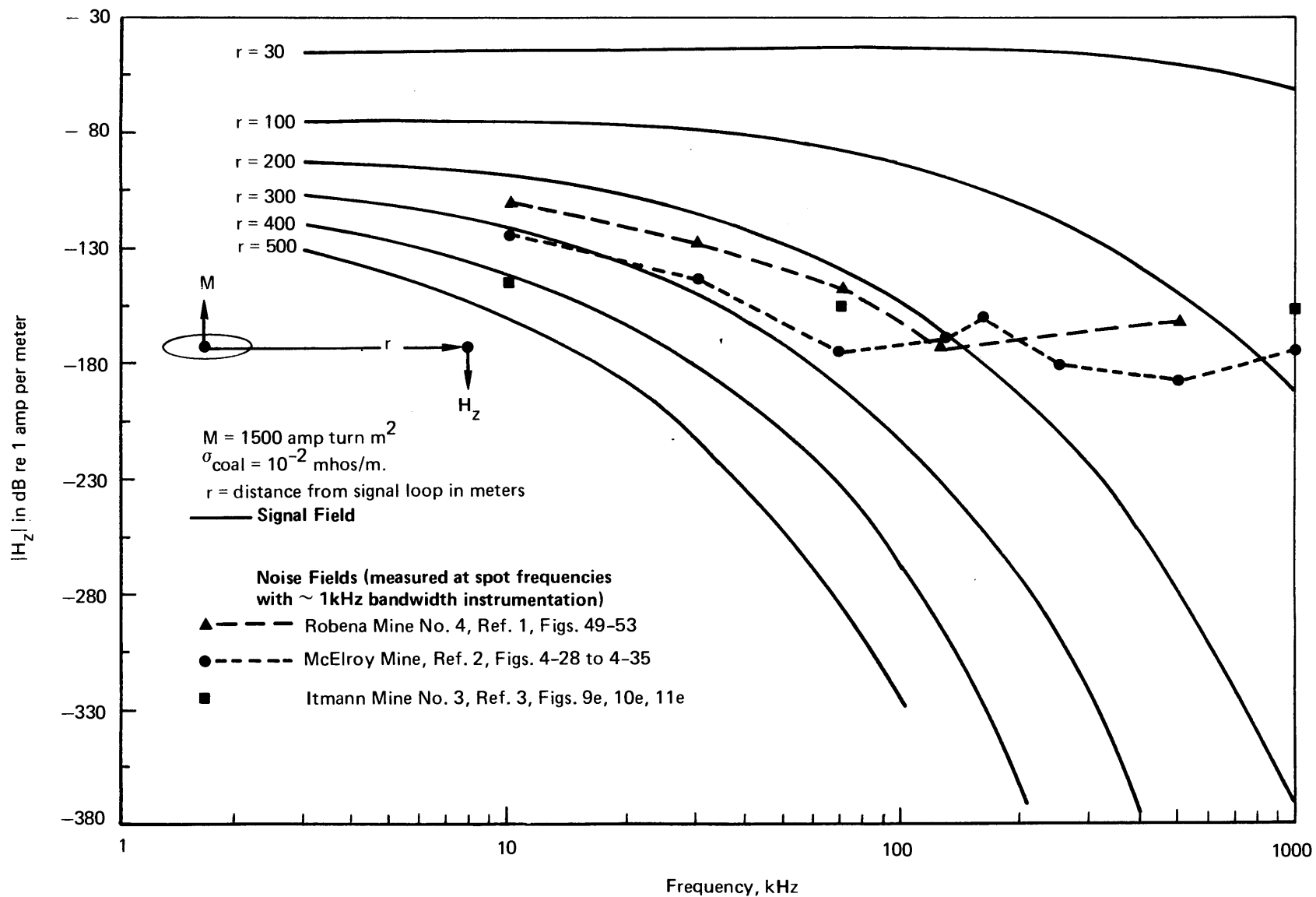


**FIGURE 2-4** COMPARISON OF LOOP SIGNAL IN CONDUCTING MEDIUM (FROM FIGURE 2-2) AND MINE NOISE IN HAULAGEWAY (NORMALIZED TO 2.5kHz BANDWIDTH)



Source: Arthur D. Little, Inc. and National Bureau of Standards.

FIGURE 2-5 MAGNETIC FIELD STRENGTH  $|H_z|$  FROM A LOOP ANTENNA IN A CONDUCTING MEDIUM AND RMS MAGNETIC FIELD NOISE IN MINES (NORMALIZED TO A 10Hz BANDWIDTH)

Examination of Figures 2-2, 2-3 and 2-4 reveals achievable ranges in the vicinity of about 50 meters for marginal quality conventional SSB voice communication, and then only above about 100-200 kHz. These range expectations, based on direct-loop-to-loop coupling between man-sized loops in a homogeneous conducting medium of  $\sigma = 10^{-2}$  Mho/m. (without the aid of any nearby conductors) in the presence of representative noise levels in operating mines, are unacceptably low compared with the desired range of 1,350 ft (412 m). At "quiet" times or locations these performance ranges can be expected to increase somewhat, but probably not drastically if the mine is not in an emergency power-down condition. Increasing the transmit moment from 0.5 to 2 amp - m<sup>2</sup> will not make a significant difference either. Section D of this chapter examines the range implications for a different propagation model which to date has been found to apply in several mines.

b. Narrowband Paging

A second reference example (a somewhat extreme one) has also been examined for the same homogeneous conducting medium having  $\sigma = 10^{-2}$  Mho/m, to see if it would produce a significant improvement in range. Namely, it was assumed that the very large transmit moment ( $M = 1500$  ampere - m<sup>2</sup> for a pillar - encircling single-turn loop) and the very narrow bandwidth ( $B = 10$ Hz) associated with recently developed audio frequency call alert mine paging systems could be safely generated and maintained over the 10 kHz - 1 MHz frequency band of interest. Such a transmitter strength and configuration might be associated with a fixed base station or repeater. The corresponding signal and noise field strength levels were computed and compared with each other to determine the increase in range that would occur. The above signal level and bandwidth changes represent a 94 dB improvement in signal-to-noise ratio. In practice such a large increase will be unattainable at the higher frequencies because of the high voltages required (because of the loop inductance) to generate the current levels in the transmit loop to produce the  $M$  of 1500 amp-m<sup>2</sup>, and because the pillar-encircling loop lying in the horizontal plane is unsuitable for exciting the favorable TEM propagation mode in a three-layer model, which now appears to be a more representative model for coal mines.

The signal field strengths were calculated as before, using the infinitesimal magnetic dipole field approximation, which will be accurate enough for estimating maximum operating ranges beyond 100 meters, in spite of the rather large finite size of the pillar-encircling loop. Thus, the signal field strength curves can be obtained by scaling up the Figure 2-2 signal curves, and the noise curves can be obtained by scaling down the Figure 2-2 noise curves. The rescaled signal and noise curves are plotted in Figure 2-5. These curves indicate that between about 200 kHz and 1 MHz, ranges would be limited to about 100-200 meters, but that between about 10 kHz and 200 kHz, it may be possible to achieve communication ranges out to between 200 and 300 meters, which still fall short of the 1,350 ft (412 m) range goal. Furthermore, this would represent only the "talk out" range from a base station. Because of the significantly lower signal strength available from a man-carried transmitter compared to that available from the pillar mounted transmitter, the "talk back" range from the mobile miner would still be substantially smaller and inadequate.

Thus, we find that if the mine environment is found to behave like a homogeneous conducting medium having a conductivity of  $10^{-2}$  Mho/m or greater, the desired range goal will be unattainable. However, it has been found that some mines may possess much more favorable wave propagation characteristics that tend to improve the outlook. These are discussed in the following section of this chapter.

#### D. THE THREE-LAYER MODEL

A second, and more plausible model, namely the three-layer propagation model has been developed recently by Arthur D. Little, Inc.<sup>(4, 5)</sup> to explain the unexpectedly favorable results of radio transmission measurements<sup>(6)</sup> made at frequencies in the 50 kHz to 1 MHz band with loop antennas in a conductor-free area of a coal mine, Consolidation Coal's Ireland Mine near Moundsville, West Virginia. The measurements indicate that communication ranges in excess of 1,000 ft are attainable in this mine when both transmit and receive loop antennas are oriented to lie in a common vertical plane. The model which explains the observed behavior is one in which the coal is assumed to have a low conductivity compared with that of the surrounding rock above and below the seam. The propagation mode is then considered to be approximately a dipolar, two dimensional TEM mode with vertical E-field and circumferential H-field in a horizontal slot (the coal seam) between two identical, higher conducting, half spaces (the rock). This model, as did the homogeneous medium model, ignores the presence of the mine tunnels, a good approximation in view of the large ratio of wavelength to tunnel dimensions. The model also represents a considerable simplification of the stratification of the layers of rock above and below the coal. We do not intend to justify this model or present detailed derivations here, since that is amply treated in the cited references. We only plan to excerpt, summarize, and use the results of that investigation for the purpose of assessing transmitter requirements to attain the 1,350 ft (412 m) communication range goal.

- 
4. Arthur D. Little, Inc., "Propagation of Radio Waves in Coal Mines" Chapter IV, Final Report on Task F, Task Order No. 1, Contract No. H0346045, October, 1975.
  5. A. G. Emslie and R. L. Lagace, "Propagation of Low and Medium Frequency Radio Waves in a Coal Seam", Radio Science, Vol. 11, No. 4, pp. 253-261, April, 1976.
  6. T. S. Cory, Summary Data Report No. 2 - "Mine Wireless Propagation Test Program - Ireland Mine Test Data at Medium Frequency", prepared for Collins Radio Group of Rockwell International for U.S. Bureau of Mines under Contract H0346067, Subcontract C-615171.

## 1. Signal Field Strengths

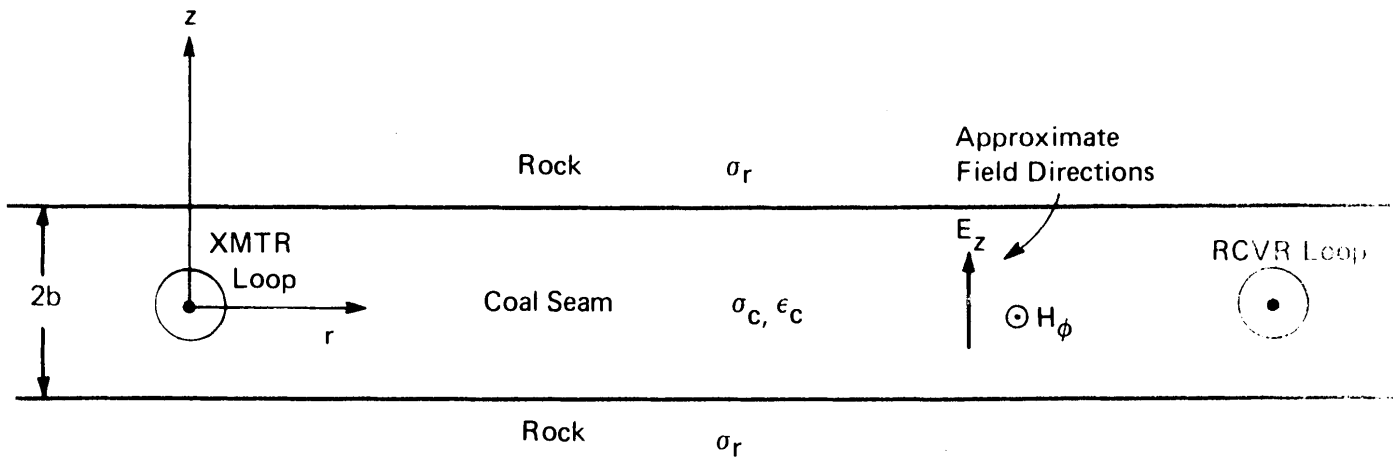
The three layer model is represented in Figure 2-6 which shows a cross section of the simplified geometry with the transmitting and receiving loop antennas in the vertical plane containing the path of propagation. The conductivity,  $\sigma_c$ , of the coal seam of thickness  $2b$  is considered to be several orders of magnitude less than the conductivity  $\sigma_r$  of the adjacent rock. The vertically-oriented transmitting loop antenna produces, along the path of transmission in the coal seam, a horizontal magnetic field  $H_\phi$  and an approximately vertical electric field  $E_z$ . The fields are almost constant over the height of the coal seam. In the rock above and below the seam the fields die off exponentially in the positive and negative  $z$ -directions, respectively. At large radial distances from the antenna the fields decay exponentially at a rate determined by an effective attenuation constant  $\alpha$ , which depends on losses both in the coal and in the rock and on the dielectric constant of the coal. There is also a  $1/\sqrt{r}$  factor at large radial distances  $r$  due to the cylindrical spreading of the wave.

The zero-order mode magnetic field  $H_\phi$  in the plane of the transmitting loop is given by

$$H_\phi = \frac{iMk^2}{8b_e} H_1^{(2)'}(kr) \quad (6)$$

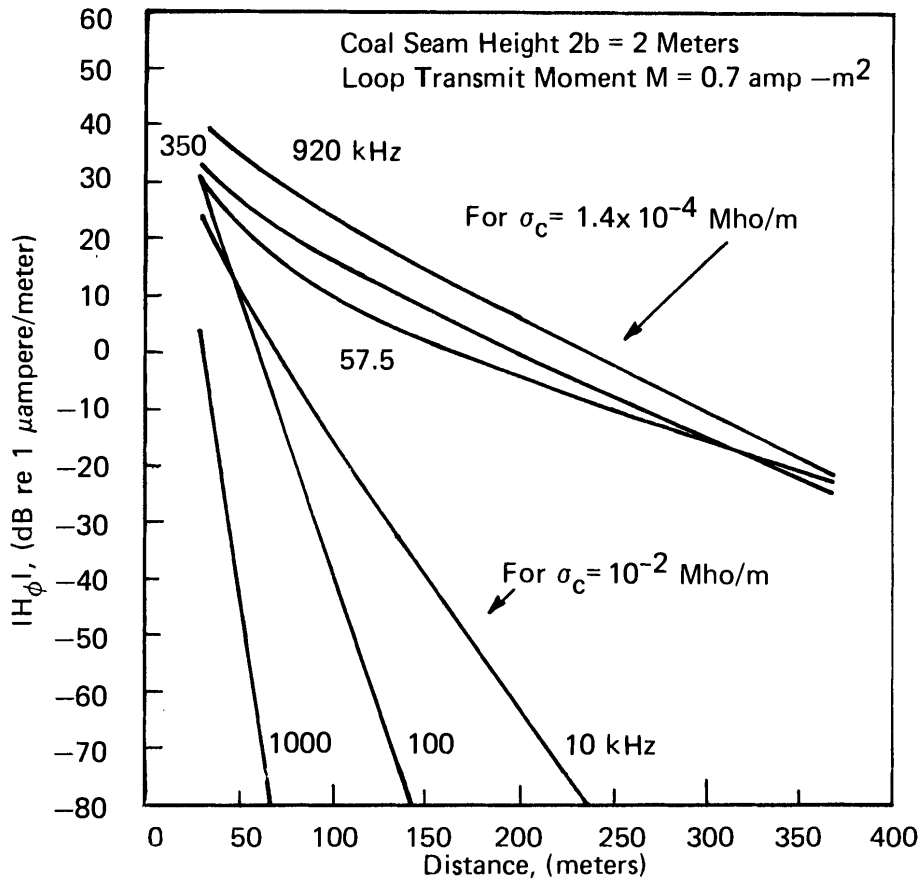
where

- $M = NIA$  is the magnetic moment of the transmitting loop antenna
- $b_e = b + 1/2 \delta_r$  is the effective half-height of the coal seam
- $\delta_r = z$ -direction skin depth in the rock
- $k = \beta - i\alpha$  is the complex propagation constant in the radial direction  $r$
- $H_1^{(2)'}(kr) =$  derivative of the first order Hankel function for an outgoing wave



Source: Arthur D. Little, Inc.

FIGURE 2-6 THREE LAYER MODEL GEOMETRY FOR LOW AND MEDIUM FREQUENCY RADIO WAVE PROPAGATION



Values of Coal Permittivity and Surrounding Rock Conductivity are Identical for all Curves, Namely  $K_c = 7$ ,  $\sigma_r = 1.0$  Mho/m

Source: Arthur D. Little, Inc.

FIGURE 2-7 THEORETICAL MAGNETIC FIELD STRENGTH PLOTS VERSUS DISTANCE AND FREQUENCY FOR THREE LAYER MODEL FOR TWO VALUES OF COAL CONDUCTIVITY,  $\sigma_c = 1.4 \times 10^{-4}$  Mho/m AND  $\sigma_c = 10^{-2}$  Mho/m



A detailed derivation for  $H_{\phi}$ , together with formulas for the phase and attenuation constants  $\beta$  and  $\alpha$  expressed in terms of the conductivities ( $\sigma_c, \sigma_r$ ) of the coal and the rock, permittivity  $K_c$  of coal, the frequency  $f$  and the half-height  $b$  of the coal seam are given in references 4 and 5. The common radial skin depth in both coal and rock is  $\delta = 1/\alpha$ .

The best overall fit of the above propagation model to the Ireland mine experimental data was found<sup>(4, 5)</sup> to occur for coal and rock conductivities of  $1.4 \times 10^{-4}$  Mho/m and 1.0 Mho/m, respectively, using an assumed coal dielectric constant of 7 (a value consistent with dielectric constant data obtained by NBS).<sup>(7)</sup> Although these values of conductivity are reasonable for bituminous coal and rock shales, they do lie close to extreme values for each. Namely, the value of  $1.4 \times 10^{-4}$  Mho/m for the conductivity  $\sigma_c$  of the coal required to make the theory fit the experimental data lies within the lower part of the range of conductivity values for bituminous coals; whereas the conductivity value  $\sigma_r$  of 1.0 Mho/m required of the adjacent rock layers, although high, lies within the uppermost part of the range of reported conductivity values for some types of shales and slates under certain conditions<sup>(8)</sup>.

Using these conductivity values, theoretical magnetic field strength curves have been computed and plotted in Figure 2-7 at three frequencies (57.5, 350, and 920 kHz) for a transmit loop source strength of  $M = 0.7$  ampere - m<sup>2</sup> which is oriented and positioned as shown in Figure 2-6 in a high-coal seam of thickness  $2b = 2$  meters. Also plotted for comparison in Figure 2-7 are field strength curves at the three frequencies of 10, 100, and 1000 kHz for the same source strength and configuration, seam thickness, and rock conductivity, but for the substantially higher coal

---

7. D. A. Ellerbruch and J. W. Adams, "Microwave Measurement of Coal Layer Thickness", Nat. Bureau Stand. (U.S.) NBSIR 74-387, September, 1974.

8. E. I. Parkhomenko, Chapter III, Electrical Resistivity of Rocks, Electrical Properties of Rocks, Translated from Russian and Edited by G. V. Keller, Plenum Press, N.Y. 1967

conductivity of  $\sigma_r = 10^{-2}$  Mho/m used in the homogeneous medium model in Section C of this chapter. The higher value of  $\sigma_c$  lies within the upper part of the range of values for bituminous coal<sup>(8)</sup>. Examination of Figure 2-7 reveals that dramatic changes in propagation loss can occur as the conductivity of the coal is increased from  $10^{-4}$  to  $10^{-2}$  Mho/m. The low coal conductivity produces a substantially lower signal attenuation rate and only moderate variations of signal strength with frequency for the indicated ranges of distance and frequency. On the other hand, the higher coal conductivity results in substantially increased attenuation rates and large variations with frequency, that in turn cause the strongest signals to occur at the lowest frequencies, as in the homogeneous model.

## 2. Range Estimates for FM Voice

Plotted in Figures 2-8 and 2-9 are comprehensive noise plots which we have used together with the field strength curves of Figure 2-7 to arrive at new range estimates for wireless voice communication with man-carried personal radio systems in mines. We chose in this instance, a narrowband FM radio communication system having an IF bandwidth  $B = 12$  kHz, receiver noise figure  $F = 6$  dB, transmit magnetic moment  $M = 0.7$  amp-m<sup>2</sup>, and loop effective turns-area  $NA = 1$  m<sup>2</sup>, similar to a system presently being developed for wireless mine communication applications by Collins Radio Group on Bureau of Mines Contract H0346047. The rms noise levels used to characterize the mine electromagnetic noise environment in Figures 2-8 and 2-9 were derived from samples of magnetic field, time-averaged, rms noise levels measured (with 1 kHz bandwidth instrumentation) at spot frequencies in the frequency range of interest in three coal mines by Bensema, Kanda, and Adams<sup>(1, 2, 9)</sup> of the National Bureau of Standards. In the frequency band of interest, the average rms noise levels generally decrease at a rate on the order of  $1/f$  with increasing frequency, and exhibit relatively large variations during typical mine work shifts. The magnitude of these long term variations in average rms level also decrease with increasing frequency in the LF to MF band, commonly being on the order of 45-50 dB at frequencies below about 100 kHz and decreasing to about 25-30 dB at frequencies around 1 MHz.

---

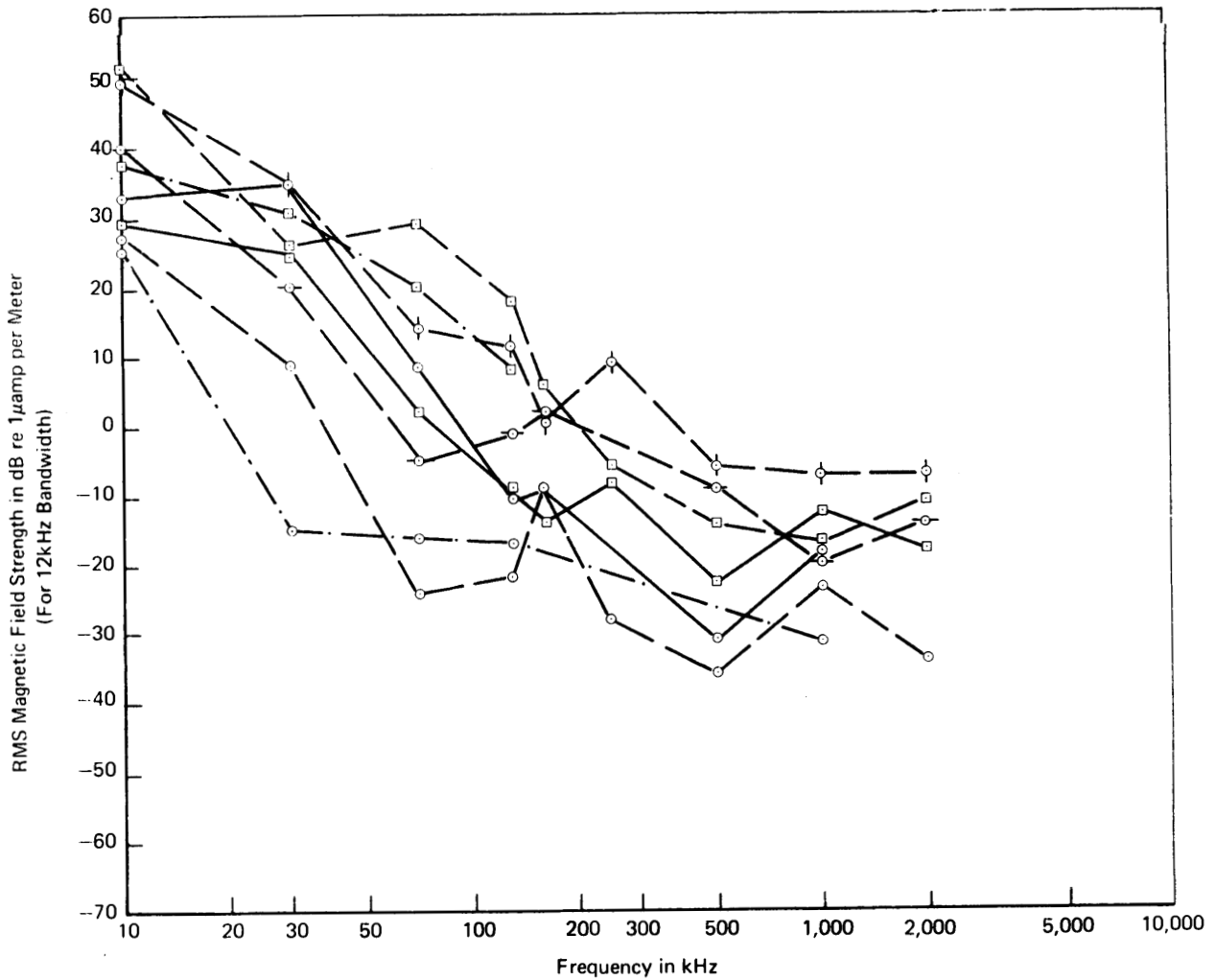
9. W. D. Bensema, M. Kanda and J. W. Adams, "Electromagnetic Noise in Itmann Mine", Nat. Bur. Stand. (U.S.) NBSIR 74-390, June, 1974.

Plotted Noise Levels Normalized to 12kHz Bandwidth – Measured with 1kHz Instrumentation Bandwidth

- Vertical Field Component
- - - Vertical Component – “Quiet Time”
- Horizontal Field Component

McElroy Mine – Continuous Miner Section and Nearby Rail Haulageway

- Near end of rail haulage line
- ◊ Near intersection of rail haulageway and conveyor belt
- ◇ Near operating continuous mining machine
- Near section power distribution center



Source: National Bureau of Standards (Report NBSIR 74-389, June 1974)

**FIGURE 2-8 REPRESENTATIVE RMS MAGNETIC FIELD NOISE LEVELS MEASURED IN THE McELROY COAL MINE**

Plotted Noise Levels Normalized to 12kHz Bandwidth – Measured with 1kHz Instrumentation Bandwidth

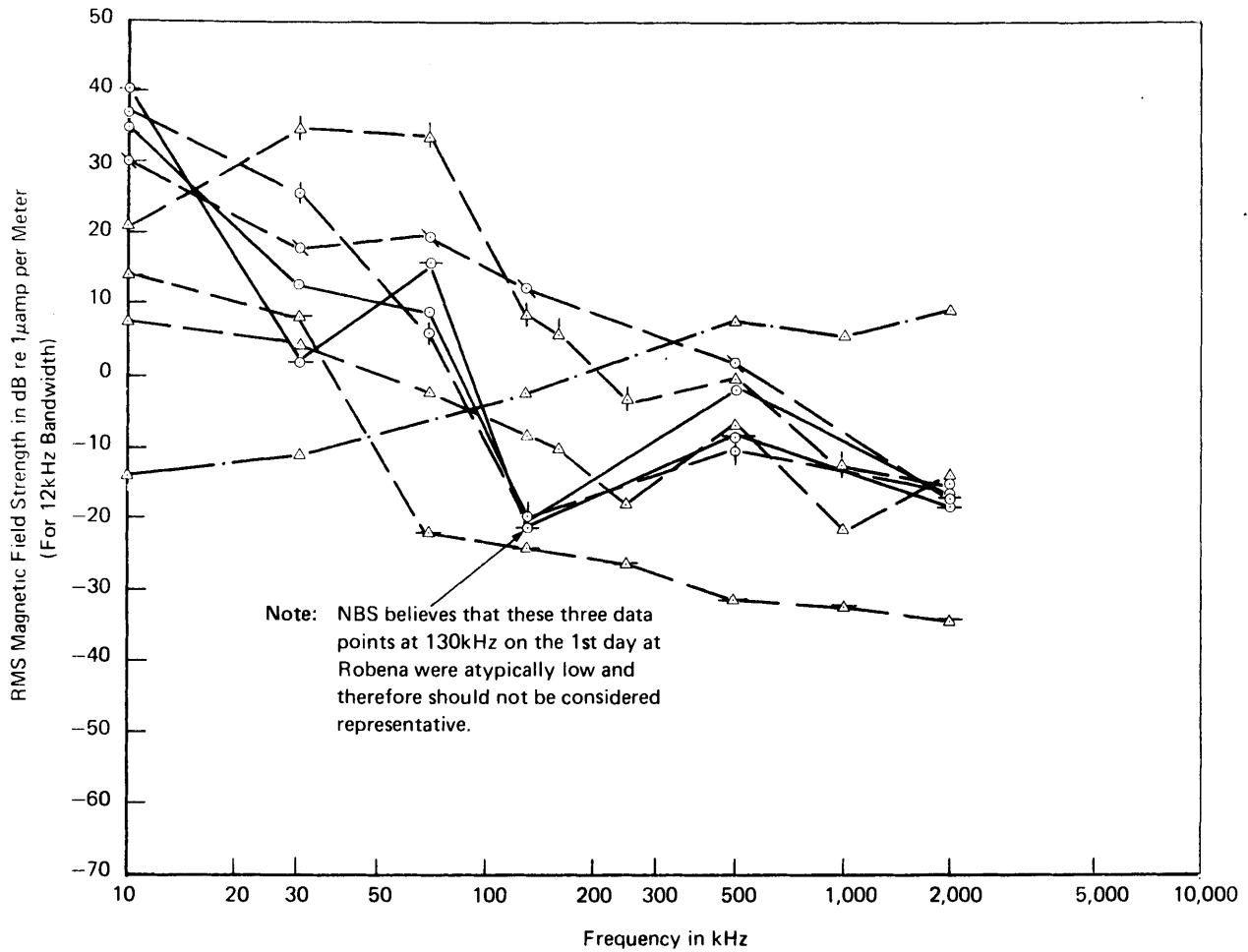
- Vertical Field Component
- - - Vertical Component – “Quiet Time”
- Horizontal Field Component

Itmann Mine – Longwall Panels

- △ At longwall face head end – Farley panel
- ▽ 230 ft from longwall face – Farley panel
- △ At longwall face head end near main conveyor belt – Cabin Creek panel

Robena Mine – Rail Haulageway serving continuous miner section. All curves for same location approximately 300 meters from face area

- Horizontal (E-W) – 1st day
- ◊ Horizontal (N-S) – 1st day
- ◇ Vertical – 1st day
- ⊗ Vertical – 2nd day



Source: National Bureau of Standards (Reports NBS Technical Note 654, April 1974 Robena; and NBSIR 74-390, June 1974, Itmann)

FIGURE 2-9 REPRESENTATIVE RMS MAGNETIC FIELD NOISE LEVELS MEASURED IN THE ROBENA AND ITMANN COAL MINES

The wireless communication ranges are estimated for the above radio system and noise parameters and a radio circuit grade of performance goal within the Circuit Merit Figure #3 classification, the minimum figure normally considered for commercial radio service. To obtain this level of performance the minimum average rms carrier-to-noise ratio at the receiver must be at least 10 dB or better for the mine noise conditions prevailing during the communication intervals.

The range estimates are shown in Table 2-1 for active-mine electromagnetic noise conditions and quiet receiver-noise-limited conditions. Table 2-1 shows that only very short and inadequate communication ranges are predicted for all noise conditions and frequencies for the high conductivity coal case ( $\sigma_c = 1.0 \times 10^{-2}$  Mho/m), as was the case for the homogeneous medium model. The extremely high rates of signal attenuation for this case also make communication ranges very insensitive to even large upward or downward changes in local levels of average rms electromagnetic noise. For the low conductivity coal case ( $\sigma_c = 1.4 \times 10^{-4}$  Mho/m), the communication ranges are substantially increased to more practical values that approach the 412 m (1,350 ft) range goal. However, these extended ranges are also more sensitive to variations in local rms electromagnetic noise levels, because of the greatly reduced rates of signal attenuation when the coal conductivity is low. This effect is illustrated in Table 2-1 by the wide spans in estimated ranges under active-mine noise conditions. Active-mine noise levels can also occasionally fall below intrinsic receiver noise levels. When this occurs, the maximum range will be limited by, and identical to, that dictated by receiver noise not mine noise. These receiver-noise-limited ranges are also shown in Table 2-1.

TABLE 2-1

RANGE ESTIMATES FOR WIRELESS COMMUNICATION WITH PERSONAL PORTABLE FM  
RADIOS IN A HIGH-COAL SEAM

(Seam Height of 2m, and  $K_c = 7$ , bounded by rock of conductivity  $\sigma_r = 1.0$  Mho/m, for coal conductivities of  $1.0 \times 10^{-2}$  and  $1.4 \times 10^{-4}$  Mho/m)

Frequency (kHz)	Coal Conductivity $\sigma_c$ (Mho/m)	Communication Range in Meters(ft)			
		Noise Conditions			
		Receiver Noise		Active Mine Noise	
10	$1 \times 10^{-2}$	45	(150)	5-45	(50-150)
100	$1 \times 10^{-2}$	65	(200)	30-65	(100-200)
1000	$1 \times 10^{-2}$	45	(150)	25-40	(75-125)
57.5	$1.4 \times 10^{-4}$	140	(450)	15-140	(50-450)
350	$1.4 \times 10^{-4}$	290	(950)	120-290	(400-950)
920	$1.4 \times 10^{-4}$	365	(1200)	175-340	(575-1125)

Source: Arthur D. Little, Inc.

### 3. Discussion of Implications

The findings of the three layer model based on the Ireland mine experimental data indicate that communication ranges within striking distance of the 1,350 ft (412 m) goal are attainable under some noise conditions in at least one mine having the right combination of rock and coal conductivities, in particular, a low value of coal conductivity. If this behavior is found to be common in coal mines, it is conceivable that the range goal could be reached through the clever application of of currently available antenna and transmitter technology. However, it is reported<sup>(8)</sup> that the conductivity of coal can take on a wide range of values, encompassing at least two orders of magnitude, which could result in different seams or mines within the same seam having drastically different attainable communication ranges. Therefore, it is important to determine whether the favorable Ireland mine conditions are typical or exceptional for bituminous coal mines in the United States. This should be accomplished by performing similar propagation measurements in several more coal mines in several of the major coal seams, to obtain data from mines having both similar and different geological properties regarding both the coal seam and the surrounding rock. Only then will it be possible to confidently determine the most favorable operating frequency, and the associated performance limits, for a mine wireless communication system using currently available technology in the 10 kHz to 1 MHz band.

Such a measurement program has been defined and is presently being implemented for the Bureau of Mines by a measurement and analysis team consisting of T. Cory/Spectra Associates/Collins Radio Group on Contract H0366028 and Arthur D. Little, Inc., on Contract H0346045, Task Order No. 4, respectively. The preliminary findings to date indicate that two other mines also in northern West Virginia and in the Pittsburgh seam exhibit behavior and coal conductivities similar to that found in the Ireland mine, while another mine in Illinois in the Herrin No. 6 seam exhibits significantly higher signal attenuation rates by about a factor of three and a coal conductivity of about  $10^{-3}$  Mho/m. Thus, the issue remains unresolved at the time of this writing. However, if large

variations in conductivity turn out to be common from mine-to-mine, it is unlikely that improved antenna technology alone will ever be capable of providing the significant improvements in system performance that will be required for 10 kHz to 1 MHz operation in mines with high conductivity coal. An assessment of the likely impact of antenna technology on performance is discussed in the following chapter.

It should be noted that the quiet-area range predictions of Table 2-1 should be most applicable for conductor free areas such as the part of the Ireland mine in which the signal propagation measurements were made; whereas the active-area range predictions are probably pessimistic, because the active, noisy areas are generally those where conductors such as trolley wire/rails and power and telephone cables are also present. In the latter situation one would expect that communication ranges could be considerably increased by the lower-loss transmission line type of propagation made possible by the inductive coupling of the fields from man-carried loops to such nearby conductors. Single conductors or cables will act as one element of a transmission line, with the highly conducting rock and/or moderately conducting coal serving as the return current path, while trolley lines have the rails as return conductors. Since miners requiring radio communications are very likely to be working in the vicinity of such conducting structures, this situation, as opposed to the completely conductor-free situation, may become an equally important operational requirement influencing the choice of frequency. Therefore, the coupling of loop antennas to two-wire transmission line structures is treated in Chapter IV. On the other hand, methods of reducing the deleterious effects of mine generated radio noise should not be overlooked as a means of improving the signal-to-noise performance and thus the communication range. For example, the effective level of received noise can in some cases be reduced by up to 10-20 dB by simple processing, such as clipping and blanking, if the noise is highly impulsive in nature. The potential benefits of yet another method, a special noise cancelling diversity reception technique that may be particularly suited to the mine noise environment, are presented in Chapter V.



### III. ANTENNA TECHNOLOGY

#### A. SUMMARY

Transmit antenna technology available in the VLF through MF bands is examined for its utility in portable mine wireless radio applications. In particular, an assessment is made of the feasibility of developing compact, portable transmit antennas that will efficiently generate radio waves in coal mines. The size of such antennas relative to wavelength classifies them as electrically small antennas which, by their very nature, are poor radiators. No major breakthroughs have occurred, or are likely to occur, to change this fact. Thus, the VLF-MF mine wireless communication problem is one of optimizing the near field and induction field coupling between two loosely coupled portable electromagnetic field transducers (antennas) in the physical and noise environment of a mine. The problem is made more difficult by the mine's lossy conducting medium which introduces considerable signal attenuation.

The choice of a specific antenna should, therefore, not be based on its radiation efficiency. Instead it should be based on the overall power efficiency and practicality achievable by the complete transmitter-antenna system, in producing the largest usable signal at the desired range within the practical constraints of system overall size, weight, convenience of use, intrinsic safety, and ruggedness for roving miners. Thus, it is concluded that conventional air-core bandolier loop antennas, and perhaps smaller ferrite-loaded loop antennas, will continue to be the most suitable and reasonable choice for roving miner portable radio applications at frequencies below about 1 MHz. Furthermore, a transmit moment of about  $2.5 \text{ amp-m}^2$  (peak) appears to be a practical upper bound for intrinsically safe portable units for use by miners. Thus, the completely wireless range capabilities will not be significantly better than those predicted for units having a transmit moment of  $0.7 \text{ amp-m}^2$ . For fixed station applications, horizontal-wire and vertical-rod mode exciters may also offer comparable or better performance than planar air-core loops, but in-mine measurements will be needed to resolve the matter.

The following sections of this chapter treat some of the basic principles and limitations of small antennas operating below 1 MHz in both free space and conducting media, together with an overview of specific antenna types considered for manpack portable applications and for base station applications. The types of antennas treated are the class of electrically small antennas in general and, specifically, conventional whip antennas, active whip antennas, conventional air-core loop bandolier antennas, ferrite loaded loops, specially resonated multi-turn air core loops, self-resonant air-core helical loop antennas, horizontal-wire mode exciters, and vertical-rod mode exciters. There is an extensive body of published reference information which covers the subject matter in considerable detail. The approach taken in this chapter is to provide an overview of this antenna technology and its significance to the mine communications problem at hand. The reader is referred to the specific references to obtain a more detailed treatment of the material.

## B. ELECTRICALLY SMALL ANTENNAS

The desire is to obtain a small, lightweight, unobtrusive, effective antenna that can be conveniently worn by a roving miner for use with a personal radio operating somewhere in the VLF to MF range of 10 kHz to 1000 kHz (1 MHz). The antenna's impedance characteristics should also be relatively unaffected by the antenna's position on the miner's body and the antenna's proximity to his body or structures found in underground coal mines.

Resonant length dipoles, monopoles, and loops have maximum dimensions on the order of a quarter to one-half wavelengths, which make them good radiators, namely, good couplers of power from a transmitter to the surrounding space. They produce radiation resistances typically on the order of 35 to 80 ohms and zero net energy storage, or reactive impedance, at their resonant length frequencies. Therefore, they can achieve very high efficiencies, be conveniently driven from conventional sources, and easily meet conventional single-channel bandwidth requirements.

Electrically small antennas present a considerably different and more difficult design problem than the more conventional type of resonant length antennas. An electrically small antenna is defined as one whose size is a small fraction of the wavelength, more specifically less than 1/10 of a wavelength. Such antennas possess fundamental limitations on their electrical characteristics and performance that are directly attributable to their size compared to wavelength alone. Portable antennas for roving miner applications at frequencies below 1 MHz fall well within the small antenna size limits. Therefore, their performance will in fact be governed by the limitations and characteristics imposed on electrically small antennas.

### 1. Electrical Smallness

Free space wavelengths for operating frequencies from 10 kHz to 1000 kHz take on values of 30,000 to 300 meters respectively. Comparing these wavelengths to the maximum conceivable dimension  $d = 1$  meter for a personal antenna worn by a roving miner, we get  $\frac{1}{30,000} \leq \frac{d}{\lambda} \leq \frac{1}{300}$ ,

which immediately places such an antenna well inside the category of "electrically small" antennas, namely, antennas having  $d < \frac{\lambda}{10}$ . The more the size of an antenna is decreased with respect to wavelength the more it behaves as a high-Q, lumped-element energy storage device and as a very poor radiator of power to the surrounding space. These limitations are fundamental and are imposed by the antenna's size compared to wavelength, as illustrated in a classic paper by Chu<sup>(1)</sup> in 1948 and by Harrington<sup>(2)</sup> and Wheeler.<sup>(3,4)</sup> Thus, electrically small, lossless, whip-type dipole antennas behave as capacitors, and loop-type antennas behave as inductors. Their input impedances are highly reactive and have only a very small resistive part defined as the radiation resistance--a resistance whose value decreases rapidly with decreasing frequency (i.e., increasing wavelength).

## 2. Radiation Resistance

The radiation resistance  $R_r$  is a measure of the power radiated by an antenna. It is given by<sup>(5)</sup>

$$R_{re} = 80\pi^2 \left(\frac{h_e}{\lambda}\right)^2, \quad R_{r\ell} = 320\pi^4 \left(\frac{NA}{\lambda}\right)^2, \quad (1, 2)$$

for dipole and loop antennas respectively, where  $h_e$  is the effective height of the dipole and N and A are the number of turns and area of the loop. Note the strong inverse dependence on wavelength. The radiation resistance  $R_r$  is the real part of the input impedance of a lossless antenna, and  $\frac{1}{2}I_o^2 R_r$  represents the real power radiated.

Namely:

$$P_r = \frac{1}{2}I_o^2 R_r, \quad (3)$$

where  $P_r$  is the total radiated power computed by integrating the electromagnetic power density in the far field over the surface of a sphere concentric with the antenna, and  $I_o$  is the antenna input current which produces the radiated field. Substituting into (1), (2), and (3) practical antenna dimensions of 0.5 meter diameter for a 10-turn loop, a 0.25 meter effective height\* for a dipole, and a 1 ampere input current to each from a portable mine wireless unit operating at 300 kHz, we find that the radiation resistances and radiated powers

-----  
\*For an electrically small unloaded dipole having a triangular distribution of current which is maximum at the terminals and zero at the ends, the effective height is one-half the dipole length.

are:

$$R_{re} = 5.5 \times 10^{-6} \text{ ohm}$$

$$R_{r\ell} = 1.5 \times 10^{-9} \text{ ohm}$$

$$P_{re} = 2.75 \text{ } \mu\text{w}$$

$$P_{r\ell} = .0007 \text{ } \mu\text{w}$$

for the dipole and loop antenna respectively. At a frequency of 30 kHz, the upper boundary of the VLF band, the above values would of course be further reduced by a factor of  $\frac{1}{100}$  for the dipole and  $\frac{1}{10,000}$  for the loop. When compared with the resistive losses associated with practical antennas, these radiation resistances become insignificant. This fact accounts for the extremely low efficiencies attainable from man-carried antennas at these low operating frequencies. Thus, other factors take on a much greater importance than efficiency in forming a basis for antenna selection.

### 3. Efficiency

The efficiency of the antenna alone is defined as the ratio of the power radiated to the sum of the power radiated and the power dissipated in the ohmic resistance  $R_d$  associated with the antenna conductors,

$$E_a = \frac{P_{rad}}{P_{rad} + P_{dis}} = \frac{R_r}{R_r + R_d} \quad (4)$$

This is the best that can be done. For example, if the above-mentioned 10-turn, 0.5 meter diameter loop was made of #16 AWG copper wire, its resistance of 0.73 ohm including skin and proximity effects would give the negligible antenna efficiency of only  $2 \times 10^{-7}\%$ . The efficiency of the transmitting system is further degraded by the resistance associated with the source impedance, and the resistance associated with any tuning circuitry that may be required to drive the highly reactive antenna from practical power sources. These equivalent resistances must be added to the value of  $R_d$ , thereby reducing  $E_a$ . To arrive at the overall system efficiency, which impacts on power supply requirements, and in particular battery life, account must also be taken of coupling coefficients and losses associated with impedance matching and coupling circuits, and the efficiency of the transmitter/power amplifier electronics too. See Wheeler<sup>(2,3)</sup> and Watt<sup>(6)</sup> for concise treatments of these topics.

#### 4. Quality Factor-Q

The high-Q, reactive nature of the small antenna points to the need for tuning and matching circuits to provide the transmitter with the proper real impedance load to optimize efficiency, power transfer, or some other performance parameter. The tuning and matching elements, like the antenna itself, are not ideal. Thus, resistive loss is introduced by these elements, which reduces the attainable efficiency and Q, and increases the antenna circuit bandwidth.

Figure 3-1 from reference (7) presents a curve of the behavior of the intrinsic Q of electrically small antennas, based on the work of Chu.<sup>(1)</sup> The quantity "a" represents the radius of the minimum size sphere within which the antenna can be enclosed. This Q is a measure of the electromagnetic energy stored in the near field of the antenna compared to the power radiated into the far field by the antenna. Namely,

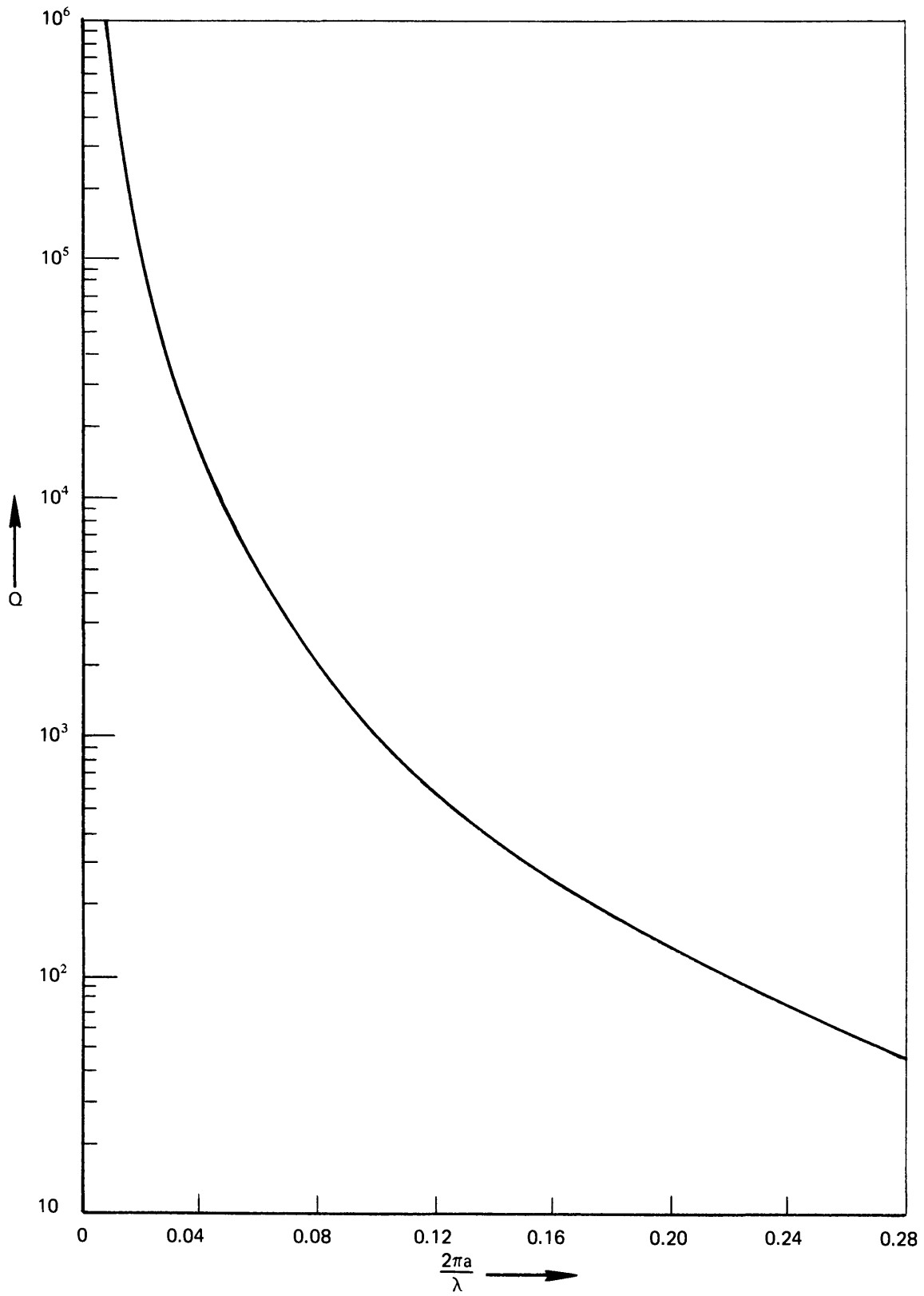
$$Q_r = \frac{\omega \times \text{peak stored energy}}{\text{average power radiated}}$$

Note the strong dependence on the radial dimension "a" expressed in wavelengths in Figure 3-1 and how rapidly Q increases with decreasing antenna size compared to wavelength, leading to the very narrow, intrinsic bandwidths characteristic of electrically small antennas.

At an operating frequency of 300 kHz, the 0.5 meter maximum antenna size of interest gives a  $2\pi a/\lambda$  value of approximately 0.001, which from Figure 3-1 results in a  $Q_r$  well in excess of  $10^6$ . The antenna's intrinsic radiation bandwidth ( $\Delta f = f_o/Q$ ) is therefore less than about 0.1 Hz at 300 kHz. Fortunately, neither of these values of  $Q_r$  or  $\Delta f$  is desirable or attainable in practice for roving miner portable radio applications. For example, net Q's of about 100 are typical for the antenna and its tuning circuit as a result of resistive type losses. This results in a more practical bandwidth of 3 kHz at 300 kHz, but in a poor net radiation efficiency of much less than 0.01% (from the alternate efficiency expression  $E = Q_{lr}/Q_r$  presented below).

#### 5. Power Factor

The intrinsic antenna behavior can also be conveniently expressed in terms of the radiation power factor introduced by Wheeler:<sup>(3)</sup>



Source: Reference 1.

FIGURE 3-1 BEHAVIOR OF ANTENNA INTRINSIC Q [BASED ON CHU<sup>(1)</sup>]

$$P_{fr} = \frac{R_r}{\omega L} = R_r \omega C = \frac{1}{Q_r} \quad (5)$$

where  $R_r$  is the radiation resistance and  $L$  and  $C$  are the intrinsic inductance and capacitance of the loop and dipole antennas respectively. This concept of power factor is a convenient and descriptive one for understanding antenna behavior and limitations of performance. For example the expression for antenna efficiency, including the resistance of the tuning elements, can be written as

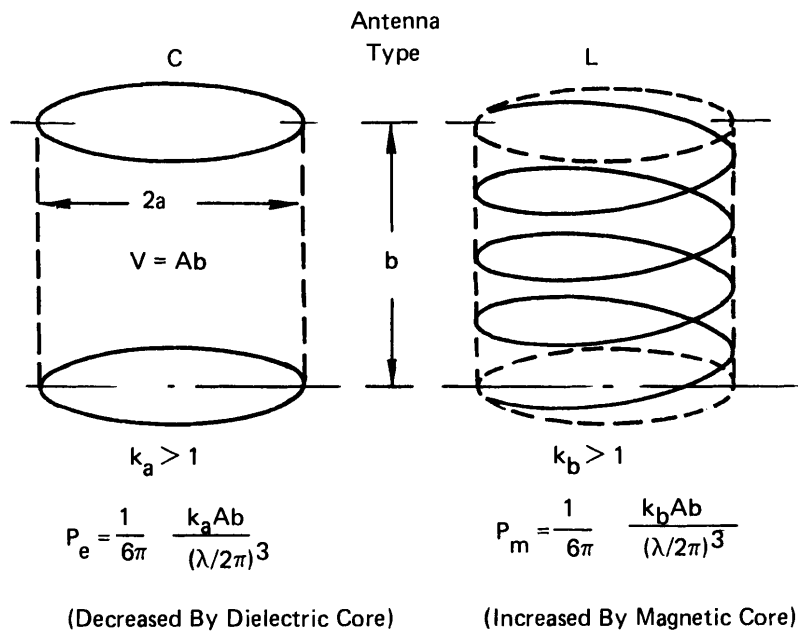
$$E = \frac{pf_r}{pf_r + pf_\ell} = \frac{R_r}{R_r + R_\ell} = \frac{Q_{\ell r}}{Q_r} \quad (6)$$

where  $pf_\ell = \frac{R_\ell}{\omega L} = R_\ell \omega C = \frac{1}{Q_\ell}$ ,  $R_\ell$  is the ohmic resistance of the antenna and tuning elements,  $Q_\ell$  is the  $Q$  due to these ohmic losses alone, and  $Q_{\ell r}$  is the  $Q$  which includes both ohmic and radiation losses.  $pf_\ell$  will of course be increased further by the real part of the source impedance seen by the tuned antenna circuit, and  $pf_r$  will be decreased by the efficiency of coupling to the tuned circuit. The reader is referred to Wheeler<sup>(3)</sup> for a more detailed presentation and for sample efficiency calculations for some specific antenna types.

## 6. Effective Volume

Wheeler also presents the extremely useful concepts of antenna effective volume,  $V'$ , and the volume of what he denotes as a "radian sphere,"  $V_s$ , or a "radian cube,"  $V_c$ .  $V'$  is the physical volume of the antenna multiplied by a shape factor greater than unity,  $k_e$  for electric dipole-type antennas and  $k_m$  for magnetic dipole-type (loop) antennas, as depicted in Figure 3-2 from Wheeler.<sup>(4)</sup> The shape factors are defined to have values such that the indicated inductance and capacitance formulas give the correct values of  $L$  and  $C$  for specific antenna geometries of interest.<sup>(3,4)</sup>  $V_s$  is the volume of a sphere of radius equal to one radian length, namely  $\frac{\lambda}{2\pi}$ , and  $V_c$  is the volume of a cube with side dimensions of one radian length  $\frac{\lambda}{2\pi}$ . It has been shown<sup>(1,8)</sup> that the radiated power in the far field of an electrically small ( $d < \frac{\lambda}{10}$ ) antenna of either type is accompanied by stored energy which is mostly located in the antenna near field within the radian sphere.





Source: Reference 4,

**FIGURE 3-2 EFFECTIVE VOLUMES AND RADIATION POWER FACTORS FOR ELECTRICALLY SMALL ANTENNAS**

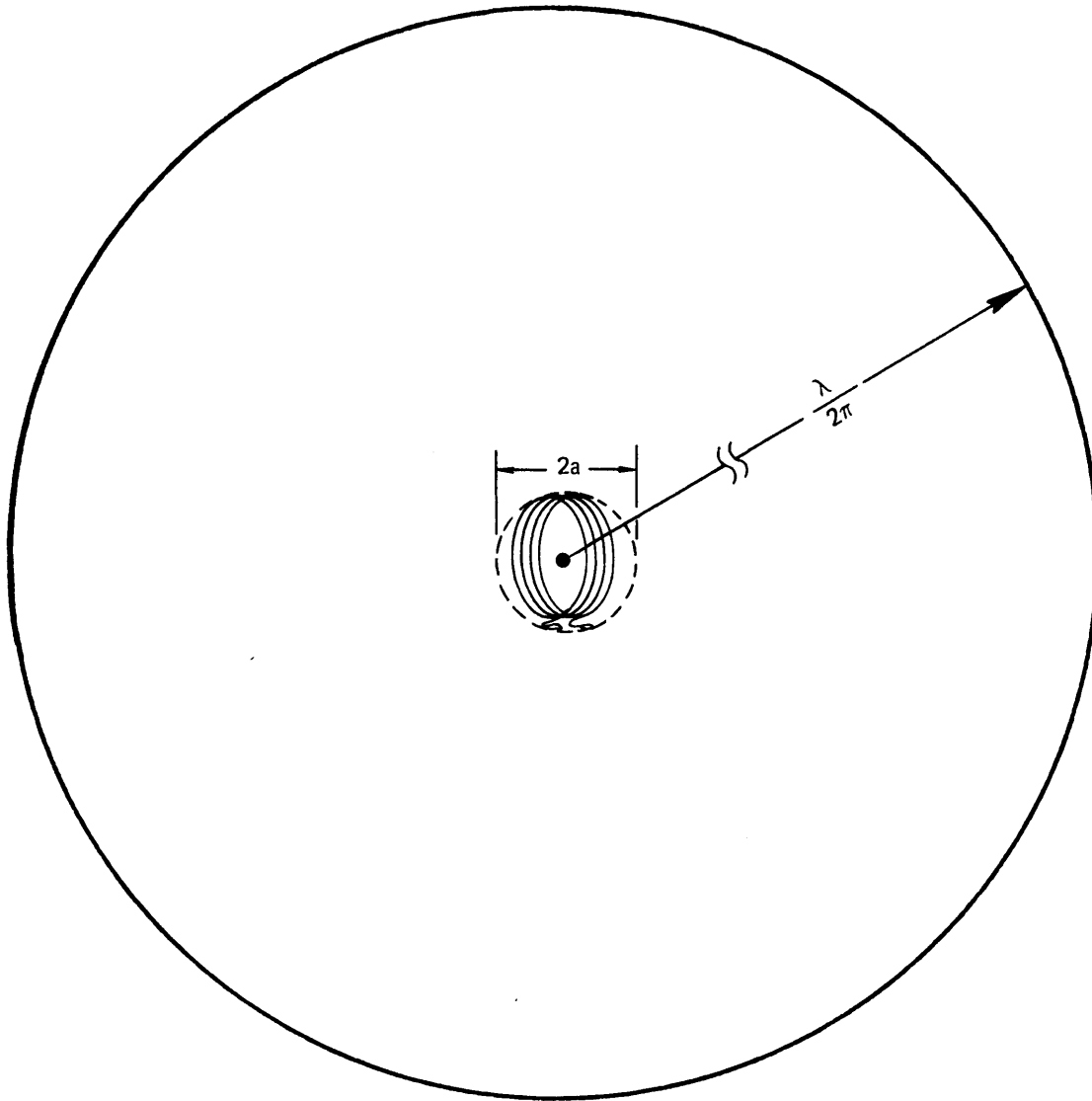
Furthermore, the radiation power factor,  $pf_r$ , which is the ratio of this radiated power to  $\omega$  times the stored energy, is found to be proportional to the ratio of the antenna's effective volume  $V'$  and the volume of either the radian sphere  $V_s$  or radian cube  $V_c$ . Namely,

$$pf_r = \frac{2}{9} \frac{V'}{V_s}, \quad pf_r = \frac{1}{6\pi} \frac{V'}{V_c}. \quad (7,8)$$

These expressions allow a very convenient and rapid method of computing the radiation power factor (together with the Q and radiation resistance) and comparing it with the circuit ohmic loss power factor to determine the efficiency of the tuned antenna.

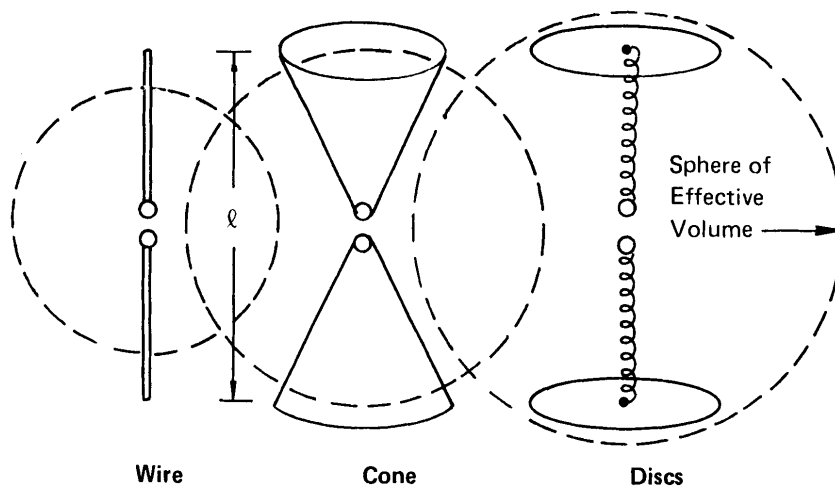
Figure 3-3 illustrates how well the volumetric comparison method allows a quick grasp of the fundamental limitations imposed by antenna size alone on the radiation power factor, the Q, and the radiation resistance. Figure 3-4 depicts comparative examples<sup>(4)</sup> of the effective volumes of several common dipole and loop antenna types. The figure reveals that long and thin electric dipoles occupy a much larger effective volume than the volume of the physical conductors. Note also that the effective volume of a multiturn "flat" square loop is not much different from that of a corresponding single turn loop, and that the effective volume for both is approximately given by the volume of a sphere of diameter equal to the side dimension of the loops. It can also be shown<sup>(3,4)</sup> that short, flat air-core loops provide a much larger effective volume than long, thin, solenoid-type air-core loops of comparable maximum dimensions. The converse is true for electric dipole antennas; namely, the long thin type provides a better volume utilization than a short capacitor-plate type.

An exception to this rule is the loop antenna loaded with a long thin high-permeability core as depicted in Figure 3-4. In this case the loop's effective volume is similar to that for a comparably-sized long thin dipole, where the loop dimensions now include those of the core; namely, the thin dipole antenna shape factor applies in computing the effective volume. Thus, in some applications a core-loaded loop may offer shape advantages that outweigh the somewhat greater

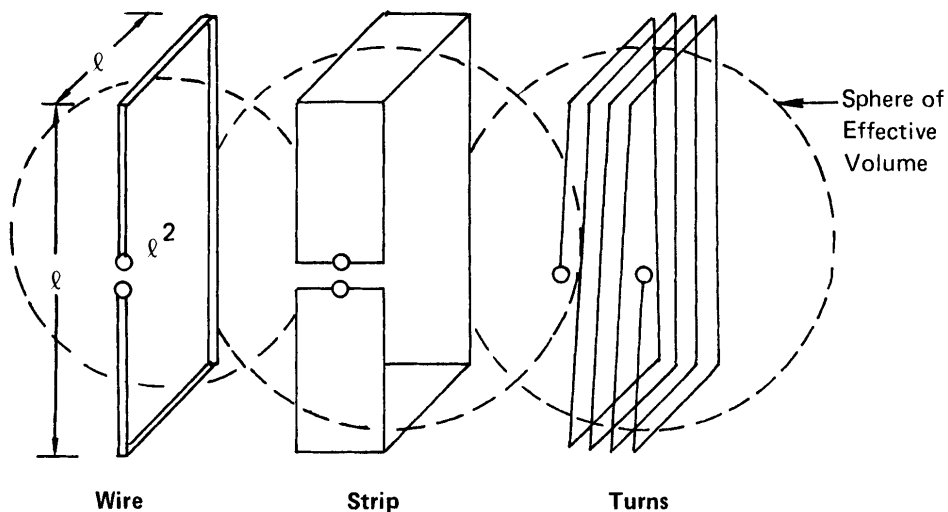


Source: Arthur D. Little, Inc.

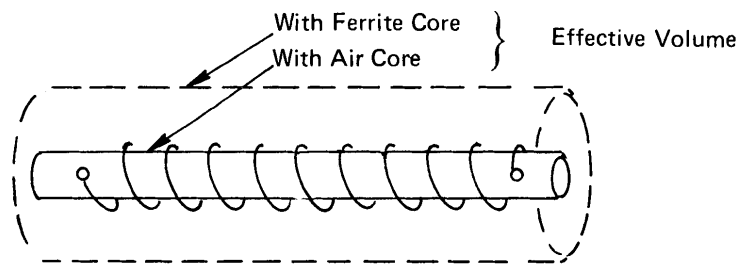
**FIGURE 3-3 ILLUSTRATION OF RADIATION POWER FACTOR LIMITATIONS  
IMPOSED BY ANTENNA EFFECTIVE VOLUME RELATIVE TO  
VOLUME OF A RADIAN SPHERE**



(a) Dipoles



(b) Loops



(c) Air And Ferrite Core Loops

Source: Reference 4.

FIGURE 3-4 COMPARATIVE EXAMPLES OF THE EFFECTIVE VOLUMES OF SEVERAL COMMON ANTENNA TYPES

effective volume offered by a flat air-core loop of equal maximum dimension. Additional limitations imposed by the properties of the core material must, of course, also be considered in practice. The opposite behavior is experienced by electric antennas loaded with dielectric material; namely, the effective volume is reduced by the presence of the material.

Applying this effective volume method to either a thin electric dipole or flat air core loop of maximum dimensions  $d = 0.5$  m gives a radiation power factor and  $Q_r$  on the order of  $10^{-9}$  and  $10^9$  respectively. Taking the ratio of  $Q_r$  to a practical tuning circuit  $Q_{lr}$  of 100 results in a negligible radiation efficiency of 0.00001%.

#### 7. Application Implications

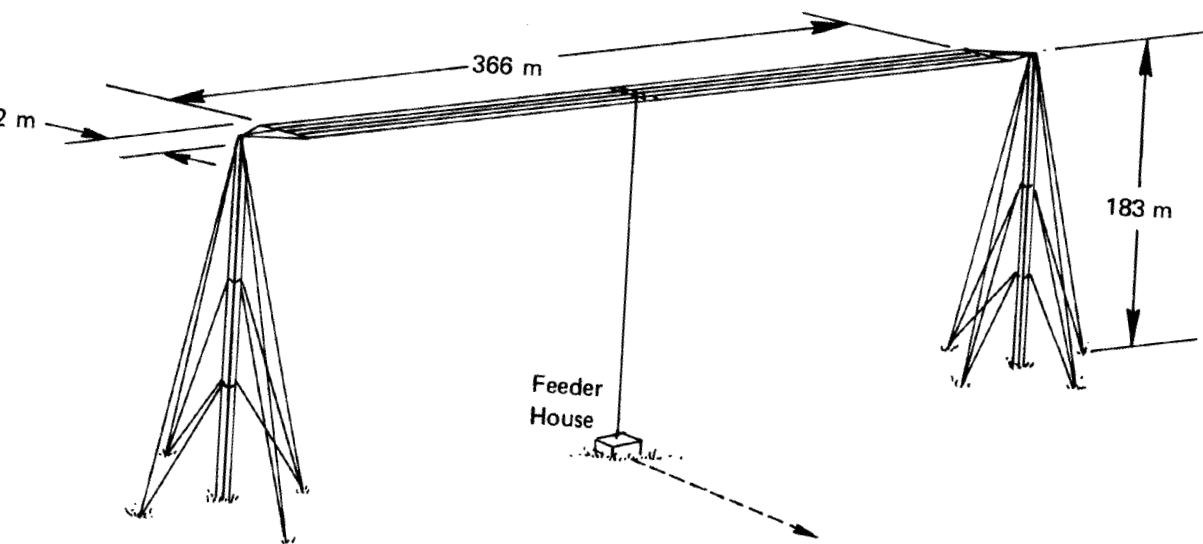
The above described fundamental limitations imposed on electrically small antennas are severe. Thus, it is not surprising that portable two-way radio systems for most conventional applications on the surface are designed to operate at frequencies in the VHF and UHF bands and to a lesser extent in the HF band, bands in which wavelengths become less than, or comparable to, the size of a person. However, the HF band, with the exception of some military applications, is still by and large mainly utilized for radio communication between either fixed stations or sizable mobile platforms such as ships, planes, and motorized vehicles, which can accommodate larger antennas than people can. Even man-carried HF military transceivers, such as the PRC-74, need to utilize clumsy inductively loaded whips about 2 meters long.<sup>(9)</sup> However, the efficiency of even optimally loaded 2 meter whips falls off rapidly at the low end of the HF band when the whip becomes less than about  $0.05 \lambda$ .<sup>(10)</sup>

Below HF the problems get rapidly worse, even for fixed station transmitters. To achieve reasonable efficiencies, the ability to construct large, low loss antenna structures tuned by large low loss circuit elements becomes important. The tall radio towers used by AM broadcast stations in the MF band are perhaps some of the more familiar examples.<sup>(11)</sup> At LF the problem worsens and the antenna structures and tuning circuits get larger and more difficult to

design,<sup>(11,12)</sup> such as the one shown in Figure 3-5. At VLF the antennas become huge structures which stretch the state-of-the-art of both electrical and structural design technologies in order to achieve high efficiencies.<sup>(6,11,4,13)</sup> Thus, VLF transmissions between fixed and mobile stations are generally one way, by necessity.

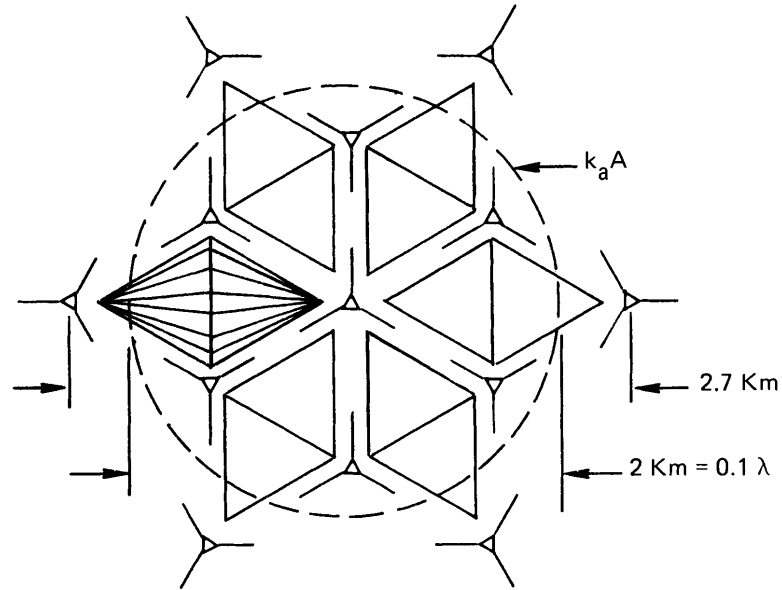
Two Navy VLF transmitters, one at Cutler, Maine,<sup>(6)</sup> and the other at Northwest Cape, Australia,<sup>(6,4)</sup> represent extreme examples in that they are the largest antennas in the world and yet still fall within the defined limits of electrically small antennas. Figure 3-6 depicts plan and elevation drawings of the Australian antenna installation,<sup>(4)</sup> which is over 1000 feet high, more than 1.5 miles in diameter, and operates at a frequency of about 15 kHz ( $\lambda = 20$  km) at an efficiency greater than 50% (the Cutler, Maine, installation is greater than 80% efficient). It is basically a vertical electric monopole (whip) antenna over an extensive man-made ground plane. It is heavily top-loaded with diamond-shaped cable grids to increase the antenna capacitance and provide a uniform vertical current distribution. These antennas are good examples of the extreme measures required at VLF to get high efficiency operation. For a comprehensive treatment of VLF radio systems in general and antenna system design problems in particular, the reader is referred to the text by Watt.<sup>(6)</sup>

To attain the Navy's overall system objective of very long (global-type) ranges, which at VLF takes a megawatt of radiated power, the option of throwing away high multiples of this radiated power into an inefficient antenna system is not available to the designers. As shown in Section III.B.3 of this chapter, high efficiency requires the radiation resistance to be on the order of, and preferably greater than, all ohmic losses in the antenna structure and tuning and matching networks. To accomplish this at VLF requires as great a physical height as practically possible together with extensive top loading to increase the antenna's effective height, and thus the radiation resistance. It also requires the difficult and specialized design of the antenna structure, tuning elements, and ground plane<sup>(6,11,12)</sup> to reduce all possible ohmic losses to on the order of 0.1 ohm, the approximate value of the radiation resistance.

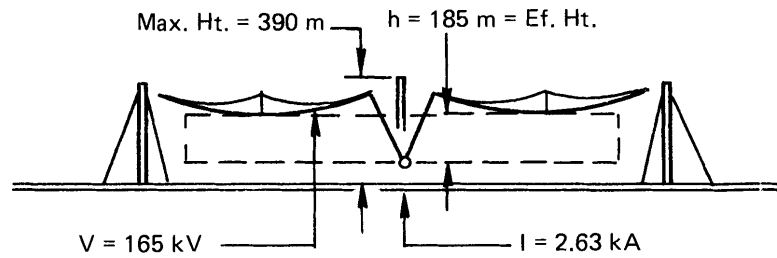


Source: Reference 12.

FIGURE 3-5 EXAMPLE OF AN LF BAND T - ANTENNA



(a) Plan View



$f = 15.5 \text{ kHz}$	$\lambda = 19.3 \text{ Km}$
$R_r = 0.144 \text{ ohm}$	$X = 63 \text{ ohms}$
$P_r = 1 \text{ MW}$	$VI = 435 \text{ MVA}$
$pf_r = .0023$	

(b) Elevation View

Source: Reference 4.

**FIGURE 3-6 EXAMPLE OF STATE-OF-THE-ART  
LARGE VLF ANTENNA IN NORTHWEST CAPE AUSTRALIA**



Since the antenna is still small electrically, it still behaves basically as an energy storage element having high reactance (63 ohm) compared to its radiation resistance (0.14 ohm). It therefore has a high intrinsic Q and narrow intrinsic bandwidth. One of the prices of achieving a high efficiency, by keeping the total ohmic resistance comparable to the low radiation resistance, is the antenna's narrow resonance bandwidth of about 130 Hz at 15 kHz. This is accompanied by huge amounts of reactive power, 435 MVA, 2.63 KA at 165 KV, which the antenna and tuning element structures must also accommodate, in addition to the real input power of 2 MW into about 0.3 ohm, 1 MW of which gets radiated.

The narrow bandwidths imposed by high efficiency VLF antenna systems constrain such systems to coded data-type communications instead of voice. In the Navy VLF submarine communications application this affects the maximum allowable bit rate of transmission, which is not considered an unacceptable limitation. In a mine wireless radio voice communications application the high-Q, narrow bandwidth problem is a severe one, and of course unacceptable. The mine wireless application **requires at least about 2.5 kHz of bandwidth for a single-sideband system and about 12 kHz for a conventional narrowband FM system.** Thus, **the transmit antenna size constraint for portable mine wireless voice communication applications, together with the system bandwidth required, make a goal of high radiation efficiency not only unattainable, but also undesirable for the VLF, LF, and even MF, radio bands from 10 kHz to 1000 kHz.**

#### 8. Impact of Conducting Media

When electrically small antennas are immersed in a conducting medium as in the case of the mine wireless application, additional factors come into play which dominate the choice of methods and antennas to optimize radio system performance. First and foremost is the severe signal attenuation introduced by the resistive losses experienced by the waves in the conducting medium. The conductivity of the medium introduces power dissipation external to the antenna conductors. This reduces both the radiated and reactive fields and

powers that would be present in a free space medium, thereby greatly reducing the attainable communication range. This effect is well depicted in Figure 2-1 in the preceding chapter. Furthermore, the free space definitions of radiation resistance and radiated power are no longer meaningful measures of performance or antenna efficiency. The so-called radiated power is no longer a fixed value independent of distance in the antenna far field, and the radiation resistance is no longer a measure of the input power coupled to or consumed by the medium external to the antenna.

Limitations imposed by signal attenuation and representative mine development practices have led to the relatively modest range goal of 1350 feet for the portable, or mine wireless system, a range which falls well within the free space near field region, and by and large, within the induction field region in a coal mine conducting medium. Consequently, the mine wireless communication situation is reduced to a near and induction field coupling problem between two loosely coupled and mobile electromagnetic field transducers (antennas) embedded in a lossy medium. Thus, the choice of antenna for the portable mine wireless application will not be based on its radiation efficiency, but on:

- the overall power utilization efficiency of the transmitter-antenna system in producing the largest usable signal strength at the desired range, and
- the overall practicality of its implementation with regard to overall system size, weight, convenience, and mine worthiness for the roving miner application.

Before proceeding to the discussion of specific antenna types in the following section, we compare the behavior of the received signals produced by the principal field components of electrically small loop and dipole transmit antennas embedded in a conducting medium. The portable antennas retain their electrically small classification because the reduced wavelength (defined as  $\lambda = 2\pi \times$  skin depth in the conducting medium) remains much greater than the antenna size for the frequencies and conductivities of interest. Equations for the  $E_{\theta}$  and  $H_{\theta}$  field

components produced by ideal infinitesimal electric and magnetic dipole sources, respectively, are used to compare the loop-to-loop response with the dipole-to-dipole response. The field component equations apply for the condition  $\sigma \gg \omega\epsilon$ , which generally applies throughout the frequency band and range of conductivities of interest for the portable mine wireless application.

$$\text{For dipoles: } E_{\theta} = \frac{Ih}{4\pi r^3 \sigma} (1 + \gamma r + \gamma^2 r^2) e^{-\gamma r} \sin\theta \quad (9)$$

$$\text{For loops: } H_{\theta} = \frac{NIA}{4\pi r^3} (1 + \gamma r + \gamma^2 r^2) e^{-\gamma r} \sin\theta \quad (10)$$

$$\text{where } \gamma^2 = j\omega\mu\sigma - \omega^2\epsilon\mu \approx j\omega\mu\sigma.$$

The equations are for z-axis oriented infinitesimal dipole and loop antenna elements, <sup>(14)</sup> and I is the uniform current in the antenna elements. The equations apply for a loop fully insulated from the medium, and a dipole insulated along its length but grounded to the medium at each end of the dipole. h is the length of the dipole element, A is the area of the current loop, and N is the number of turns in the loop.

Taking the ratio of the open circuit output voltage induced in the receive antenna of each pair of like antennas (i.e., dipole-dipole, loop-loop), we get the comparison factor

$$F_{d,\ell} = \frac{V_{oc}(\text{dipoles})}{V_{oc}(\text{loops})} = \frac{I_d h^2}{N^2 I_{\ell} A^2 \omega\mu\sigma} \quad (11)$$

Substituting into (11) the representative values of  $h = 0.5$  m,  $A = 0.2$  m<sup>2</sup> based on a 0.5 m loop diameter,  $N = 10$  turns,  $\mu = \mu_0 = 4\pi \times 10^{-7}$  h/m, conductivity  $\sigma = 10^{-2}$  mho/m, and frequency  $f = 300$  kHz, we find that  $F_{d,\ell}$  reduces to

$$F_{d,\ell} = \left( \frac{I_d}{I_{\ell}} \right) \quad (12)$$

Therefore, it becomes apparent that based on this measure of performance for antennas in a conducting medium, the advantage enjoyed by the dipole over the loop in free space does not apply in a conducting medium. A

similar conclusion was reached by investigators<sup>(15,16)</sup> at the University of Innsbruck in Austria during the course of a VLF through-the-earth communications project funded by the U. S. Air Force. Furthermore, when the difficulty of driving the antennas to obtain the required currents  $I_d$  and  $I_\ell$  is also factored into this comparison equation, **the loop antenna is clearly seen to be the most favorable antenna.**

For example, the resonant impedance of a tuned loop having a bandwidth of 12 kHz at 300 kHz is about 10 ohms, whereas the practical grounded dipole source is faced with the spreading resistance of its two ground connections to the medium. These two connections can take on values greater than 200 ohms, based on a simple 0.5 m ground rod termination at each end of the dipole in a medium having  $\sigma = 10^{-2}$  mho/m. If both antennas are driven by the same voltage, the resultant performance factor  $F_{d,\ell}$  is given by:

$$F_{d,\ell} = \frac{h^2}{N^2 A^2 \omega \mu \sigma} \left( \frac{Z_\ell}{Z_d} \right) . \quad (13)$$

Substituting the above parameter values, and taking into account the increase in the effective length of the dipole antenna caused by the insulated ground rod terminations, we find that  $F_{d,\ell} \approx 0.1$ . Since the medium conductivity  $\sigma$  also appears in the numerator of  $F_{d,\ell}$  when  $Z_d$  is the spreading resistance of ground rods, this performance comparison should remain insensitive to the conductivity of the medium for the conductivities and frequency band of interest. The lower resonant impedance of the loop will also allow better receiver utilization of the induced open circuit voltage. Thus, the loop exhibits a clear performance advantage over a typical grounded-dipole antenna.

The advantage of the loop becomes greater when compared to a whip-type dipole antenna,<sup>(6)</sup> which would be the practical choice over the grounded dipole for a roving miner's portable radio. This whip would be a completely insulated antenna not grounded to the medium at each end. The impedance of this antenna worn by a miner standing in a tunnel will be a high capacitive reactance instead of the modest resistance of the grounded dipole. The spatial coupling to the surrounding medium would also be reduced.

Examining the impact of the input impedance change, we find that the capacitance represented by the short whip worn on a person is very low (approximately 10 pf), and subject to large variations<sup>(17,18)</sup> due to "stray" capacitances such as those introduced by the whip's variable proximity to the body and mine environment and by the large tuning coils required to resonate such a small capacitance at 300 kHz. This situation typically requires that a lumped capacitance much larger than the antenna capacitance be placed in parallel with the antenna, to allow the use of a practically sized tuning inductor at 300 kHz, and to prevent changes in the resonant frequency caused by variations in the effective antenna capacitance. This lower reactance shunt path will divert most of the tuned circuit current into the large shunt capacitor instead of the high reactance antenna. Antenna current reductions of 100 to 1 are not uncommon, thereby putting the short whip-type dipole antenna at a considerable practical disadvantage for the present roving miner application. The following sections of this chapter discuss the feasibility and potential utility of specific antenna types.

### C. PORTABLE MANPACK ANTENNAS

#### 1. Conventional Whip Antennas

The objective for the portable mine wireless application is to obtain an antenna that is not only effective but small, rugged, and convenient for a miner to wear. Electric dipoles or whip antennas fail to meet this objective in all respects at the desired operating frequencies in the mine environment. Therefore, only a brief review of some of the major shortcomings is given below.

The size, convenience, and ruggedness problem can be appreciated by comparison with HF band manpack hardware used for tactical radio communications by the military, a user which generally attempts to optimize the same characteristics of concern to a mine wireless application. A case in point is the PRC-74 transceiver which requires a 6-foot, inductively loaded whip to achieve reasonable performance on the surface over most of the HF band.<sup>(9)</sup> However, the performance of even such whips, with inductive loading optimally placed about 0.4 of

the way up the whip, falls off rapidly below about 6 MHz when the whip becomes less than  $0.05 \lambda$ .<sup>(10)</sup> A semi-flexible whip structure of this type and length is totally incompatible with underground roving miner mine wireless applications. The military also considers it highly inconvenient, particularly so in jungles, but tolerates it because of the practical necessities of tactical military communications on the surface. The magnitude of the problem of course becomes much more severe at frequencies in the MF and lower bands of interest for mine wireless radio, particularly when a miner is likely to consider even a 25 cm whip unreasonable.

Whip effectiveness with respect to signal strength produced in a conducting medium and the ease of generating such a signal from a practical transmitter is also poor. The previous section of this chapter showed that ideal loop antennas are more effective than ideal grounded-dipole antennas in a conducting medium at the operating frequencies of interest. The problems and performance associated with whips rapidly worsen for portable manpack applications, making loop antennas the clear choice for portable mine wireless applications.

As mentioned briefly in Section III.B.8 an ideal electrically small whip of about 1 meter length over a perfect ground plane is characterized by a very small capacitance of approximately 10 pf,<sup>(17)</sup> which results in a very high capacitive reactance at frequencies in the 100 kHz to 1 MHz band. The tuning difficulties imposed by this whip antenna, even in such a simple environment, become apparent by looking at the experience at HF with 6-foot whips; namely, they are nearly impossible to resonate with a practical series lumped inductor below 6 MHz because of the whip's high capacitive reactance.<sup>(17)</sup> For example, a 10 mh inductor is required to resonate a 10 pf capacitor at 300 kHz. The problems worsen when such a whip must be worn on the body of a person in a manpack application. The whip's geometry, and its high capacitive reactance below low band VHF, make the whip's input impedance strongly affected by the whip's closeness to and position on a person's body, and by the person's immediate local environment, his position within it, and his "connection" to it via his feet or other parts of the body.<sup>(17,18,19)</sup>

The practical problems associated with tuning and driving the high and widely variable input impedance of such an antenna configuration become intolerable. Thus, it becomes desirable, if not necessary, in practice to: either set the unit down away from the body and surrounding objects; or incorporate circuit elements that minimize the antenna impedance variations seen by the transmitter and receiver and at the same time simplify the tuning coil design. Only the latter option is operationally allowable for the MF mine wireless application. A typical means of accomplishing this latter option is by adding a large, lumped shunt capacitor in parallel with the whip. This of course shunts a large portion of the transmitter output current away from the whip, leading to the correspondingly large reduction in overall system effectiveness discussed in Section III.B.8.

In summary, problems associated with whip antennas for use in portable manpack applications are not new, nor are they unique to the mine wireless application. They have been and continue to be a source of considerable concern and difficulty at both low band VHF and HF, with the problems becoming particularly acute at the low end of the HF band. Thus, it is not surprising that conventional whip antennas are incompatible with the MF band mine wireless radio application.

## 2. Active Whip Antennas

A moderate amount of attention has been given since the mid-1960's to investigations of the potential advantages of so-called active antennas which incorporate a transistor into the whip antenna structure itself. Investigations have included the frequency range from VLF to UHF, and both receiving and transmitting applications. (20-29)

Receiving applications got most of the attention until the early 1970's when effort devoted to transmit applications was increased. (20,21,22,23,24)

The intent of this section is not to present a detailed explanation and assessment of this work, but to briefly describe and comment on an active transmitting configuration that has been reported (20,21) to offer certain performance advantages over that of a conventional series-tuned whip antenna in the MF band. Our conclusion is that this active antenna configuration does not overcome the considerable disadvantages

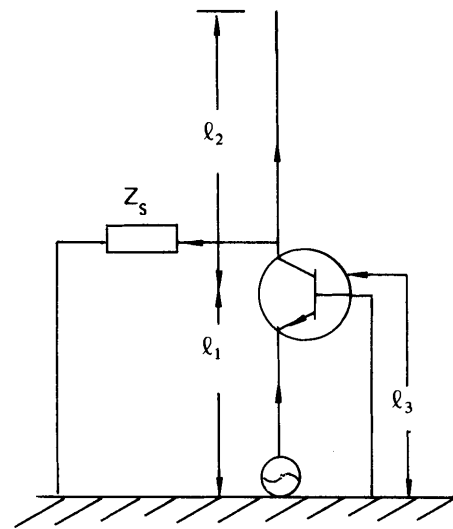
associated with whip-type antennas for portable mine wireless applications, and moreover it is significantly more wasteful of power than the conventional tuned whip.

Figure 3-7 depicts the fed-emitter base loop (FEBL) transmitting antenna configuration which is considered by active antenna investigators<sup>(20,21)</sup> to be favorable for transmitting applications.  $Z_s$  is the collector bias resistor connected to the DC power supply. The optimum transistor position for a transmit application is the one that maximizes the current moment  $Ih$  of the antenna. This occurs for the FEBL configuration of Figure 3-7 when the transistor is at ground plane level<sup>(20)</sup> as shown in Figure 3-8. This transistor position maximizes the collector and emitter currents, and also eliminates radiation field cancellation caused by rf currents flowing in the negative direction in the bias resistor lead. By using a 3000 ohm collector bias resistor of value much less than the antenna capacitive reactance (for  $C_A \approx 7$  pf), the investigators obtain a relatively frequency independent resistive input impedance of about 30 ohms at the emitter-base terminals of a 1 meter long transistorized antenna. Thus, "so-called" resonant operation at a real input impedance is obtained with an electrically short, capacitively reactive antenna without using a tuning inductor. Furthermore, the impedance seen by the transmitter is buffered from variations in antenna reactance caused by the environment and frequency over a wide range in the MF and HF bands.

However, the bias resistor in parallel with the whip antenna's high capacitive reactance provides a low impedance shunt path for the collector current as shown in the equivalent circuit of Figure 3-9a, thereby diverting most of the available current away from the antenna as in the case of capacitance shunting of conventional whips discussed previously. In addition, this shunting resistor greatly increases the power dissipation of the total antenna circuit over that required to produce the same antenna current in a series-tuned antenna equivalent circuit of Figure 3-9b.

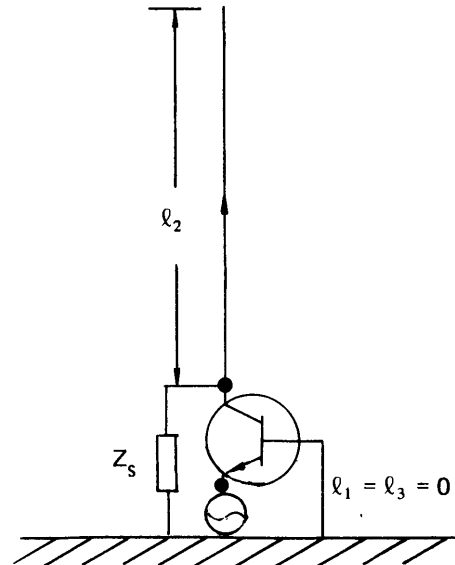
In reference (20), the above described active antenna configuration is compared at a frequency of 1.24 MHz with a series-tuned antenna





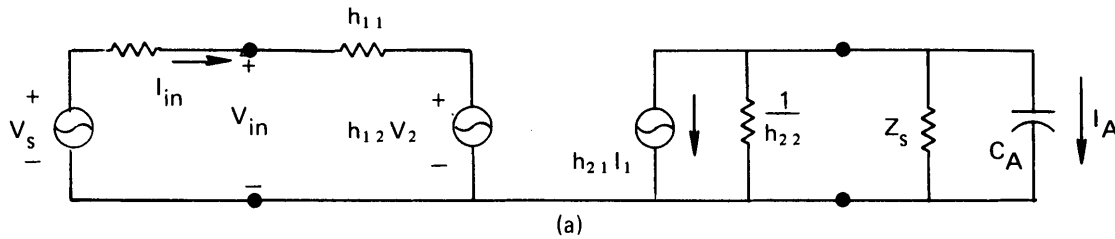
Source: Reference 20.

**FIGURE 3-7 ACTIVE TRANSMIT ANTENNA FEBL CONFIGURATION**



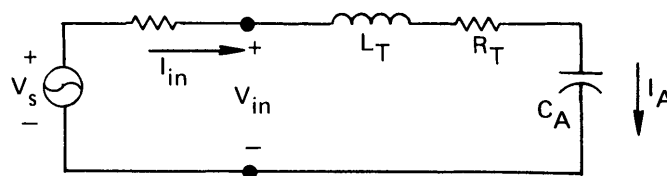
Source: Reference 20.

**FIGURE 3-8 FEBL CONFIGURATION FOR MAXIMIZING ANTENNA CURRENT MOMENT**



(a)

Equivalent Circuit For FEBL Transmit Configuration Of Figure 3-8



(b)

Equivalent Circuit For Series Tuned Conventional Whip  
Source: Arthur D. Little, Inc.

**FIGURE 3-9 EQUIVALENT CIRCUITS**

circuit having a Q of about 120 (10 kHz bandwidth). By neglecting the power dissipated in the bias resistor, the active antenna is shown to exhibit a "so-called" power gain disadvantage of about 9 dB compared to the tuned antenna circuit. If account is also taken of the power dissipated in the bias resistor, this disadvantage increases considerably to about 27 dB; namely, the active whip antenna dissipates at least 27 dB more power than an equivalent series-tuned whip antenna.

Finally, the antenna current values obtained from the active antenna configuration examined in reference (20) are characteristic of the levels obtainable from a 12 volt battery suitable for a miner's portable radio. These values of 0.4 ma at 1.2 MHz and 0.1 ma at 300 kHz are clearly inadequate, except perhaps for extremely short range, near-field applications in free space. Thus, although active antennas may offer certain performance advantages over conventional whips in some applications, they offer no practical benefits as transmit antennas for MF portable mine wireless radios.

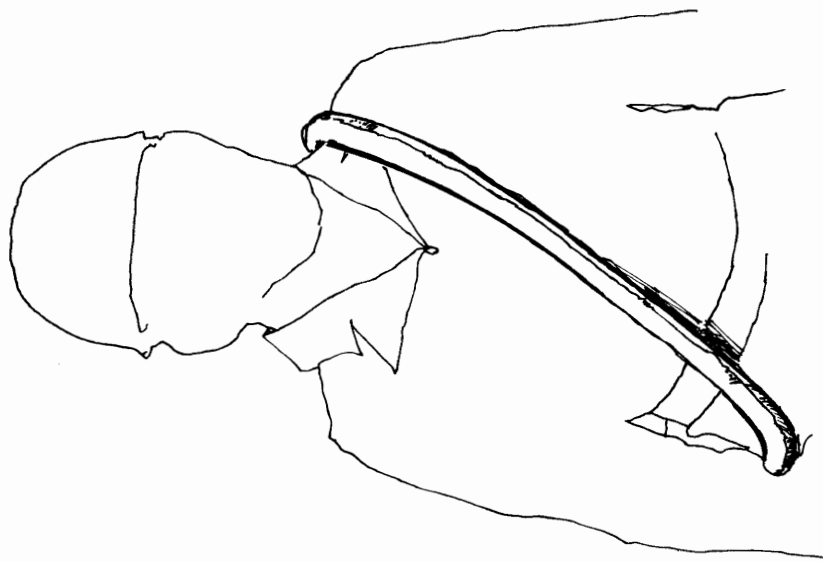
### 3. Conventional Loop Antennas

Conventional air-core loop antennas represent one of the most suitable and effective choices for the MF mine wireless roving miner application. Thus, it is not surprising that the South Africans (30,31) and the British (32,33,34,35) have adopted the use of such antennas for rescue type, portable MF band communications in mining and fire fighting applications respectively. Similar developments are also occurring within the U. S. coal mining community. (36,37,38,39,40) However, the state-of-the-art is such that, even with such loops, a completely wireless range goal of 1350 feet in coal mines is likely to be attainable only in the most favorable mine environments (41,42,43) (see Chapter II). On the other hand, ranges on the order of 1 - 3 km have been reported (30, 31,35,36,40,44,45) when such loop antennas are employed in the vicinity of mine electrical conductors (see Chapter IV for representative calculations).

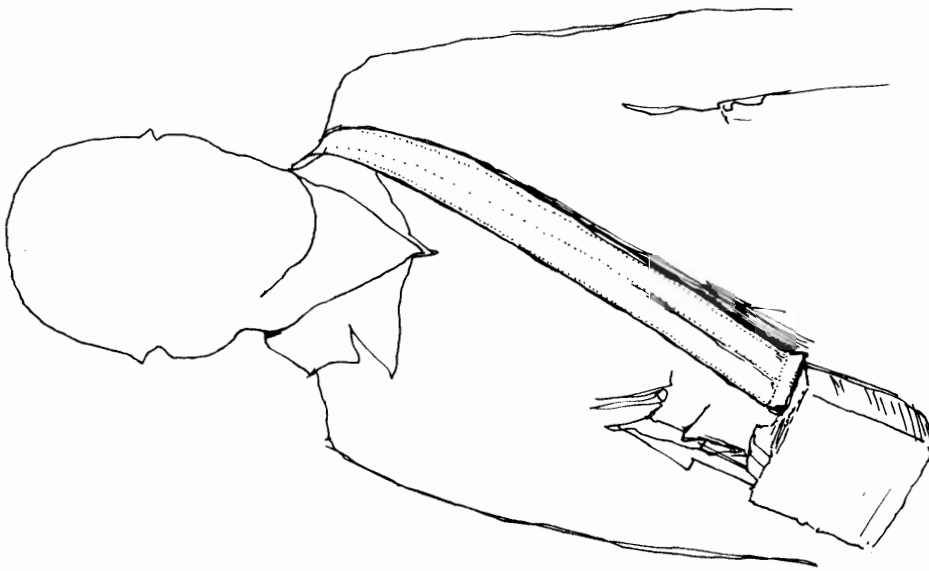
The conventional loop antenna has a large number of positive attributes for roving miner applications. At the low frequencies of interest it is an inductively reactive device whose magnetic fields

and input impedance remain, for all practical purposes, unaffected by its location on and closeness to the body of a person, and also by the local mine environment. The stray capacitance problems associated with whip antennas are avoided. The moderate inductive reactance of a typical loop configuration, having on the order of 10 turns, can be easily tuned by readily available practical capacitors in the MF band. The loop can be readily formed into a lightweight, rigid or flexible, bandolier shape. This allows the area of the loop, and therefore the transmit magnetic moment, to be maximized within a form factor that can be tailored to protect the loop from damage while providing the least inconvenience to the miner wearing it. Some examples of current designs are presented below.

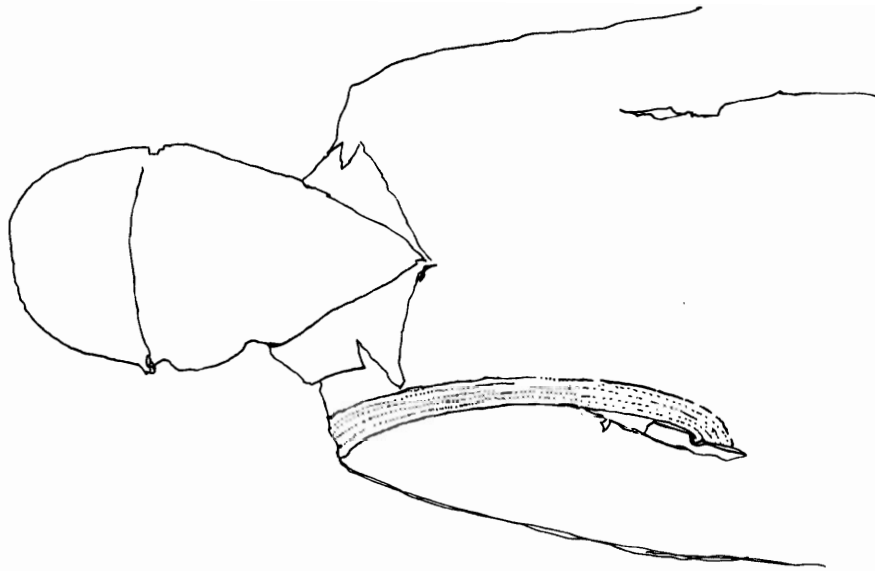
Rigid units like the tubular elliptically shaped bandoliers depicted in Figure 3-10a are used with the South African radio<sup>(30)</sup> (SAR) at 335 kHz and the Collins Radio mine wireless radio prototypes<sup>(37)</sup> at 520 kHz. They provide the advantage of a fixed area, and therefore fixed transmit moment and loop inductance, but the disadvantage of somewhat greater awkwardness than flexible bandolier configurations. Representative flexible units include: the strap-type depicted in Figure 3-10b used by Plessey in its Inductorfone TGR.1 unit<sup>(35)</sup> at 140 kHz and by Lee Engineering Division of Consolidation Coal Co. in prototype units<sup>(36)</sup> at 425 kHz, and garment-type depicted in Figure 3-10c where the turns (typically stranded wire) are sewn in the desired shape into the person's work uniform or into a specially designed jacket or pull-over worn by the radio-equipped person. **For example, the Plessey #PRD2200 unit used by firefighters in large buildings at 2.5 to 3.5 MHz is incorporated into a special jerkin,<sup>(33)</sup> whereas one of the Lee Engineering prototype units<sup>(36)</sup> at 425 kHz has the loop sewn into a pair of miner's coveralls approximately as shown in Figure 3-10c. The Russians<sup>(45)</sup> have also made use of loop antennas, in a hand-carried configuration, for mine radio communications at 78 kHz. The loop orientation which results from wearing a bandolier type of antenna (i.e., in a nearly vertical plane) also closely approximates the ideal orientation for coupling to the quasi-TEM mode of propagation in the**



a. Rigid Oval Tubular Type



b. Flexible Strap Type



c. Garment Type

Source: References 30, 35, 36, 37 and Arthur D. Little, Inc.

FIGURE 3-10 SKETCHES OF SEVERAL BANDOLIER LOOP ANTENNA CONFIGURATIONS

coal seam waveguide (see Figure 2-6). The following paragraphs are devoted to examining some design guidelines and performance limits of such antennas for a portable mine wireless radio application.

The first design objective is to generate the largest practical antenna magnetic moment within the constraints imposed by intrinsic safety, reasonableness of size and form factor for wear by a miner, and practical tuning and matching elements. The second and equally important design objective is to produce this magnetic moment by the most efficient use of the energy stored in the battery of the portable unit. The first objective affects the maximum attainable range, while the second affects the maximum allowable operating time between battery recharges, or conversely, the minimum size battery required to obtain the minimum desired operating time (such as a normal work shift). Furthermore, the signal attenuation and electromagnetic noise encountered in typical coal mines is so severe that attempts to achieve small-to-moderate increases in transmit magnetic moment, at the expense of overall transmitter efficiency or power dissipation, are generally not warranted. In a roving miner application, it is better to have a smaller, lighter-weight, longer-lasting unit that has a somewhat shorter range than a unit that has 100 - 200 feet greater range under some highly favorable mine conditions, but is too heavy and bulky for the miner to wear, or has too short an operating time between recharges.

**The transmit moment is maximized by maximizing the product  $M = NIA$  of the loop, where N is the number of turns, I is the current flowing in the turns, and A is the area enclosed by the turns of wire.** The maximum reasonable loop area for a roving miner application is about  $0.25 \text{ m}^2$ . Both the SAR and the Collins Radio prototype MF units<sup>(30,37)</sup> use a rigid tubular elliptically shaped bandolier (SAR -  $0.66 \text{ m} \times 0.42 \text{ m}$ , Collins Radio -  $0.61 \text{ m} \times .47 \text{ m}$ , 2 ft. x 1 ft.) having an area about  $0.22 \text{ m}^2$ . The Lee Engineering units<sup>(36)</sup> use a strap-type bandolier of dimensions  $0.56 \text{ m} \times .33 \text{ m}$ , and a garment-sewn circular loop having the same perimeter as the elliptical strap unit and an area of about  $0.15 \text{ m}^2$ .

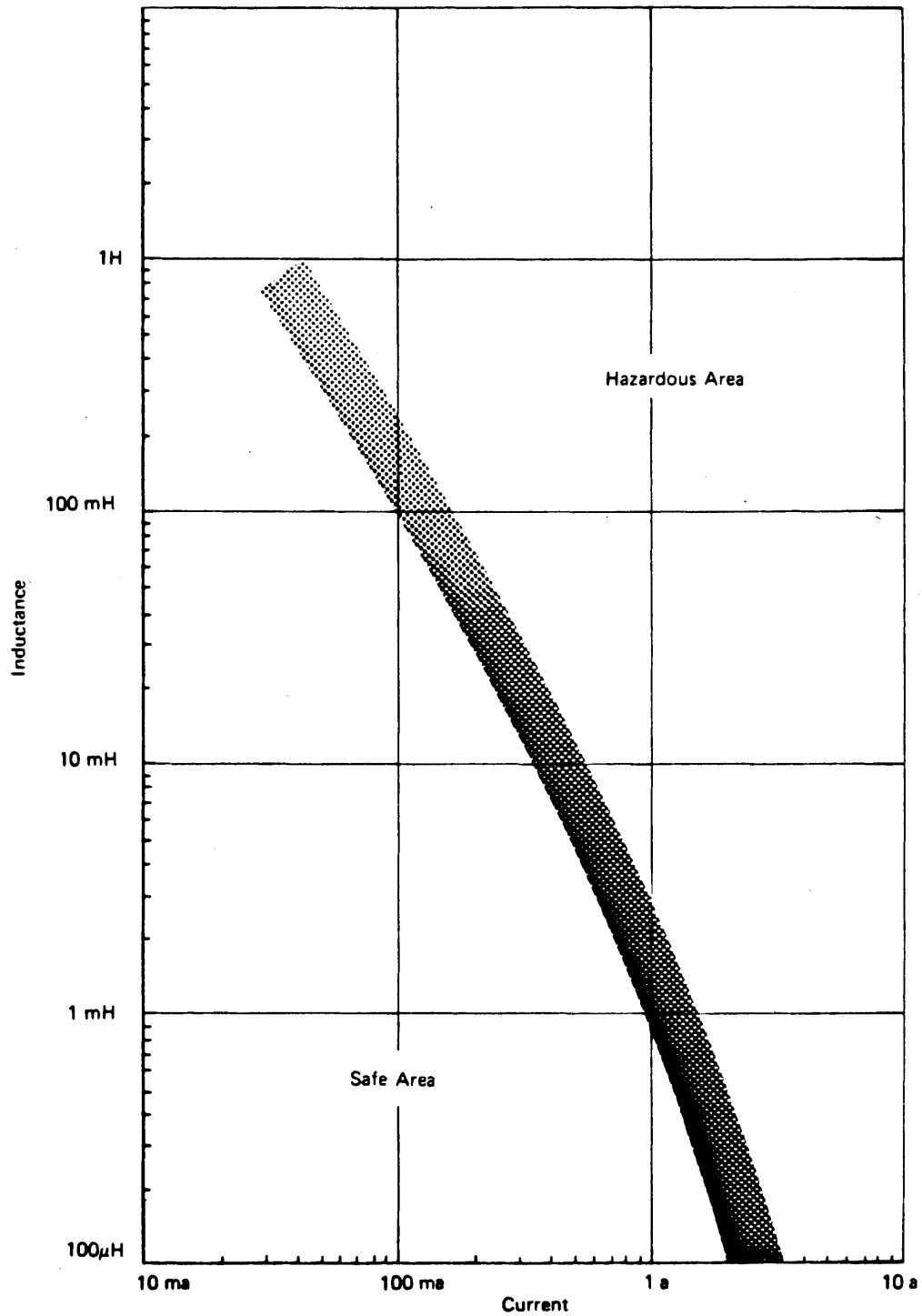
A practical number of turns appears to be in the 5 to 15 turn range (SAR and Collins - 7 turns, Lee Engineering - 12 turns). The inductance of an air-core loop having a diameter  $d$  and a single layer winding of width  $w$  is given by the equation

$$L = kA^{1/2}N^2 \text{ microhenries} \quad (14)$$

from Watt,<sup>(6)</sup> where  $A$  is the loop area in square meters,  $N$  is the number of turns, and  $k$  is the inductance form factor which depends on the ratio of  $d/w$ .  $k$  is a slowly changing function for the  $d/w$  range of present interest, varying from a value of about 1.8 for  $d/w = 5$  to a value of about 3.6 for  $d/w = 50$ . Thus, a loop having an area  $A = 0.25 \text{ m}^2$ , 10 turns, and an effective  $d/w$  ratio of about 25 ( $k = 3$ ) results in an inductance of about 150  $\mu\text{h}$ , which can be easily series-tuned with practical capacitor values on the order of 1000 pf in the 300 - 500 kHz frequency band. Reducing the turns to 7 gives about 75  $\mu\text{h}$ , which is close to the measured values of 60  $\mu\text{h}$  and 82  $\mu\text{h}$  for the SAR and Collins loop antennas, respectively. Thus, the capacitor values required for tuning increase accordingly to between 1000 pf and 5000 pf, depending on the inductance value and operating frequency.

A bandwidth of 12 kHz in the 300 to 500 kHz band requires a  $Q$  of 25 to 42 respectively. For a series-tuned 8-turn,  $0.25 \text{ m}^2$ , loop of nominal 100  $\mu\text{h}$  inductance, this means a real impedance level of 7.5 ohms at the resonant operating frequency. Thus, an rms loop current on the order of 1 ampere is obtainable from a transmitter operating from a 12 volt battery supply. A double totem pole, class D, transistor bridge output stage is one example of a highly efficient way to utilize the full battery voltage on both positive and negative half cycles. This allows the generation of a practical rms transmit moment,  $M = NIA$ , of about  $2 \text{ amp-m}^2$ , a value nearly equal to that of the Collins Radio prototype unit, and slightly higher than the moment of the SAR unit.

The intrinsic safety curve shown in Figure 3-11<sup>(46,47,48)</sup> is based on the findings of the Mining Enforcement and Safety Administration (MESA) for DC inductive circuits. It reveals that for an inductance of 100  $\mu\text{h}$  the rms current of 1 ampere is already close to the band



Source: Ref. 46.

**FIGURE 3-11** MINIMUM IGNITING CURRENT AS A FUNCTION OF AN INDUCTIVE CIRCUIT FOR AN 8.3% METHANE/AIR MIXTURE

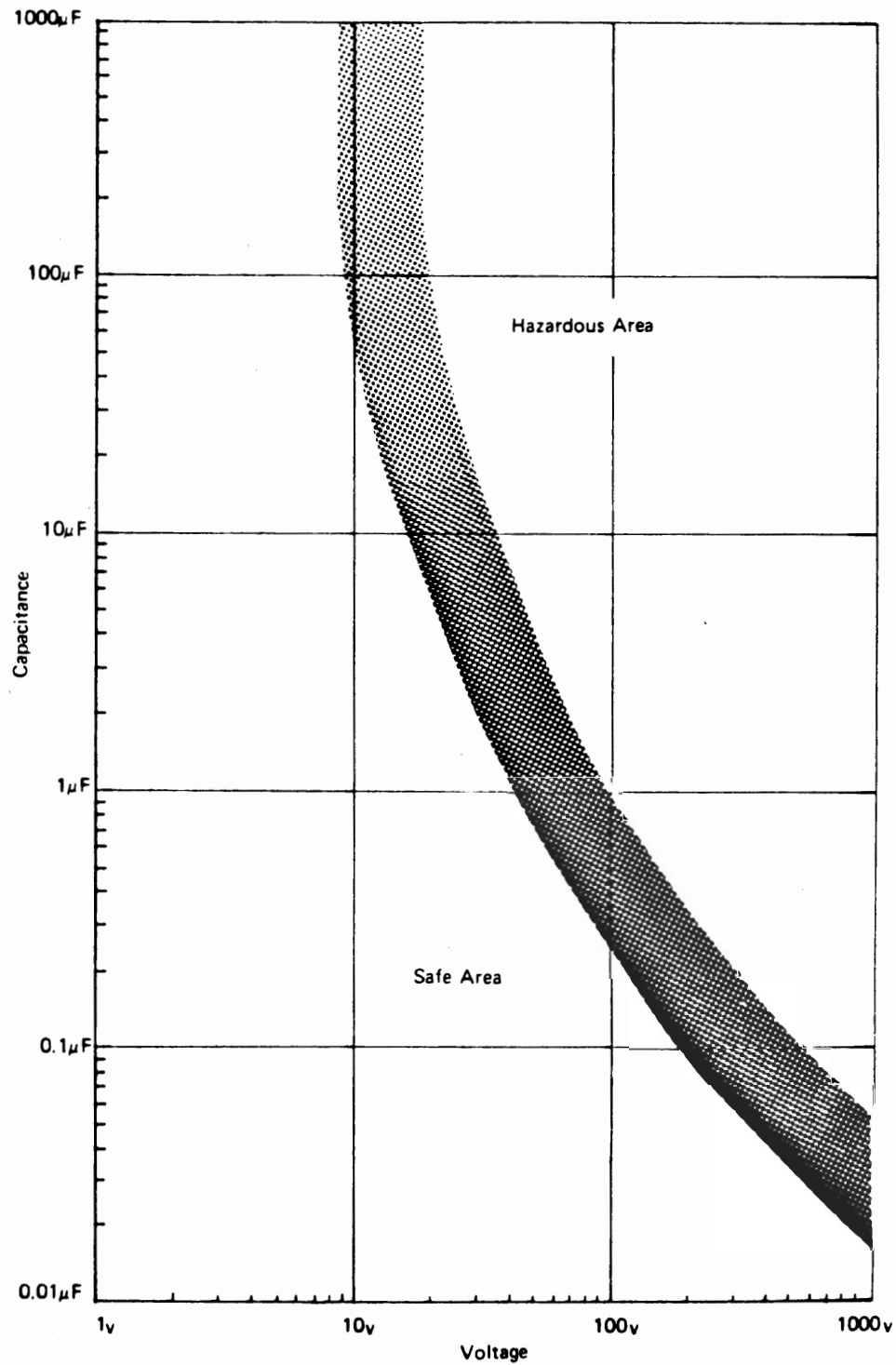
defining the zone of maximum safe current level. In AC applications, this level must represent the peak current<sup>(48)</sup> level, so the 1 amp rms level compared to the allowed 2 amps peak includes a modest safety factor. It can be seen from the plot that significant gains in transmit moment cannot be obtained from increases in current at this inductance. Nor can they be obtained by increasing the number of turns, since the inductance, and also the resistance for a fixed bandwidth requirement, increases more rapidly (as  $N^2$ ) than the moment (as  $N$ ), thereby reducing the maximum attainable and intrinsically safe current.

In the other direction, namely reducing turns, the current at resonance will increase as the inductance and therefore the resistance decrease. **To avoid problems with stray circuit and cabling inductance, the loop inductance should be kept above about 10  $\mu$ h.** This allows a 3 to 1 reduction in turns, a 9 to 1 reduction in L and R, a corresponding 9 to 1 increase in I, and a net increase of 3 to 1 in magnetic moment M. However, even this modest increase in M is unrealizable in practice. The intrinsic safety curve becomes increasingly steep below 1 mh and particularly below 100  $\mu$ h,<sup>(46,48)</sup> thereby allowing at most perhaps a 1.5 to 1 increase in current, which results in a net decrease in M instead of an increase. The practically achievable moment for a 7-turn loop having an inductance of about 75  $\mu$ h, like the SAR and Collins loops, will be about the same as that for the 8-turn, 100  $\mu$ h loop, and the 1 amp rms in the 7.5 ohm load will dissipate 7.5 watts.

The rf voltage across the tuning capacitor (and the loop inductor) at an operating frequency of 500 kHz will be as high as 318 volts rms (450 V-peak) for a 1000 pf capacitor carrying a current of 1 amp rms. These voltages fall well within the safe area of the intrinsic safety plot for capacitors<sup>(46)</sup> shown in Figure 3-12.

It should also be realized that existing intrinsic safety curves are based on DC circuit experience. The subject becomes much more complex<sup>(48)</sup> for AC applications, so the DC-based curves serve only as approximate design guidelines for the MF band radio application. In the end, verification of the MF mine wireless portable radio's intrinsic safety will be determined only after the radio, including the





Source: Ref. 46.

**FIGURE 3-12 MINIMUM IGNITION VOLTAGE AS A FUNCTION OF CAPACITANCE FOR IGNITION OF AN 8.3% METHANE/AIR MIXTURE**

antenna, has successfully completed methane ignition tests conducted by MESA in its special test facility.

The above discussion shows that practical values of magnetic moment  $M$  for a portable MF band unit are not likely to exceed the values of about  $2.5 \text{ amp-m}^2$  peak available with present prototype equipment. This represents only a 12 dB improvement in signal levels over those obtained in the performance estimates of Chapter II for a moment of  $0.7 \text{ amp-m}^2$ . In highly favorable mine attenuation and noise environments, this may result in a range increase of about 300 ft. over that predicted in Table 2-1 of Chapter II. In fair-to-poor mine environments, range increases of less than 50 ft. will occur and the completely-wireless communication range will remain hopelessly small in these situations as shown in Chapter II and reference (41).

The major objective for MF mine wireless radios should therefore be to obtain the most reasonable value of magnetic moment consistent with a transmitter/antenna circuit design that provides the most efficient use of the battery's energy supply. This will lead to a portable system with the smallest battery size, and therefore smallest portable unit size and weight, for satisfying the principal operational requirements, of which the wearability and operating lifetime between charges are as important, if not more so, than the magnitude of the transmit magnetic moment. This suggests the use of MF transmitters designed to operate in a large-signal mode (such as the one mentioned above) to obtain efficiency benefits similar to those of switching-type transmitters at lower frequencies, and optimized for driving a portable unit antenna having a relatively low tuned impedance at the operating frequency.

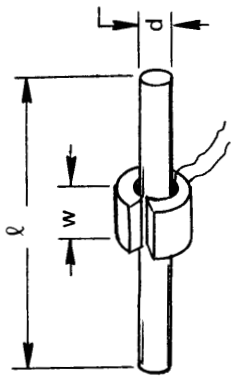
In summary, air-core, bandolier-type loops provide a feasible, practical solution to the MF wireless radio antenna problem, but at a price of minor-to-moderate inconvenience to the miner, depending on whether the antenna is sewn into a garment or fashioned into a flexible or rigid bandolier. The most suitable and practical configuration for a particular mine application is best determined by in-mine trials with prototype designs. The convenience of wear offered by the garment

and flexible bandolier configurations will be somewhat offset by the smaller and slightly variable transmit moments and inductances. The inductance variation could possibly, but not necessarily, introduce the inconvenience of minor retuning of the antenna on different sized individuals. This can be easily checked by experiment. Finally, the transmit moments of presently available prototype units are representative of what is attainable within the operational constraints of the coal mine MF wireless application; and overall portable system improvements will most likely take the form of increased efficiency of transmitter utilization of battery energy, and consequently reduced overall size and weight of the portable units.

#### 4. Ferrite-Loaded Loops

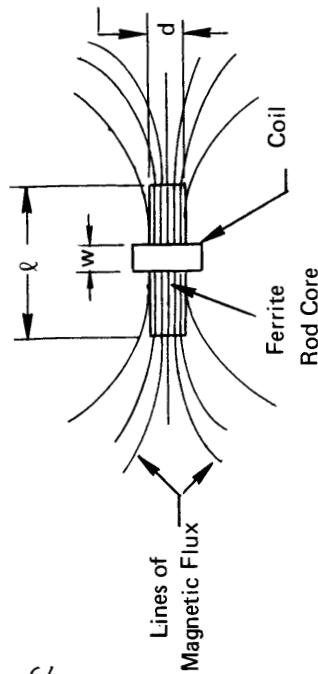
In many applications, loops loaded with magnetic core materials offer equal or improved performance in a considerably reduced cross-sectional area and volume over that of an air-core loop.<sup>(6)</sup> Perhaps the most familiar example of such an antenna in the MF band is the small, ferrite loop-stick receiving antenna used in small transistor pocket radios. A typical configuration for many ferromagnetic core loop antenna applications is shown in Figure 3-13.<sup>(6)</sup> If such an antenna could provide the required magnetic moment within a cylindrical volume of 10 in. length by 2 in. diameter, it would become quite attractive for a portable mine wireless radio, because it could then be mounted horizontally to the radio unit itself or to the miner's belt on which the cap lamp battery and self-rescuer are attached. The brief feasibility calculation described in the following paragraphs shows that the practically attainable transmit moment for such a ferrite-core loop compares favorably with that obtainable with an air-core bandolier loop. Thus, experimental effort should be devoted to verifying its feasibility, and if confirmed, to establishing the optimum antenna design for a portable mine wireless radio.

When a loop loaded with a high-permeability ferrite core or rod, as shown in Figure 3-13, is placed in an ambient magnetic field, the magnetic flux passing through the cross-sectional area enclosed by the loop is greatly increased.<sup>(6,11,49,50)</sup> The high-permeability rod, in



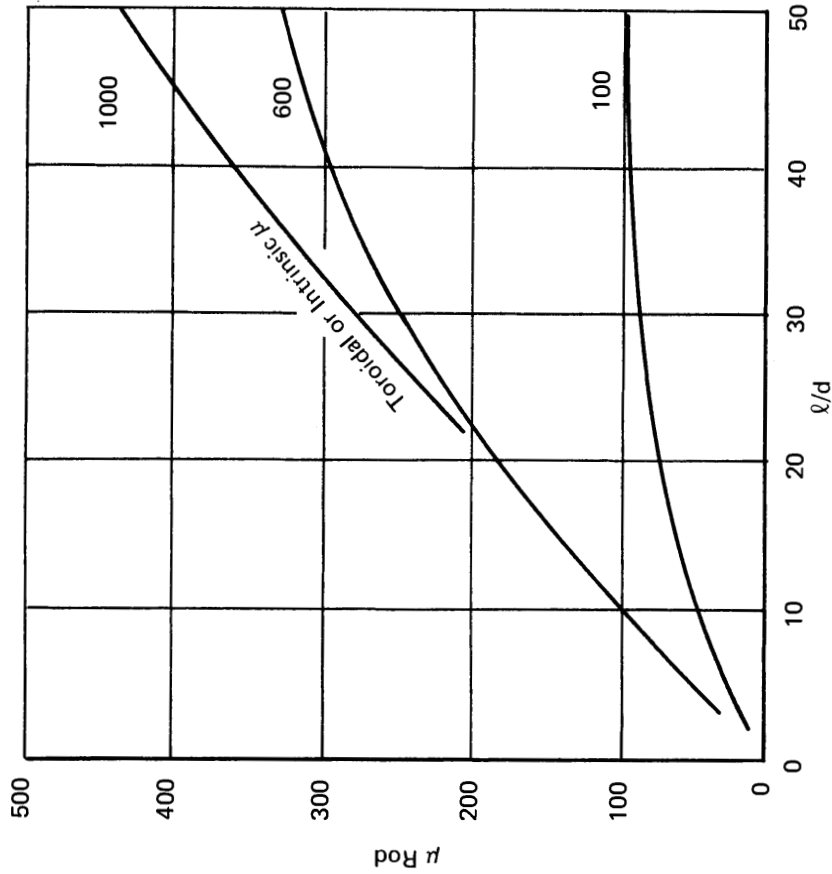
Source: Ref. 6

FIGURE 3-13 TYPICAL CONFIGURATION FOR LOOPS LOADED WITH FERROMAGNETIC CORES



Source: Ref. 11.

FIGURE 3-14 SKETCH OF FLUX CONCENTRATION CAUSED BY HIGH PERMEABILITY ROD



Source: Ref. 11.

FIGURE 3-15 APPARENT PERMEABILITY,  $\mu$ , ROD, AS A FUNCTION OF ROD  $l/d$  AND ROD INTRINSIC PERMEABILITY,  $\mu$

effect, gathers and concentrates the magnetic flux lines in the vicinity of the rod, and causes them to pass through the rod which threads the loop, as depicted in Figure 3-14. This greatly increases the "captured" flux, the "effective area," and therefore the induced open circuit output voltage of the loop acting as a receive antenna. The presence of the rod can also be viewed as increasing the effective permeability of the medium surrounding the antenna, thereby creating the increased flux linkage and output voltage of the loop. By reciprocity, it can be shown that the magnitude of the fields generated by such a loop, when acting as a transmit antenna, will be similarly improved by a rod of magnetic material. The transmit improvement will be identical to that for reception within the linear operating region of the material. In practice, significant improvements in transmit magnetic moment can be realized with practical materials until the materials are driven into saturation.

The presence of the magnetic rod core causes the flux linked and produced by the loop, the loop inductance, and the loop Q, to be increased by different amounts. The amount of increase depends on the shape and size of the rod and on the relative permeability,  $\mu$ , of the rod material, also referred to as the intrinsic permeability of the rod material when measured in a toroid ( $\mu_{\text{toroid}}$ ).<sup>(6,11)</sup> A considerable amount of analytical and experimental work has been done<sup>(6,11,50,51,52,53)</sup> to quantitatively describe how the above quantities depend on the intrinsic permeability of the rod material, on the shape or  $l/d$  ratio of the rod, and on the length of the rod compared to the length of the loop or coil, namely the  $l/w$  ratio.

Referring to Figure 3-14, the best overall practical performance of ferrite rod antennas generally occurs when  $l/d \leq 20$ ,  $l/w \leq 8$ , and  $l/D \leq 4$ . Furthermore, as illustrated in Figure 3-15, when the intrinsic permeability  $\mu$  is greater than about 500 to 600, the effective permeability of the rod  $\mu_{\text{rod}}$  becomes essentially independent of the intrinsic  $\mu$ . This is particularly so for the  $l/d$  range of principal interest for the MF mine wireless radio, namely  $l/d \leq 20$ . Figure 3-15 shows the apparent or effective permeability of the rod,  $\mu_{\text{rod}}$ , (increase in

received flux or transmitted field strength for the loop) as a function of length-to-diameter ratio,  $\ell/d$ , of cylindrical rods having various intrinsic or toroidal permeabilities,  $\mu$ . The increase in the inductance of the coil or loop caused by the rod can be expressed as an increase in the coil permeability,  $\mu_{\text{coil}}$ . The increase in  $\mu_{\text{coil}}$  is generally much less than the increase in  $\mu_{\text{rod}}$ , except when the  $\ell/d$  ratio is not much larger than unity, <sup>(6,11)</sup> and  $\mu_{\text{coil}}$  generally increases with the length of the coil on the rod. **The Q of the coil is also increased by the presence of the rod, so the rod material  $\mu Q$  product in the frequency band of interest is generally an important design parameter.** A plot of typical  $\mu Q$  product behavior as a function of frequency below 10 MHz can be found in reference (51).

To assess the feasibility of using a ferrite rod loop antenna for the portable mine wireless MF radio, a rod material form factor and size is chosen that offers favorable performance, is compact enough to be conveniently worn by a miner, and is readily available from suppliers. A 10 in. long, 1 in. diameter ( $\ell/d = 10$ ) rod of manganese-zinc (MnZn) ferrite material typically used for antenna rods in the LF and MF bands from about 100 kHz to 2 MHz is assumed. <sup>(54,55)</sup> This material typically **has a saturation flux density  $B_{\text{sat}}$  of about 0.3 tesla and an intrinsic initial permeability  $\mu$  of 500 to 1000.**

The saturation flux density defines the maximum moment that a given volume of the material can produce. This maximum  $M_{\text{sat}}$  is given by

$$M_{\text{sat}} = \frac{B_{\text{sat}} V_{\text{rod}}}{\mu_0}, \quad (15)$$

when the flux density is uniformly distributed over the volume.  $B_{\text{sat}}$  is the saturation flux density in teslas,  $V$  is the volume of the rod in  $\text{m}^3$ , and  $\mu_0 = 4\pi \times 10^{-7} \text{h/m}$ . Substituting for  $B_{\text{sat}}$ ,  $V_{\text{rod}}$ , and  $\mu_0$ , we find that the maximum attainable moment for the rod is  $M_{\text{sat}} = 31 \text{ amp-m}^2$  peak, a value greater than 10 times the maximum intrinsically safe moment obtainable with a practical bandolier air-core antenna. However, as shown below, it is not possible to generate this maximum moment in an intrinsically safe manner or with a practical 12 volt transmitter.

On the other hand, generating the 2.5 amp-m<sup>2</sup> (peak) moment obtainable with an air-core bandolier does appear to be feasible, thereby offering the system designer a potentially attractive alternative to the air-core bandolier loop.

The magnetic moment, M, in the material's linear region below saturation is given by

$$M = NIA\mu_{rod} \quad (16)$$

where N is the number of turns in the loop, I is the loop current in amperes, A is the area in m<sup>2</sup> enclosed by the loop, and  $\mu_{rod}$  is taken from Figure 3-15. For the chosen rod having an intrinsic  $\mu$  of 500 to 1000 and  $\ell/d$  of 10, we find from Figure 3-15 that  $\mu_{rod} = 100$ . Thus, equation (16) shows that to generate the air-core bandolier peak moment of 2.5 amp-meter<sup>2</sup> would require an NI product of 49 compared to the NI product of 14 required for the 7-turn air-core bandolier loop discussed in the previous section. Thus, if the ferrite-loaded loop could be driven with the same maximum peak current of 1.4 amperes, the number of turns required would be N = 35.

A single-layer winding which distributes the 35 turns over a length of w = 2 in. in the center of the 1 in. diameter rod is chosen. For a solenoidal coil with this form factor, the simple air-core inductance formula applies<sup>(56)</sup>

$$L_o = \frac{N^2 a^2}{9a + 10w} \text{ microhenries,} \quad (17)$$

which then must be multiplied by  $\mu_{coil}$ <sup>(6,11)</sup> to obtain the inductance when it is ferrite loaded.

$$L = L_o \mu_{coil} \quad (18)$$

N is the number of turns, a is the coil radius in inches, and w is the coil length in inches. The value of  $\mu_{coil} = 10$  is used, based on the finding that for rods having an  $\ell/d$  ratio of 12,  $\mu_{coil} \approx \mu_{rod}/10$ .<sup>(52,6)</sup> Thus, substituting for  $\mu_{coil}$ , a, w, and N in (17) and (18) gives a ferrite-loaded loop inductance of L = 125  $\mu$ h, a value close to that obtained with an 8-turn air-core bandolier antenna.

The bandwidth of 12 kHz at an operating frequency of 500 kHz requires a Q of 42. To achieve this Q at 500 kHz, a series-tuned real

impedance level ( $R = \omega L/Q$ ) of 6.7 ohms is required. This results in a slightly lower peak current of about 1.2 amperes than the 1.4 amperes assumed above for estimating the number of turns ( $N = 35$ ) required to produce the desired magnetic moment of  $2.5 \text{ amp-m}^2$  peak.

Therefore, we find that this ferrite-loaded loop configuration is nearly equivalent to the 8-turn bandolier loop configuration of the previous section in all respects, including its location inductance and current-wise with respect to the safe region boundary on the intrinsic safety plot of Figure 3-11. As in the case of the bandolier loop, a modest decrease in the number of turns allows the moment to be optimized with respect to the intrinsically safe current/inductance levels. In this case about 28 turns should provide the desired peak moment of  $2.5 \text{ amp-m}^2$  at the inductance and peak current levels of about  $80 \mu\text{h}$  and 1.8 amperes respectively. Similar results can also be achieved by distributing the 35 turns over a greater length of the rod.

The above example also illustrates that the maximum achievable moment  $M_{\text{sat}}$ , defined by the saturation flux density  $B_{\text{sat}}$  and volume of the ferrite rod, would require current levels in excess of those which are intrinsically-safe and greater than the 12 volt power supply could supply to the real impedance level imposed by the bandwidth requirement. As in the case of the air-core bandolier loop, the maximum intrinsically-safe moment is constrained to be about  $2.5 \text{ amp-m}^2$ . However, the prospect of achieving the  $M = 2.5 \text{ amp-m}^2$  performance with a much smaller antenna than the bandolier loop makes the ferrite-loaded loop very attractive for the roving miner application. In fact, the example suggests that this moment could be achieved with even a smaller volume core than the one used in the example. The favorable performance of ferrite loaded loops as receiving antennas <sup>(6,11,51)</sup> make their use doubly attractive. Therefore, effort should be directed toward verifying this predicted performance. This is best accomplished experimentally, as will the future optimization of any practical design, should the feasibility be confirmed.

##### 5. Special Multiturn Loop (MTL) Antennas

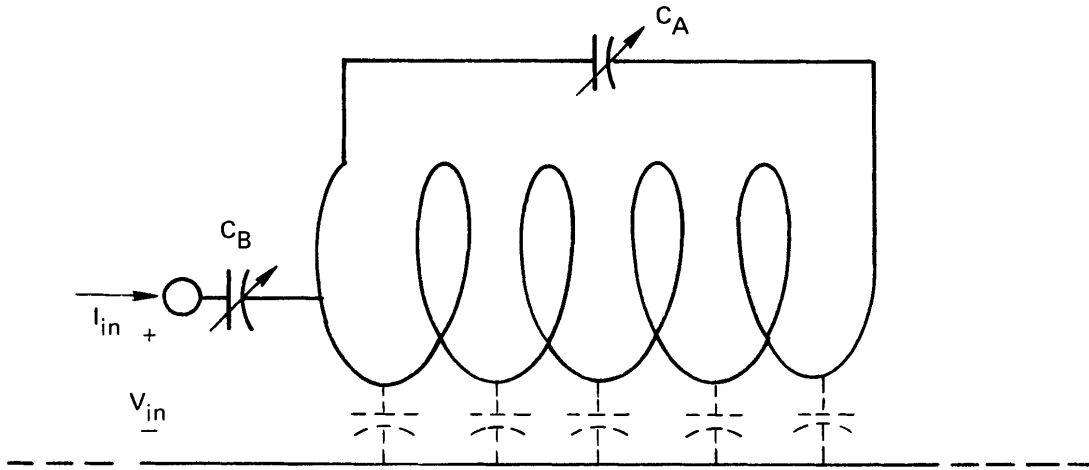
The Ohio State University and others have been studying and developing a class of electrically small antennas called multiturn loop (MTL) antennas. <sup>(7,57,58,59,60,61,62)</sup> The objective has been to



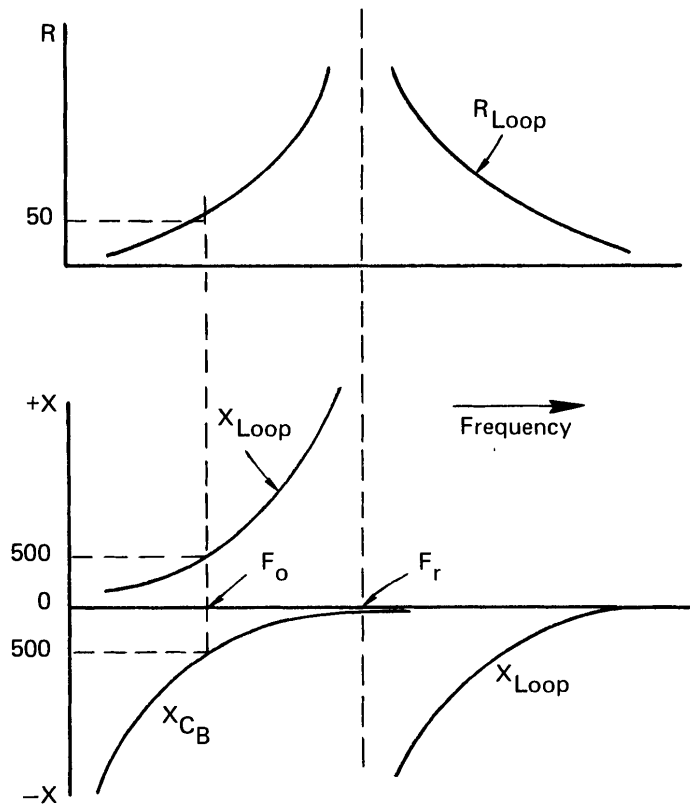
provide improved performance in terms of antenna system radiation efficiency, or comparable performance in a smaller and more convenient volume, than that obtainable with whips tuned by generally high-loss coils in the HF band and in the low and high VHF bands. Although these MTL antennas may offer size and/or performance advantages for some applications in the HF and VHF bands, they are by and large inappropriate for the portable mine wireless MF band application.

MTL antennas are low-loss, high-Q, single-layer coil structures having  $\ell/d$  ratios near unity, and consisting of from 3 to 10 turns of tubular or strip conductor, spaced about 2 to 4 conductor diameters apart. The axis of the MTL coil is positioned parallel to, and at a short height above, a ground plane. Tuning and matching is accomplished with two low-loss capacitors. As depicted by the antenna schematic in Figure 3-16a, the coil's self-capacitance between turns, and between the turns and the ground plane, is supplemented by the parallel tuning capacitor  $C_A$  to produce a parallel resonance at a frequency,  $f_r$ , above the desired operating frequency,  $f_o$ . Below  $f_r$ , the parallel combination of  $C_A$  and the coil structure exhibits an input impedance having real and inductively reactive parts as shown in Figure 3-16b. This impedance is in series with the capacitive reactance of the matching capacitor,  $C_B$ . To obtain the desired value of real input impedance, the value of  $C_A$  is adjusted, which shifts  $f_r$  so as to produce the desired real part of the parallel coil-capacitor circuit impedance at the operating frequency,  $f_o$ . Then, the matching capacitor  $C_B$  is adjusted to cancel the inductive reactance of the antenna structure at  $f_o$ . The result is a high-Q, narrow bandwidth, tuned antenna structure capable of moderate-to-high radiation efficiencies. Best results are generally obtained when the largest structure dimension is greater than at least  $\lambda/50$  (preferably greater than  $\lambda/20$ ) and the length of the conductor forming the turns is between  $\lambda/8$  to  $\lambda/4$ .

Two examples of portable MTL applications are the prototype packet MTL antenna developed for the PRC-77 low-band VHF (30-76 MHz) military transceiver<sup>(57,58)</sup> and a prototype shoulder-mounted MTL antenna for high-band VHF police personal radios.<sup>(61)</sup> The size of each MTL would



a. Schematic Diagram of MTL Antenna



b. Impedance Characteristics of MTL Antenna

Source: Reference 7.

FIGURE 3-16 MTL ANTENNA DIAGRAM AND IMPEDANCE CHARACTERISTICS

be compatible with a portable mine wireless application. The low-band VHF packset MTL is a 4-turn square coil of dimensions 2-1/2 x 2-1/2 x 4-1/2 inches long, mounted to the base of the PRC-77 radio, and enclosed in a fiberglass protective cover which extends 5-1/2 inches below the packset, which is carried as a backpack by a soldier. This MTL was found to compare favorably to a 3 ft. whip over the 30-76 MHz band, but to also experience tuning and pattern problems as a result of the antenna's high Q and its closeness to the body. The high band VHF shoulder-mounted MTL is 2.7 x 2.7 x 0.7 inches high, mounted above a 4.5 x 6.5 inches shoulder-pad type of ground plane. This MTL was found to compare favorably with a 6 inch helical whip over the 150-170 MHz band, but to also experience problems similar to those for the low-band VHF packset MTL. Both required tuning after being mounted on the person, and the performance of both depended on body positions and orientations. At MF band wavelengths, which are between 2 and 3 orders of magnitude greater than those at VHF, the problems associated with portable-sized MTL units will become significantly more severe.

In the VLF to MF band of present interest, the MTL dimension requirements with respect to wavelength are clearly incompatible with the sizes desired for portable mine wireless units, and even for semi-permanent fixed installations in coal mines. The ground plane requirement is similarly incompatible. Furthermore, as cited in Section III.B, high antenna efficiency requires high antenna system Q, which is also incompatible with the bandwidth required for mine wireless FM voice communications in the VLF to MF band. Thus, the principal attribute of ideal MTL antennas is neither desired nor attainable for the mine wireless application. Therefore, although MTL antennas may offer performance advantages over other antennas for portable radio applications<sup>(57,58,61)</sup> in the VHF band, and for shipboard applications<sup>(7)</sup> in the HF band, MTL antennas are inappropriate for MF band mine wireless applications.

#### D. FIXED STATION ANTENNAS

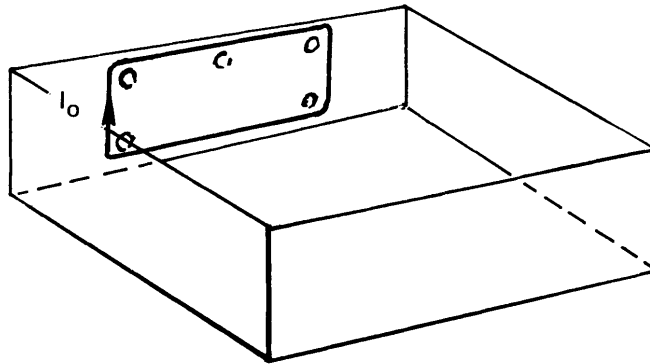
This section briefly considers some alternative antenna types and radio wave coupling methods that are suited to mine wireless radio fixed installations such as base stations or repeaters.

##### 1. Vertical Plane Loops

Air-core planar loops, series tuned, provide a practical choice for the mine wireless radio portable units. They also provide the most convenient way of generating the largest magnetic moment per unit weight of antenna for a fixed radio installation. This is especially so when space is available to span a large area with the loop as is usually the case in coal-mine tunnels. The planar loop combines the desirable attributes of high magnetic moment, well-defined and stable impedance characteristics, and ease of installation and maintenance.

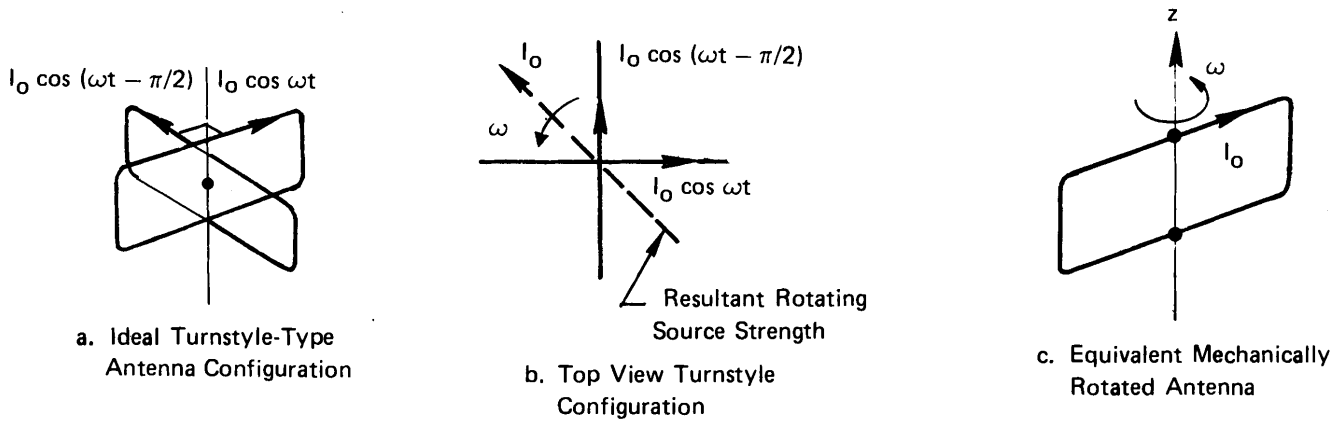
A practical loop configuration for a fixed installation is a rectangular air-core loop, series tuned, and formed in a vertical plane so that it can be "hung" or mounted on the wall or rib of the mine tunnel as depicted in Figure 3-17. The vertical orientation of the planar antenna is the most favorable for exciting the desired zero-order, quasi-TEM mode having horizontal magnetic field  $H_\phi$  and vertical electric field  $E_z$  in coal seams (Section II.D, Figure 2-6). Maximum signal strengths will occur at positions in the plane of the loop ( $\phi = 0^\circ$ ), and minimum signal strengths at locations in the vertical plane perpendicular to, and passing through the center of, the loop ( $\phi = 90^\circ$ ), according to the  $\cos \phi$  angular dependence of a magnetic dipole (loop) source.

The angular dependence of the mode excitation presents a nonuniform area coverage problem that is somewhat more serious than the one experienced by a miner wearing a bandolier-type loop antenna. For example, the miner can always rotate his body position to maximize his received signal-to-noise ratio. However, the same result can be obtained with fixed station installations by installing a second vertical planar loop oriented perpendicular to the first loop, and driven with a current equal to, and  $90^\circ$  out of phase with, the current in the first loop as shown in Figure 3-18. This is a turnstyle type of antenna installation<sup>(11)</sup>



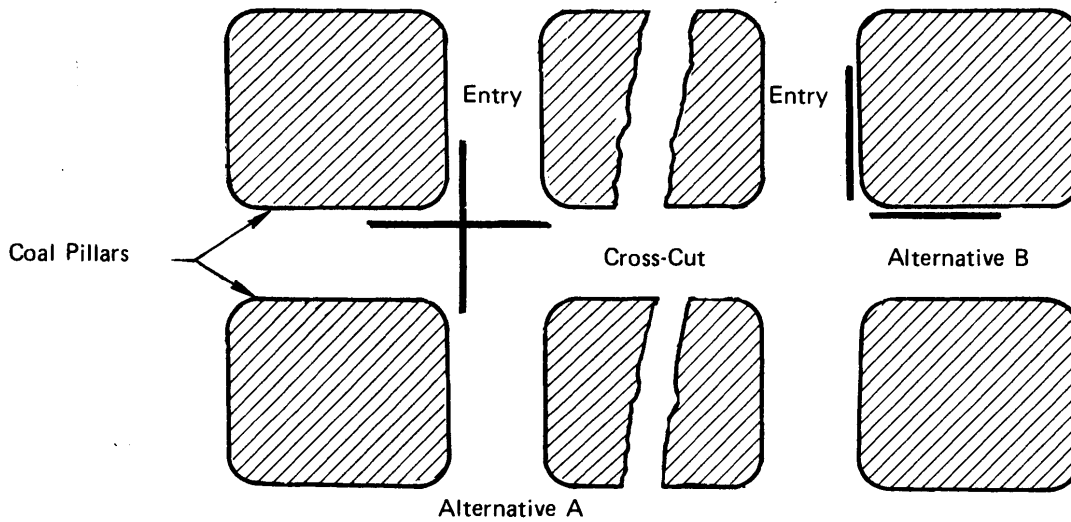
Source: Arthur D. Little, Inc.

**FIGURE 3-17 WALL-MOUNTED FIXED STATION LOOP IN COAL MINE TUNNEL**



Source: Arthur D. Little, Inc.

**FIGURE 3-18 FIXED-STATION TURNSTYLE LOOP ANTENNA CONFIGURATION**



Source: Arthur D. Little, Inc.

**FIGURE 3-19 TURNSTYLE ANTENNA INSTALLATION POSSIBILITIES IN A COAL MINE ENVIRONMENT**

that creates an electrically rotating antenna and source field equivalent to that of a mechanically rotated one (one rotation per cycle of the excitation), thereby providing omnidirectional antenna coverage in the coal seam horizontal plane.

Ideally, the two loops should have a common center as shown in Figure 3-18. This provides a common electrical phase center for the waves and minimizes mutual coupling between the two loops. Although it is possible to install two common-centered perpendicular vertical loops in coal mines by spanning the intersection of an entry and a cross-cut as in Figure 3-19a, it may not be a practical option in mine entries used by vehicles for the movement of men and material, unless special precautions are taken to protect the loop conductors.

An alternative installation which avoids the need for such protection is shown in Figure 3-19b, whereby the loops are mounted on the perpendicular entry and cross-cut walls near the corner of a coal pillar. The non-coincident phase centers should not present any problems in the MF band of interest, but the mutual coupling between the loops may adversely affect the tuning and driving of the loops. The severity of these coupling effects, together with electrical and/or spatial means of minimizing any significant ones, will probably have to be eventually determined or verified experimentally.

Finally, the most favorable length-to-height ratios, and number of turns, for fixed station rectangular loops will probably be best determined by experiment. The quasi-TEM mode of propagation excited in the coal seam, together with the thickness of the seam, are likely to impose limits on the increase in signal strength obtainable by increasing the length of a single-turn rectangular loop having a height approximately equal to the tunnel height in the coal seam. Once beyond the point of diminishing return with respect to loop length, additional increases in loop magnetic moment could be obtained by adding turns. Practical size constraints for typical in-mine installations could also lead to increased turns, as could the desire to increase the loop inductance to allow the loop to be resonated with capacitors that may be more conveniently available and practical.

The wall-mounted loop presently used for the prototype MF mine wireless fixed installations in high-coal seams is a one-turn, 6 feet high by 24 feet long loop giving an  $NA = 12 \text{ m}^2$  and a loop inductance of 27  $\mu\text{h}$ . It is driven with a peak current of about 1 amp to produce a magnetic moment of  $14 \text{ amp-m}^2$ . The bandwidth of 12 kHz requires a Q of 42 and a series-tuned real impedance level of about 2 ohms at a 500 kHz operating frequency.

Simple in-mine experiments should be performed to determine the relationship between loop length and signal strength produced in the plane of the loop at distances beyond about 100 - 200 meters from the loop. The results may reveal that a shape factor based on length-to-height ratio must be applied to the geometrical area to obtain an effective area from which the effective magnetic moment of the loop can be determined. A long piece of insulated wire capable of being driven from one end and any one of several other points along its periphery should be suitable for conveniently forming, mounting, and driving rectangular loops of different length on the wall of a mine tunnel.

## 2. Alternative Mode Exciters

### a. Horizontal Grounded Long Wires

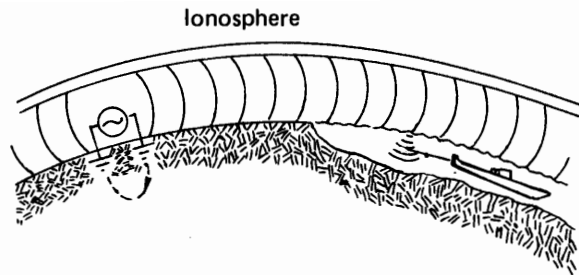
Mode excitation techniques or antennas<sup>(63,64,65,66)</sup> similar to those used for the Navy's proposed worldwide ELF Sanguine communications system may also be applicable for mine wireless radio fixed installations. This section briefly describes some of the attractive similarities between the two applications, presents the results of some preliminary feasibility calculations for coal mines, and suggests some avenues of further investigation that appear promising.

As discussed in Section II.D of this report, recent and continuing analyses<sup>(41,42,43)</sup> and measurements<sup>(40,44)</sup> have shown that coal seams bounded above and below by sedimentary rock behave as lossy parallel plate waveguides with respect to the propagation of radio waves in the LF and MF frequency bands. At ELF, the conducting ionosphere and surface

of the earth form the upper and lower boundaries of a similar parallel plate earth-ionosphere waveguide within which transmitted ELF waves travel around the world with very low attenuation, to be received by submerged submarines as depicted by Figure 3-20. Perhaps the most important difference between the two waveguides is that the coal seam waveguide is filled with a lossy medium, the coal itself, in addition to being bounded by lossy media above and below, thus introducing shunt loss in addition to the series loss of the "plates" in both waveguides. The spherical shell nature of the earth-ionosphere waveguide introduces only a different geometrical spreading loss factor. However, neither of these differences, the shunt loss nor the spherical shell, changes the basic nature of the quasi-TEM mode of propagation in the waveguide. In fact the Sanguine problem was initially treated in terms of cylindrically spreading waves in a flat-earth, parallel plate waveguide. A spherical "focusing" correction factor was applied to the cylindrical wave solution afterwards. Thus, the excitation methods for one waveguide should be largely applicable to the other.

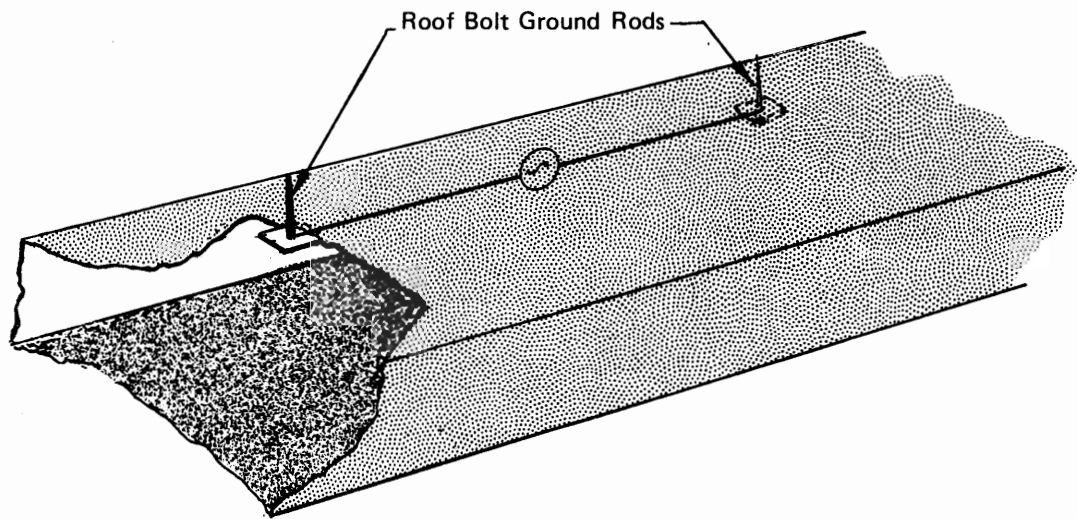
The Sanguine investigators found that the most effective and feasible transmitting antenna configuration for their application was a parallel array of grounded, center-driven, long wire antennas. A single long horizontal wire is the simplest form of such an antenna. However, to achieve the required current moment  $I\ell$  requires an excessively long antenna (and thus land having the desired conductivity) and/or unreasonably high currents. High currents lead to two consequences that are undesirable for both the Sanguine and mine wireless applications, namely excessive power dissipation and environmentally nonpermissible field or current levels. A parallel array greatly reduces the maximum linear dimensions of the antenna, and distributes the required current moment over an area which in turn allows the use of several parallel wires, each carrying a fraction of the total current required. Furthermore, it was found that a spacing between horizontal wires (in the Sanguine case, 0000 AWG copper to carry 100 amperes) of about 2 skin depths provides a favorable compromise between overall system performance, power dissipation, and cost for the intended application. The reader is referred to references (63,64,65) for a more detailed treatment.





Source: Ref. 63.

**FIGURE 3-20 PROPAGATION AT ELF IN THE EARTH-IONOSPHERE WAVEGUIDE**



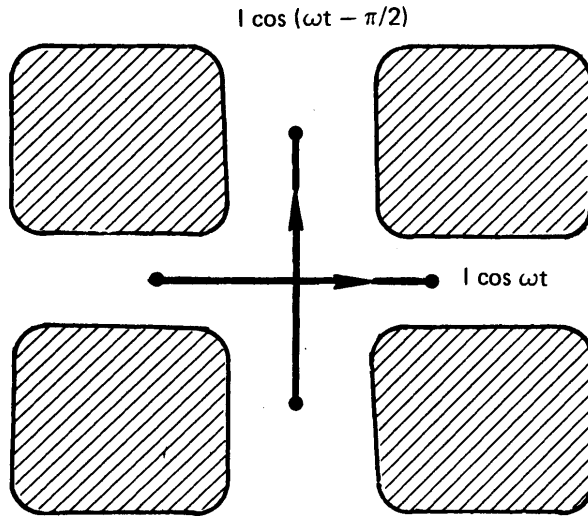
Source: Arthur D. Little, Inc.

**FIGURE 3-21 SKETCH OF A GROUNDED LONG WIRE ANTENNA INSTALLED IN A COAL MINE TUNNEL**

Thus, one can visualize a mine wireless fixed station application that employs one or more horizontal long wire antennas strung along the roof of a mine tunnel and grounded to the rock above the coal seam by roof bolts as portrayed in Figure 3-21. The long wire antenna exhibits the same  $\cos\phi$  dipole pattern angular dependence as the vertical plane loop previously discussed. Thus, omnidirectional area coverage can be obtained in the same manner as with loops, by employing a second long wire antenna perpendicular to the first and driven  $90^\circ$  out of phase with it in turnstyle fashion as depicted in Figure 3-22. Note that the long wire antenna is better suited than a loop to turnstyle installations across the intersections of mine entries and crosscuts, because it does not require a floor-mounted wire which is generally difficult to protect from damage in well-travelled intersections.

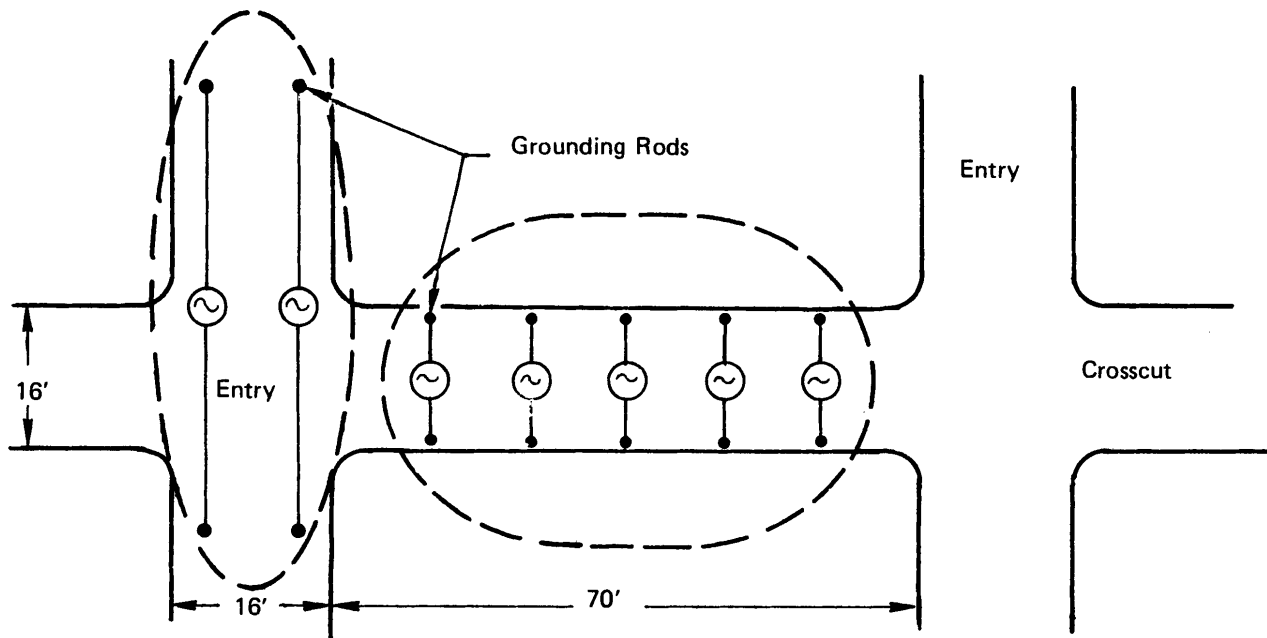
The most recent estimates<sup>(43)</sup> place the conductivity of roof rock in coal mines within the range of 0.01 to 1.0 mho/m with a value of about 0.1 mho/m being typical. At an operating frequency of 300 kHz, this produces a skin depth in the rock,  $\delta_r$ , of about 2 meters. Thus, the Sanguine  $2\delta$  separation criteria would allow at least two, and perhaps three, parallel long wires to be placed in a typical mine tunnel or entry, depending on the tunnel width in different mines or different parts of the same mine. Another possibility could involve a similar or greater number of considerably shorter long wire antennas installed in a cross-cut tunnel between two entries as depicted in Figure 3-23. In each case, the individual grounded wires could be driven by separate transmitters keyed-on simultaneously via an audio twisted pair interconnection, or driven in-parallel by a single transmitter.

The most effective configuration from the standpoint of power drain, communication range, ease of installation and maintenance, compatibility of fixed station units with the portable units, etc., would have to be determined after analyzing the results of a simple set of performance measurements in mines. Particular attention should be paid to the dependence of signal strength on the length of the long wire antenna (as suggested for the loop antenna measurements in Section III.D.1), and to the levels and variability of the impedance of simple roof bolt (and



Source: Arthur D. Little, Inc.

FIGURE 3-22 LONG WIRE TURNSTYLE CONFIGURATION IN AN ENTRY/CROSSCUT INTERSECTION



Source: Arthur D. Little, Inc.

FIGURE 3-23 LONG WIRE ARRAY CONFIGURATIONS IN A MINE ENTRY AND A CROSSCUT

perhaps other types) ground terminations for the long wires. The dependence of both signal strength and antenna input impedance on the spacing between parallel long wires also needs to be examined in mines.

The elaborate ground termination techniques available to a large and permanent, well-controlled Sanguine antenna installation will, of course, not be practical for a semi-permanent and largely uncontrolled mine installation. As a result, ground terminations achievable in a mine may be so large and/or variable as to make the horizontal long wire antenna impractical for mines. The spreading resistance of a 2 m long by 2.5 cm diameter ground rod (about the size of a roof bolt) making ideal contact along its length to rock of uniform conductivity 0.1 mho/m, is 4.2 ohm, giving a total of 9.4 ohms for the two long wire terminations. Though 9.4 ohms is reasonable, it may not be achievable in practice. A long wire antenna will also exhibit a nominal inductive reactance<sup>(63)</sup> which can be tuned out by a series capacitor if necessary.

A first-order estimate of the performance of a single, terminated long wire compared to that of a conventional rectangular planar loop antenna can be made by computing the effective magnetic moment of the long wire and its return current path in the roof. When the antenna is long compared to the skin depth in the rock, the return current flow spreads out into the roof to about one skin depth from the wire.<sup>(63,64,65)</sup> Thus, the long wire and its return current path can be approximately represented by a rectangular loop of length  $\ell$ , effective height  $\delta_r/\sqrt{2}$ ,<sup>(65)</sup> and area  $A = \ell\delta_r/\sqrt{2}$ .

An operating frequency of 300 kHz in rock having a conductivity  $\sigma = 1.0$  mho/m, gives a  $\delta_r$  value of about 2 meters which results in an effective loop height of 1.4 m. The most effective long wire antenna length,  $\ell$ , may range from slightly longer than the waveguide (seam) height as in the Sanguine case, to a length that is on the order of the effective skin depth,  $\delta$ , of the coal seam waveguide, where  $\delta$  is largely determined by the conductivity of the coal as opposed to that of the rock. The effective skin depth  $\delta$  of lossy coal seam waveguides at 300 kHz has been found<sup>(43)</sup> to vary from about 10 m in high loss seams, such as the Herrin No. 6 seam in Illinois, to as large as 100 m in low loss seams,

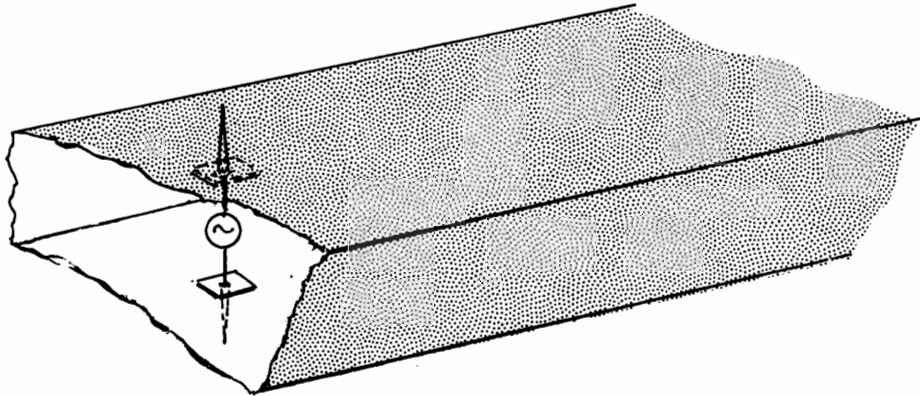
such as the Pittsburgh seam in West Virginia. Maximum wire lengths,  $l$ , between 10 and 100 m can therefore be expected. Thus, the effective loop areas of grounded long wires are seen to compare favorably with that of the 2 m x 7 m rectangular fixed station loop discussed in Section III.D.1.

Yet to be determined is whether the resultant waveguide coupling factor for the long wire is more or less favorable than indicated by the above simplified effective magnetic moment analysis, whether termination impedances comparable to the impedances of tuned loops can be achieved and easily maintained over time, and to what extent the signal strength remains proportional to wire length as the length is increased. Both analytical and experimental efforts will be required to resolve these issues.

b. Vertical Grounded Wires

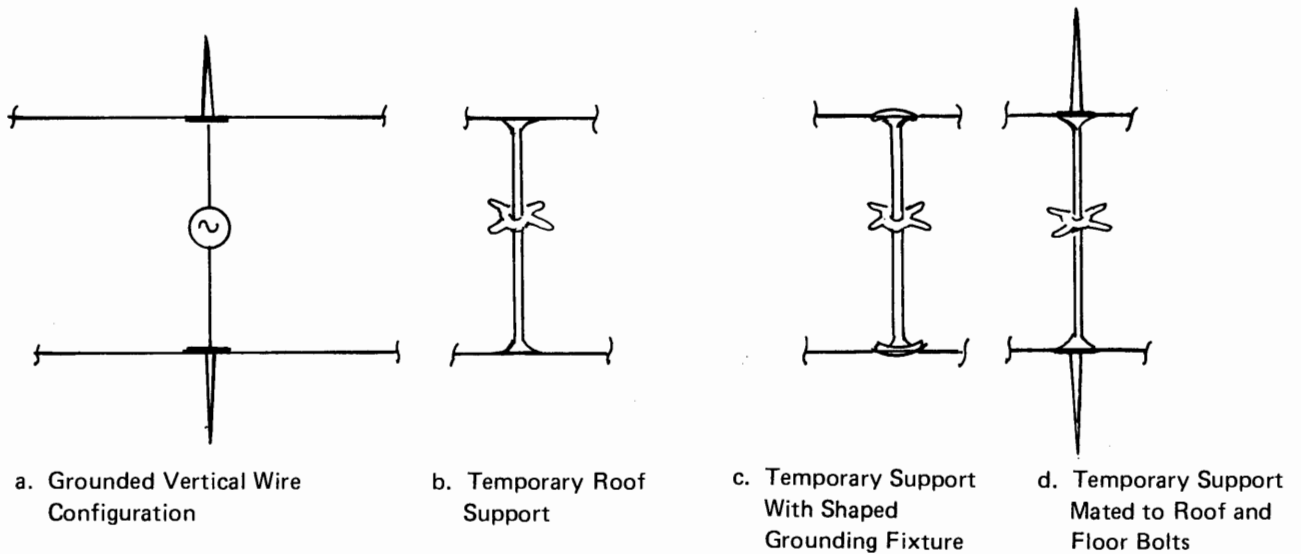
The Sanguine ELF radio system unfortunately could not use what is perhaps the ideal antenna to excite the quasi-TEM mode in the earth-ionosphere waveguide, namely a vertical current source rising out of the conducting earth and terminating in the conducting ionosphere. Although such an antenna is clearly not feasible for the Sanguine application, it does become a very real possibility for use in the coal seam waveguide. In its simplest form it could consist of a vertical center-driven wire grounded at each end to two vertical roof bolts, one in the roof and one in the bottom (floor), in a mine entry or a crosscut tunnel as depicted in Figure 3-24. It also has the advantage of producing omnidirectional coverage in the plane of the coal seam, without the addition of a second unit.

Another perhaps more convenient configuration may also be feasible, namely the use of a steel, screw-tightened temporary roof support (Fig. 3-25) commonly used in the face area prior to permanent roof bolting. Such a roof support could be mated at each end with a special fixture designed to make a good grounding connection to the roof and bottom, and to provide a means for connecting the vertical rod coupler to the transmitter. This would avoid the need to drive a roof bolt or other type of grounding rod into the bottom. The shape of the fixture surface making contact with the coal would be designed with the objective of providing



Source: Arthur D. Little, Inc.

**FIGURE 3-24 SKETCH OF A GROUNDED VERTICAL WIRE ANTENNA INSTALLED IN A COAL MINE TUNNEL**



Source: Arthur D. Little, Inc.

**FIGURE 3-25 CONCEPTUAL SKETCHES OF VERTICAL WIRE MODE EXCITER CONFIGURATIONS**

a favorably low termination resistance, and a current spreading distribution in the roof and bottom consistent with mode excitation constraints imposed by the skin depth in the rock. The shape of the contact surface must also lend itself to a convenient pressure-fit type of installation as the temporary support is screw-tightened against the roof and bottom. A similar result may also be obtainable without special shaping, by installing the vertical roof support so that it mates top-and-bottom to two previously installed roof bolt grounding rods. A secondary advantage of the structural-type of vertical mode exciter represented by the temporary roof support is that it allows the fixed station radio to be directly mounted to it, giving a physically integrated mine installation.

A first-order estimate of the performance of this vertical wire/rod terminated source has been made and compared to that of a representative vertical plane loop. The vertical monopole-type source current generates a  $\phi$ -directed magnetic field component that is independent of  $\phi$ . Solution of the wave equation for this source distribution gives the following expression for the magnitude squared of  $H_\phi$ :

$$|H_\phi|_V^2 = \frac{I^2}{8\pi} (\alpha^2 + \beta^2)^{1/2} \frac{e^{-2\alpha r}}{r} \quad (19)$$

for  $r \gg \delta$  where  $\delta$  is the effective skin depth in the coal seam waveguide,  $I$  is the source current,  $\alpha$  is the attenuation constant, and  $\beta$  is the phase constant. Ideal matching of the source current distribution to that required in the rock by the mode is assumed. The corresponding field expression for a dipole source current such as that of a rectangular planar loop is

$$|H_\phi|_L^2 = \frac{M^2}{(h + \delta_r)^2} \frac{(\alpha^2 + \beta^2)^{3/2}}{8\pi} \frac{e^{-2\alpha r}}{r} \quad (20)$$

for  $r \gg \delta$ , where  $M$  is the source loop magnetic moment,  $\delta_r$  is the skin depth in the rock,  $h$  is the height of the coal seam, and  $\alpha$  and  $\beta$  are defined above. Forming the ratio of these two field quantities gives the expression

$$R_{V/L} = \frac{I^2}{M^2} \frac{(h + \delta_r)^2}{(\alpha^2 + \beta^2)} \quad (21)$$

The ratio  $R_{V/L}$  is computed for installations in a representative high-loss coal seam having a seam height of 3 m and a low loss seam of 1.5 m height. A current of 1 ampere is used for both vertical wire and planar loop sources. A 2 m x 7 m one-turn loop ( $M = 14 \text{ a-m}^2$ ), similar to the one used for the prototype MF mine wireless system, is assumed for the comparison. The high-loss seam is characterized by values of  $\alpha = 0.047 \text{ m}^{-1}$ ,  $\beta = 0.034 \text{ m}^{-1}$ ,  $\delta_r = 2.3 \text{ m}$  at a representative operating frequency of 250 kHz. Thus, a ratio of  $R_{V/L} = 43$  is obtained, representing a 16 dB advantage over the loop. The low-loss seam is characterized by values of  $\alpha = 0.013 \text{ m}^{-1}$ ,  $\beta = 0.02 \text{ m}^{-1}$ ,  $\delta_r = 2.9 \text{ m}$  at the same operating frequency, and results in the ratio  $R_{V/L} = 132$ , representing a 21 dB advantage. In the high-loss seam, a 16 dB advantage represents only about a 130 ft. increase in the receiver-noise-limited communications range, whereas a 21 dB advantage in the low-loss seam represents about a 630 ft. increase in operating range at 250 kHz.

Thus, this method of mode coupling for fixed stations also appears to warrant a more thorough analytical and experimental investigation to see whether these favorable approximate results can be obtained in practice. This coupling method, of course, will be subject to the same potential problems associated with establishing and maintaining good grounding connections to the rock as the horizontal long wire coupling method. Therefore, the likely success of both coupling methods will depend on the results of ground rod impedance experiments performed on roof bolts and other grounding devices implanted in the roofs and bottoms of mine tunnels.

The conventional type of mine roof bolt installation, which contacts the rock at only two points, at the expansion wedge and at the base plate, will probably not provide a good enough electrical connection to the rock for the purpose of establishing and maintaining a low impedance ground. Some of the new plastic grouted bolts that fill the drill hole space between the steel roof bolt and the rock with a quick-hardening epoxy-type of plastic may create an even poorer connection if the grouting material is not conductive. However, if the plastic grouting material could be made conductive or of high dielectric constant, it



may be possible to approach the low terminal resistance of an ideal grounding rod, and to maintain it over a period of time sufficient to serve the semi-permanent needs of an advancing coal mine working section. At present, it appears that quantitative knowledge on how roof bolt and similar types of ground terminations work, vary over time, should be installed, and could be improved from an electrical standpoint, is not available. If and when this information becomes available, as a result of a carefully performed series of in-mine measurements, a more definitive assessment of the feasibility of the long horizontal wire and vertical rod mode exciting methods will be possible.

### 3. Other Loop Antennas

A considerable amount of development effort has also been devoted during the late 1960's and early 1970's to two other types of loop antenna that are worthy of brief mention, namely self-resonant helical antennas by the University of Innsbruck<sup>(15,16,67,68,69)</sup> in Austria and large ferromagnetically loaded solenoidal loop antennas by Develco, Inc.<sup>(53)</sup> in the United States. Both efforts were aimed at generating very high magnetic moments (on the order of  $1000 \text{ amp-m}^2$ ) for special-purpose, fixed-installation, through-the-earth, narrowband data communication applications in nonexplosive atmospheres, primarily in the VLF and LF bands.

The Develco ferromagnetically loaded transmit loop antennas were designed for a bore hole through-the-earth data application subject to very high shock and overpressure. The antennas, consisting of nineteen ferrite rods surrounded by a long, high turns-density solenoid coil and a protective fiberglass shell, occupied a cylindrical volume about 10 ft. long and 1 ft. in diameter, and represented state-of-the-art electrical and mechanical designs optimized for the application. The University of Innsbruck transmit antennas were designed for through-the-earth data or code communication from an underground, environmentally controlled cavity, such as might be fashioned in an underground network of tunnels. The antennas were center-fed, self-resonant, air-core helical structures consisting of a large number of turns and typically occupying a volume on the order of a meter cube. Both development efforts also included analytical and experimental investigations of the associated through-the-

earth propagation problems, and methods of optimizing ferrite-loaded receive antennas. The Develco propagation effort was primarily concerned with vertical propagation through the overburden, and the University of Innsbruck effort was primarily concerned with horizontal propagation through an underground network of tunnels in a mountain.

Although the specific antennas developed may be inappropriate for portable, intrinsically safe, mine wireless voice communication applications in the MF band, similar antennas and technology may in fact be applicable to permanently installed, one-way, wireless emergency warning or signalling applications in the ULF or VLF band for mines. The grounded horizontal long wire and vertical wire mode exciters discussed in the previous section may also be candidates for such applications. The high energy storage and/or high-power antenna/transmitter installations that would likely be required for long range, emergency warning applications could probably be located in areas of a mine where similar, high-power, nonintrinsically-safe equipment is allowed, or in specially-prepared locations where independent ventilation and sealing could be used to ensure a safe operating atmosphere even in the event of a mine disaster. Some of the antenna and signalling technology associated with the Develco ferrite-loaded cylindrical antenna systems may also be applicable to refuge shelter through-the-earth communications, especially in shelter situations where a large-area, air-core loop cannot be conveniently deployed. Further investigation will be required to determine the feasibility and suitability of these antenna and signalling techniques for narrowband emergency warning and refuge shelter signalling applications.

E. REFERENCES

1. Chu, L. J., "Physical Limitations of Omni-directional Antennas," J. A. P., Vol. 19, pp 1163-1175, December 1948.
2. Harrington, R. G., Time Harmonic Electromagnetic Fields, McGraw-Hill, New York, pp 264-316, 1961.
3. Wheeler, Harold A., "Fundamental Limitations of Small Antennas," Proceedings of the I. R. E., pp 1479-1484, December 1947.
4. Wheeler, Harold A., "Small Antennas," IEEE Trans. Antennas and Propagation, Vol. AP-23, No. 4, pp 462-469, July 1975.
5. Collins, Robert E., and Zucker, Francis J., Antenna Theory, Part 1, McGraw-Hill Book Co., New York, 1969.
6. Watt, A. D., VLF Radio Engineering, Pergammon Press, Oxford, 1967.
7. Bohley, P., Walter, C. H., and Caldecott, R., "Development of the Multiturn Loop Antenna at H. F. for Shipboard Applications," The Ohio State University Electro Science Laboratory, Final Report 3518-1, Naval Ship Systems Command Contract N00024-73-C-1023, December 1973.
8. Wheeler, H. A., "The Radiansphere Around a Small Antenna," Proc. IRE, pp 1325-1331, August 1959.
9. Ikrath, K., Kennesbeck, W., and Hoverter, R. T., "Trees Performing as Radio Antennas," IEEE Trans. Antennas and Propagation, Vol. AP-23, No. 1, pp 137-140, January 1975.
10. Hansen, Robert C., "Optimum Inductive Loading of Short Whip Antennas," IEEE Trans. on Vehicular Technology, Vol. VT-24, No. 2, pp 21-29, May 1975.
11. Jasik, Henry, Ed., Antenna Engineering Handbook, McGraw-Hill Book Co., New York, 1st Edition, 1961.
12. Jinkings, P. W., "Antenna Systems for L. F. Transmitters," Point-to-Point Communication, pp 32-45, January 1971.
13. Seely, E. W. and Wiborg, P. H., Jr., "Horizontal VLF Transmitting Antennas Near the Earth," NOLC Report 721, Naval Ordnance Laboratory Corona, Corona, California, May 15, 1967.
14. Collin, Robert E. and Zucker, Francis J., Antenna Theory, Part 2, McGraw-Hill Book Co., New York, 1969.

15. Klein, R., "Antennas for the VLF Region and LF Region," Scientific Report No. 4, AFCRL 70-0602, Contract No. F61052-69-C-0007, Univ. Doz. D. W. Bitterlich, VLF-Project, Univ. of Innsbruck, Innsbruck, Austria, September 1, 1970, NTIS No. AD719875.
16. Grisseemann, Ch., et al, "VLF/LF Antennas and Waves in Liquid and Solid Media," Final Scientific Report, AFCRL-71-0197, Contract No. F61052-69-C-0007, Univ. Doz. D. W. Bitterlich, VLF-Project, Univ. of Innsbruck, Innsbruck, Austria, December 31, 1970, NTIS No. AD725768.
17. Kueckin, J. A. "Packset Radio Antenna Measurements," IEEE International Convention Record, Part 5, pp 261-270, 1966.
18. Krupka, Zdenek, "The Effect of the Human Body on Radiation Properties of Small-Sized Communication Systems," IEEE Trans. on Antennas and Propagation, Vol. AP-16, No. 2, pp 154-163, March 1968.
19. Shepard, N. H. and Chaney, W. G., "Personal Radio Antennas," IRE Trans. Vehicular Communications, Vol. VC-10, pp 23-31, April 1961.
20. Maclean, T. S. M., and Morris, G. "Short Range Active Transmitting Antenna with Very Large Height Reduction," IEEE Trans. on Antennas and Propagation, pp 286-287, March 1975.
21. Maclean, T. S. M. and Ramsdale, P. A. "Short Active Aerials for Transmission," Int. J. Electronics, Vol. 26, No. 2, pp 261-269, 1974.
22. Maclean, T. S. M., and Ramsdale, P. A., "Active Loop-Dipole Aerials," Proc. IEE, Vol. 118, No. 12, pp 1698-1710, December 1971.
23. Anderson, A. P., and Dawoud, M. M. "The Performance of Transistor Fed Monopoles in Active Antennas," IEEE Trans. on Antennas and Propagation, pp 371-374, May 1973.
24. Fanson, Philip L. and Chen, Ku-Mu, "Instabilities and Resonances of Actively and Passively Loaded Antennas," IEEE Trans. on Antennas and Propagation, pp 344-347, March 1974.
25. Dawoud, M. M., and Anderson, A. P., "Experimental Verification of the Reduced Frequency Dependence of Active Receiving Arrays," IEEE Trans. on Antennas and Propagation, pp 342-344, March 1974.

26. Daniel, Jean-Pierre and Terret, C., "Mutual Coupling Between Antennas--Optimization of Transistor Parameters in Active Antenna Design," IEEE Trans. on Antennas and Propagation, pp 513-516, July 1975.
27. Lindenmeier, Heinz, "Active Receiving Antennas for Very Low Frequencies," Digest of the 1972 Group on Antennas and Propagation International Symposium, Williamsburg, Virginia, IEEE, New York, December 11-14, 1972.
28. Turner, E. M., IEEE Conf. Rec., XVIII Annual Conference IEEE Vehicular Technology Group, 6-8 December 1967.
29. Meinke, H., "Aktive Antennen," Nachrichtentech. Z., Vol. 19, pp 697-705, 1966.
30. "Description and Specifications for Underground Radio Transceivers for Use in the Underground Workings of Mines," Chamber of Mines of South Africa, Johannesburg, January 19, 1973.
31. Vermeulen, D. J., and Blignaut, P. J., "Underground Radio Communication and Its Application for Use in Mine Emergencies," Trans. S. A. Institute of Electrical Engineers, Vol. 52, pp 94-109, April 1961.
32. "Mystery Radio to the Rescue at Moorgate," New Scientist, p 641, March 13, 1975.
33. "Fire Ground Communications Equipment," Types PRD 2200/PRD 2201, Product Brochure, The Plessey Company Limited, Hants, England.
34. "Technical Specification for a Fire Ground Communications System," Plessey Types PRD 2200 and PRD 2201, The Plessey Company Limited, Hants, England, March 4, 1974.
35. "'Inductorfone' Equipment," Mine Telephones and Signalling Equipment, Sheet 26, Plessey Communication Systems Ltd., Manchester, England.
36. Dushac, H. M., "Two-Way Wireless Voice Communication System for Underground Coal Mines," Internal Report, Lee Engineering Division, Consolidation Coal Company, February 1976, and personal communications with Mr. Dushac.

37. Chufo, R. L., Lagace, R. L., and Wilson L. R., "MF Mine Wireless Radio," Proceedings of Bureau of Mines Technology Transfer Seminar on Mine Communications, Pittsburgh, Pa., Bureau of Mines IC Washington, June 1977.
38. Bradburn, R. A., "Communications for Haulage Loop Arounds," Proceedings of Bureau of Mines Technology Transfer Seminar on Mine Communications, Pittsburgh, Pa., Bureau of Mines IC , Washington, June 1977.
39. Bradburn, R. A., and Foulkes, J. D., "Longwall Mining Communications," Proceedings of Bureau of Mines Technology Transfer Seminar on Mine Communications, Pittsburgh, Pa., Bureau of Mines IC , Washington, June 1977.
40. Collins Radio Group, Rockwell International, "Mine Wireless Communication System," Final Report, Bureau of Mines Contract H0346067, to be published, Spring-Summer 1978.
41. Lagace, R. L., Cohen, M. L., Emslie, A. G., and Spencer, R. H., "Propagation of Radio Waves in Coal Mines," Arthur D. Little, Inc., Final Report, Task F--Task Order No. 1., Bureau of Mines Contract No. H0346045, October 1975.
42. Emslie, A. G., and Lagace, R. L., "Propagation of Low and Medium Frequency Radio Waves in a Coal Seam," Radio Science, Vol. 11, No. 4, pp 254-261, April 1976.
43. Lagace, R. L., and Emslie, A. G., "Analysis of In-Mine Electromagnetic Wave Propagation Measurements," Arthur D. Little, Inc., Final Report, Task Order No. 4., Bureau of Mines Contract No. H0346045, to be published, Fall 1977.
44. Collins Radio Group, Rockwell International, "Propagation of EM Signals in Underground Mines," Final Report, Bureau of Mines Contract No. H0366028, to be published, May 1977.
45. Zikun, G. A., Luzhnev, Yu. M., Pozhar, E. A., "Apparatus of Underground High-Frequency Mine Rescue Communication 'Donetsk-1 M'," All-Union Scientific-and-Research Institute of Mine Rescue Matters, Donetsk Plant, U.S.S.R.

46. Long, R. G., "Acceptability Guidelines for Performance Characteristics of Underground Pager Phones," Arthur D. Little, Inc., Final Report, Bureau of Mines Contract No. J0166085, April 1977.
47. Wolf, R. A., "Design of Electrical Equipment for Intrinsic Safety," Proceedings of the First WVU Conference on Coal Mine Electrotechnology, West Virginia University, August 2-4, 1972.
48. Redding, R. J., INTRINSIC SAFETY--The safe use of electronics in hazardous locations, McGraw-Hill, London, 1971.
49. Moon, P., and Spencer, D. E., Field Theory for Engineers, D. VanNostrand Company, Inc., Princeton, New Jersey, 1961.
50. Wait, J. R., "Receiving Properties of a Wire Loop with a Spheroidal Core," Canadian Journal of Technology, Vol. 31, pp 9-14, January 1953.
51. Dunlavy, J. H. Jr., "Design Aspects of Ferrite Antennas in the Frequency Range Below 30 MHz," Proceedings of the 1968 Electronic Components Conference, Washington, D. C., May 9, 1968.
52. Belrose, J. S., "Ferromagnetic Loop Aerials," Wireless Engineer, Vol. 32, pp 41-46, February 1955.
53. Rorden, L. H., Bacon, L. C., and Smith, R. L., "Underground Telemetry System Development--Design Definition Phase," Develco, Inc., Interim Report on Defense Nuclear Agency Contract No. DNA 001-74-C-0298, July 1975.
54. Snelling, E. C., "Ferrites for Linear Applications, Part I - Properties," IEEE Spectrum, Vol. 9, No. 1, pp 42-51, January 1972.
55. Snelling, E. C., "Ferrites for Linear Applications, Part II - Performance Requirements," IEEE Spectrum, Vol. 9, No. 2, pp 26-32, February 1972.
56. Sams, H. W., Handbook of Electronic Tables and Formulas, 2nd Ed., Herrington, D., and Meacham, S., Ed., Howard W. Sams and Co., Inc. Bobbs-Merrill Co., Inc., Indianapolis, 1962.
57. Bohley, P., David, R. J., and Walter, C. H., "Man-Pack Loop Antenna System," The Ohio State University ElectroScience Laboratory, Final Report 3824-2, Naval Regional Procurement Office Contract N00123-74-C-0645, December 1974.

58. Davis, R. J., "The Development of a Multiturn Loop Antenna for the AN/PRC-77," The Ohio State University ElectroScience Laboratory, Technical Report 3824-1, Naval Regional Procurement Office Contract N00123-74-C-0645, December 1974.
59. Bohley, P., and Newman, E. H., "Development of a VHF Multiturn Loop Antenna for Seismic Sensor Systems," The Ohio State University ElectroScience Laboratory, Final Report Vol. #1, United States Army Materiel Command Contract DAAG-39-72-C-0041, March 1973.
60. Newman, E., Bohley, P., and Walter, C. H., "Two Methods for the Measurement of Antenna Efficiency," IEEE Trans. on Antennas and Propagation, Vol. AP-23, No. 4, pp 457-461, July 1975.
61. King, H. E., "Characteristics of Body-Mounted Antennas for Personal Radio Sets," IEEE Trans. on Antennas and Propagation, pp 242-244, March 1975.
62. Reggia, F., "Low-Profile VHF Antennas for Seismic Detection Systems," HDL-TR-1635, U. S. Army Materiel Command, Harry Diamond Laboratories, Washington, July 1973, NTIS No. AD766703.
63. Bernstein, S. I., et al, "Long-Range Communications at Extremely Low Frequencies," Proceedings of the IEEE, Vol. 62, No. 3, pp 292-312, March 1974.
64. Burrows, M. L., "ELF Antennas," Presentation at IEEE Antennas and Propagation Society Chapter Meeting, Washington, D. C., October 19, 1971.
65. IEEE Transactions on Communications, Special Issue on Extremely Low Frequency (ELF) Communications, Vol. COM-22, April 1974.
66. Wait, J. R., "Earth-Ionosphere Cavity Resonances and the Propagation of ELF Radio Waves," Radio Science, Vol. 69D, pp 1057-1070, August 1965.
67. Nessler, N., "Theoretical and Experimental Studies of VLF and LF Waves," Final Scientific Report--1973, AFCRL-TR-73-0174, Contract No. F 44620-72-C-0052, University of Innsbruck, Innsbruck, Austria, February 28, 1973, NTIS No. AD753778.
68. Nessler, N., "Considerations on the Dimensioning of Ferrite Antenna Amplifiers in the VLF Regions," Scientific Report No. 2,



AFCRL-69-0420, Contract No. F61052-69-C-0007, Univ. Doz., Dr. W. Bitterlich, VLF-Project, University of Innsbruck, Innsbruck, Austria, July 15, 1969, NTIS No. AD695489.

69. Lukavec, R., "Measured Properties of Small Self-Resonant Helical Antennas at Low Frequencies for Application in Dissipative Media," Scientific Report No. 8, AFCRL-69-0096, Contract No. 61(052)-902, Univ. Doz., Dr. W. Bitterlich, VLF-Project, University of Innsbruck, Innsbruck, Austria, December 1, 1968, NTIS No. AD684578.

(This page intentionally left blank)

#### IV. COUPLING TO EXISTING CONDUCTORS IN MINES

##### A. SUMMARY

To evaluate the potential advantages and practicality of extending mine wireless ranges by coupling to existing conducting structures in mines, theoretical equations were developed, relating loop antenna strength, frequency, and its distance from two-wire cables and structures, to the current and voltage induced in that structure by the loop antenna. These equations allow one to compute not only the loop-to-structure coupling but also loop-to-loop coupling via the two-wire structure. Results computed for three frequencies (3, 100, and 1000 kHz) indicate that:

- performance improves with closeness to the two-wire structure, increased separation of the wires, and increasing frequency up to about 0.5-1 MHz in a mine tunnel;
- loop-to-loop communications along a haulageway appear practical in the presence of a trolley wire system and may also be usable in the presence of untwisted cables and single wires attached to the ribs;
- coupling to twisted pair cables is severely reduced over that for untwisted pairs;
- performance should be significantly reduced for loops located in tunnels adjacent to the one in which the conductors are located.

The results for representative cases of interest are plotted.

##### B. INTRODUCTION

The objective is to calculate the coupling between a loop antenna which can reasonably be carried by a miner and conductors which are commonly found in mines. The antenna loop has a magnetic moment of  $M=NIA$  where  $N$  is the number of turns,  $I$  is the current in the loop, and  $A$  is its area. For an antenna which is wrapped around a man, a reasonable source strength is  $M = 1/2$  to 4 amp-turn meter<sup>2</sup>. We will use the value 1 amp-turn meter<sup>2</sup> here. The conductors available for coupling to are:

- telephone lines (twisted and untwisted pairs);
- trailing cables (either twisted pairs, twin-leads or more complex structures);
- trolley wire/rail (approximated here by a two-wire line) and
- power distribution lines (a conventional 3-phase cable for mine use).

The simpler, in-air case will be examined to get upper bounds for performance. These results should be applicable within the haulageways where the conductors are located. Transmitter requirements will be more severe for coupling beyond the immediate tunnel cross-section in which the conductors are located because of the additional losses introduced by the coal and surrounding rock.

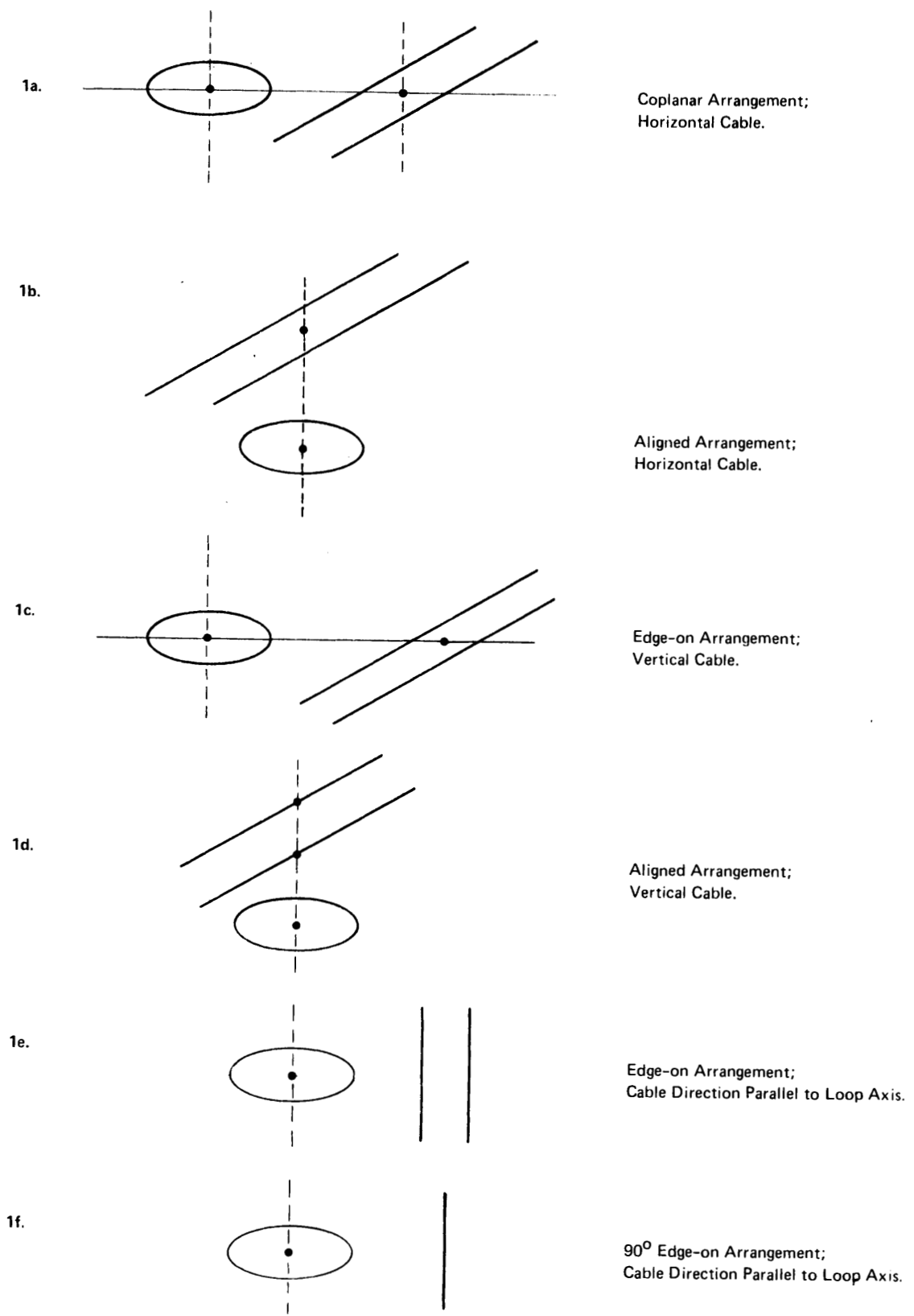
C. REPRESENTATIVE GEOMETRIES

We first examine several different cases of coupling between a loop, assumed of infinitesimal size, and twin-lead and twisted-pair conductors. The assumption of an infinitesimal loop is justified if the diameter of the loop, approximately 0.3 m, is much less than the wavelength of the signal, and the loop-to-conductor spacing. Table 4-1 summarizes several situations of interest. Figure 4-1 shows several basic arrangements of the transmitting loop with respect to simple twin-lead conductors. If the miner wears the transmitting antenna as a bandolier around his body, then situations 1a and 1b represent cases where the planes of the twin-leads and the loop are horizontal; while situations 1c and 1d represent cases where the plane of the twin-lead cable is vertical but the loop itself is still in the horizontal plane. Situations 1e and 1f represent cases where the cable direction is parallel to the

TABLE 4-1  
TYPICAL DIMENSIONS FOR STRUCTURES  
OF INTEREST IN A MINE

Frequencies	3kHz	to	1MHz
Wavelengths	$10^5$ m	to	$3 \times 10^2$ m
Trolley Lines (trolley wire to track spacings)	1m (low coal)	to	2m (high coal)
Twisted Pairs (cable diameters)	0.02m	to	0.07m
Flat Twin-Lead (lead spacings)	0.015m	to	0.05m
Three Conductor Cables (cable diameters)	0.02m	to	0.08m
Antenna-to-Cable Distances	2m	to	600m

Source: Arthur D. Little, Inc., Essex and Anaconda Catalogs



Source: Arthur D. Little, Inc.

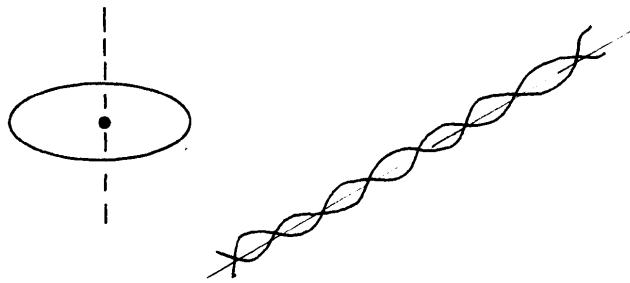
**FIGURE 4-1 DIFFERENT GEOMETRIES FOR A HORIZONTAL LOOP ANTENNA AND A TWIN-LEAD CABLE**

axis of the loop, but in case E the plane of the twin-lead cable contains the loop axis, while in case F the plane of the twin-lead cable is perpendicular to a plane containing the axis of the loop. These latter two situations where the direction of the cable is parallel to the axis of the loop are not considered as realistic alternatives. Figure 4-2 shows similar arrangements for a twisted-pair but since there is no unique plane which contains only the two wires of the twisted-pair, there are less cases of interest.

In general, the transmit loop antenna and the mine structure that is acting as the conductor will not have such simple relationships as those shown in Figures 4-1 and 4-2. The coplanar relationships in 1a and 1b are reasonable approximations for most situations where a horizontal twin-lead or a twisted-pair are mounted on the side wall of a tunnel or hung from the roof. In low coal, the conductor is unlikely to be more than 1/2 m above or below the plane of the transmitting antenna which may be 2 m to 600 m away. At 2 m the angle above or below the transmitter loop plane is  $14^\circ$  while at 600 m the angle is  $0.05^\circ$ .  $\cos 14^\circ$  is about 0.97, so the field strength at a conductor 1/2 m above the plane of the transmit loop is approximately equal to that for a conductor in the plane of the transmit loop. Assuming a 2 m high seam for high-coal, the maximum angle of the conductor above the plane of the transmitter loop is  $37^\circ$ , which has a cosine of 0.80, so the absence of coplanarity is more significant here. However, at distances greater than 6 m, the coplanarity assumption is a reasonable approximation, as shown in Figure 4-3.

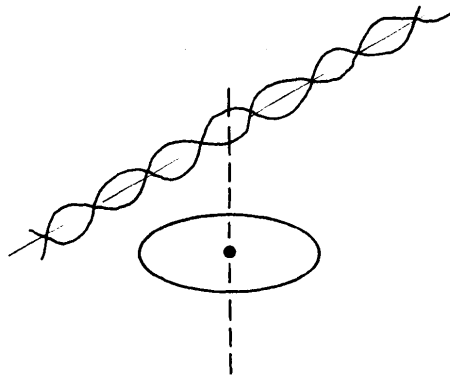
Similarly, when the twin-lead cable is in the horizontal plane and suspended from the roof away from a wall, case 1a is still a reasonable description of the situation as the transmitting loop approaches from 600 m to 6 m in high-coal, and to 2 m in low-coal. There can then be a transition region as the transmitting loop moves under the cable until the situation of 1b is achieved.

2a.



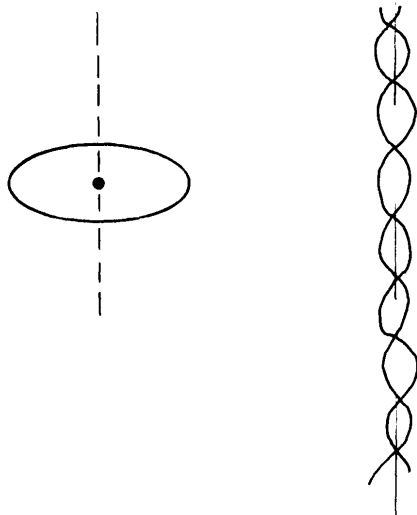
Coplanar Arrangement  
(similar to 1a and 1c)

2b.



Aligned Arrangement  
(similar to 1b and 1d)

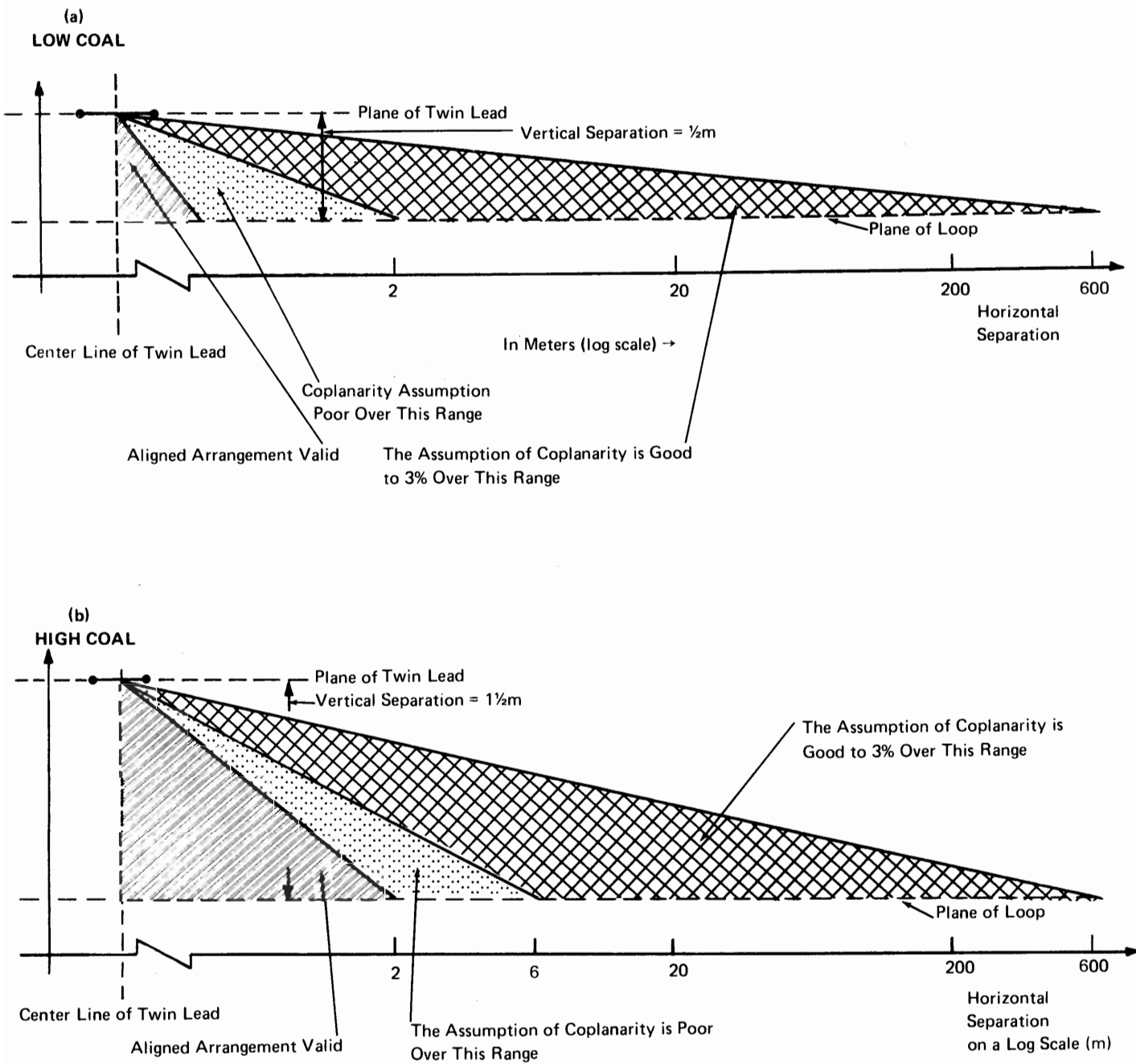
2c.



Edge-on Arrangement  
(similar to 1e and 1f)

Source: Arthur D. Little, Inc.

FIGURE 4-2 DIFFERENT GEOMETRIES FOR A HORIZONTAL LOOP ANTENNA AND A TWISTED-PAIR CABLE



Source: Arthur D. Little, Inc.

FIGURE 4-3 RANGES OF VALIDITY OF COPLANARITY ASSUMPTIONS



Similar ranges of validity apply to the case where the twin-lead cable is in the vertical plane. A special case of this is the trolley-wire system, which because of its size with respect to the tunnel dimensions, the loop position will always lay vertically somewhere between the trolley-wire and the rail return.

D. COUPLING TO SIMPLE TWO-WIRE LINES

1. Case 1a - Coplanar Geometry

a. Electric Field Method

This case has been considered in detail by Albert A. Smith, Jr. in a paper called "The Response of a Two-Wire Transmission Line Excited by the Non-uniform Electromagnetic Fields of a Nearby Loop," published in the IEEE Transactions on Electromagnetic Compatibility, EMC-16, 196-200 (1974). The equations given in this paper for the near, or inductive-field, case are valid over most of the ranges of parameters of interest to us, see Table 4-2. The variable  $\beta R = 2\pi R/\lambda$  should be much less than unity; R is the spacing between the loop and the cable and  $\lambda$  is the wavelength of the signal in air.

TABLE 4-2  
REGIONS OF VALIDITY FOR USING  $\beta R \ll 1$  CRITERION,  
THE INDUCTIVE-FIELD APPROXIMATION  
(IN AIR)

f(kHz)	3	100	1000
$\lambda$ (m)	$10^5$	$3 \times 10^3$	$3 \times 10^2$
R(m)			
2	$1.3 \times 10^{-4}$	$4.2 \times 10^{-3}$	$4.2 \times 10^{-2}$
20	$1.3 \times 10^{-3}$	$4.2 \times 10^{-2}$	$4.2 \times 10^{-1(1)}$
200	$1.3 \times 10^{-2}$	$4.2 \times 10^{-1(1)}$	$4.2^{(2)}$
500	$3.2 \times 10^{-2}$	$1.1^{(1)}$	$10.5^{(2)}$

The entries in the table are values of  $\beta R = 2\pi R/\lambda$  in air.

(1) Transition zone between inductive and radiation fields.

(2) Radiation - field zone.

Source: Arthur D. Little, Inc.

If the two-wire line is represented as a transmission line terminated at both ends by impedances, Smith has developed several simplified expressions for the current induced in the load resistance terminating the transmission line. Figure 4-4 defines the quantities of interest in the expressions. The loop is at a distance R from the center line of the transmission line and at a distance w from the start of the line. The transmission line is s long and consists of two parallel conductors spaced b apart. Both the loop and the transmission line are in the plane x-z. The electric field in the plane x-z due to the loop is a function of r only. In most mine situations, s is a large dimension, at least several hundred meters,  $b \ll R$  (see Table 4-1 for values of b), and the loop is not close to either end of the transmission line. Then, according to Smith, the following approximations can be made:

- $E_z =$  a constant depending on R over a length of the transmission line  $L = R$ .
- $E_z = 0$  over the rest of the line.
- $E_x =$  a constant depending on R over a length of the transmission line  $L = R$ , and 0 over the rest of the line.

A current is induced in the transmission line because of the non-uniform distribution of these fields. In the case of a radiation field, the current is principally induced by the phase difference of the wave over the two conductors.

The normalized expression for the current in the load at the end of the line is given by:

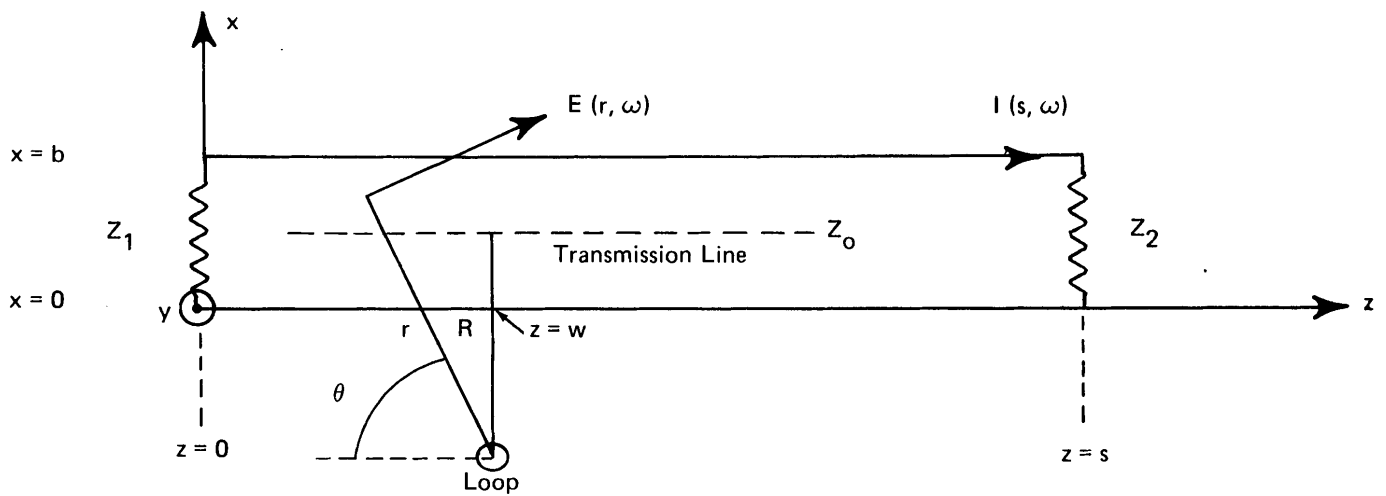
$$\frac{I(s, \omega)}{E(R, \omega)} = \frac{I_1(s, \omega)}{E(R, \omega)} + \frac{I_2(s, \omega)}{E(R, \omega)} \quad (1)$$

where

$$\frac{I_1(s, \omega)}{E(R, \omega)} = \left( -2j \sin \frac{\beta b}{2} \right) \frac{2 \sin(\beta L/2)}{D\beta} \quad (2)$$

$$\cdot \left[ Z_0 \cos \beta w + j Z_1 \sin \beta w \right] P \quad (1)$$

(1) From Smith IEEE article previously cited.



Source: Smith, IEEE Trans EMC, EMC-16 196-200 (1974)

FIGURE 4-4 GEOMETRY OF THE TRANSMITTING LOOP AND TRANSMISSION LINE FOR THE CASE OF FIGURE 4-1(a)

$$\text{and } \frac{I_2(s, \omega)}{E(R, \omega)} = \frac{bZ_0 R^2 w}{D [R^2 + w^2]^{3/2}} Q_1 + \frac{b(Z_0 \cos \beta s + jZ_1 \sin \beta s) R^2 (s - w)}{D [R^2 + (s - w)^2]^{3/2}} Q_2 \quad (1) \quad (3)$$

$$P = \frac{1 + (b/2R)^2 - j(b/R) \cot(\beta b/2)}{[1 - (b/2R)^2]^2} \quad (1) \quad (4)$$

$$Q_1 = \cos \beta [(R^2 + w^2)^{1/2} - R] - j \sin \beta [(R^2 + w^2)^{1/2} - R] \quad (1) \quad (5)$$

$$Q_2 = \cos \beta [(R^2 + (s - w)^2)^{1/2} - R] - j \sin \beta [(R^2 + (s - w)^2)^{1/2} - R] \quad (1) \quad (6)$$

$$\begin{aligned} D &= (Z_0 Z_1 + Z_0 Z_2) \cos \beta s + j(Z_0^2 + Z_1 Z_2) \sin \beta s \quad (1) \\ \beta &= 2\pi/\lambda \text{ phase constant} \\ \lambda &= \text{wavelength} \\ Z_0 &= 276 \log_{10} (200b/a) \text{ characteristic impedance} \quad (1) \\ b &= \text{spacing (meters)} \\ a &= \text{diameter (cm)}. \end{aligned} \quad (7)$$

$$L = R \quad (8)$$

$$Z_0 = Z_1 = Z_2 \quad (9)$$

Since  $s$  is usually larger than  $R$  and the loop is not near the ends of the line, it is reasonable to place  $E_x = 0$  as well as  $E_z = 0$  at the ends of the line. Then, only the term  $I_1(s, \omega)/E(R, \omega)$  due to  $E_z$  over the length of line  $L = R$  near the loop contributes to the current in the line.

As  $R$  grows larger, the nature of the loop-caused field at the line changes from inductive to radiative. Then, the equations are modified to:

$$\frac{I_1(s, \omega)}{E(R, \omega)} = \dots \text{ as above } \dots \quad (1) \quad (10)$$

except

$$P = \frac{1 - j(b/2R) \cot(\beta b/2)}{1 - (b/2R)^2}, \quad (1) \quad (11)$$

and

$$\frac{I_2(s, \omega)}{E(R, \omega)} = \frac{bZ_0 R w}{D(R^2 + w^2)} Q_1 + \frac{b(Z_0 \cos \beta s + jZ_1 \sin \beta s) R(s - w)}{D[R^2 + (s - w)^2]} Q_2 \quad (1) \quad (12)$$

with  $Q_1$  and  $Q_2$  as above and  $Z_1 = Z_2 = Z_0$ .

These complex expressions must be rearranged so that their magnitudes can be evaluated. Since the inductive-field assumption is valid over most of the ranges of interest to us, and since it is reasonable to assume that  $w > R$  for all cases of interest to us, only the expression for  $I_1$  is rearranged. Then we have:

$$\frac{I_1(s, \omega)}{E(s, \omega)} = \frac{\lambda}{\pi Z_0} \frac{\sin\left(\frac{\pi b}{\lambda}\right) \sin\left(\frac{\pi R}{\lambda}\right)}{\left[1 - \left(\frac{b}{2R}\right)^2\right]^2} \times \sqrt{\left\{ \left(1 + \frac{b^2}{4R^2}\right)^2 + \frac{b^2}{R^2} \cot^2\left(\frac{\pi b}{\lambda}\right) \right\}} \quad (13)$$

If  $b \ll 2R$ :

$$\frac{I_1(s, \omega)}{E(s, \omega)} = \frac{\lambda}{\pi Z_0} \sin\left(\frac{\pi b}{\lambda}\right) \sin\left(\frac{\pi R}{\lambda}\right) \sqrt{\left\{ 1 + \frac{b^2}{R^2} \cot^2\left(\frac{\pi b}{\lambda}\right) \right\}} \quad (14)$$

If  $R \ll \lambda$ , and  $b \ll R$ , then;

$$\begin{aligned} T = \frac{I_1(s, \omega)}{E(s, \omega)} &= \frac{\pi b R}{\lambda Z_0} \sqrt{\left(1 + \frac{\lambda^2}{\pi^2 R^2}\right)} \\ &\approx \frac{b}{Z_0} \end{aligned} \quad (15)$$

The value of this transfer admittance

$$T = \frac{I_1(s, \omega)}{E(s, \omega)} \quad (16)$$

has been evaluated below for three cases:

1. Twin-lead, telephone and power cable  
b = 0.04 m;  $Z_o = 280.6$  ohms  
R  $\leq$  20 m; T = -77dB  
R  $\geq$  200 m; T = -78dB
2. Low coal, trolley system (Two-wire line approximation)\*  
b = 1 m; a = 0.05 m;  $Z_o = 442.4$  ohms  
R  $\leq$  20 m; T = -53dB  
R  $\geq$  200 m; T = -55dB
3. High coal, trolley system (Two-wire line approximation)\*  
b = 2 m; a = 0.05 m;  $Z_o = 525.3$  ohms  
R  $\leq$  20 m; T = -48dB  
R  $\geq$  200 m; T = -50dB

Table 4-3 lists the values of electrical field strength in the plane of the loop at 2 m from a loop antenna in air as a function of frequency. It also indicates the reduction in field strength at increasing distances. Using these field strengths and the values of T given above, the values of current induced in the conductors and the matched loads have been calculated and tabulated in Table 4-4.

#### b. Magnetic Field Method

The value of these induced currents can also be estimated by an equivalent simpler method based on the voltage induced in the pair by the loop magnetic flux cutting the pair. In the above coplanar case, the  $\theta$ -component of the loop field,  $H_\theta$ , would be used, and the induced voltage estimated by using the approximation of an equivalent constant flux density distribution  $B_\theta = \mu_o H_\theta(R)$  linking an area enclosed by the separation b of the cable pair over a length L along the pair. Here, L is equal to 2R, instead of R, where R is the shortest distance from the center of the loop to the midpoint between the cable conductors as before, and  $H_\theta(R)$  is the value of loop magnetic field at this midpoint.

---

\* In practice, the trolley line characteristic impedance is closer to 200 ohms, because of the large effective diameters of the trolley wire/feed conductors and the rail return conductors.

TABLE 4-3  
VALUES OF  $E_{\phi}$  IN THE PLANE  
OF A LOOP AT A DISTANCE R AWAY IN AIR  
(Source Strength  $M = 1 \text{ amp-meter}^2$ )

<u>Frequency</u>	<u>3kHz</u>	<u>100kHz</u>	<u>1MHz</u>
R(m)			
2	480 $\mu$ V/m	15,800 $\mu$ V/m	158,000 $\mu$ V/m
20	-40dB*	-40dB*	-39dB*
200	-80dB	-79dB	-67dB
500	-96dB	-93dB	-76dB

Source: Arthur D. Little, Inc.

---

\*dB reduction with increasing distance relative to 2 meter values

TABLE 4-4  
 CURRENTS IN  $\mu$  AMPERES INDUCED IN CONDUCTORS  
 FOR THE SITUATION OF FIGURE 4-1a  
 (IN AIR)

(a) Frequency = 3kHz				
b(m)	0.04		1	2
R(m)				
2	0.06		1.0	1.7
20	$6.6 \times 10^{-4}$		$1.0 \times 10^{-2}$	$1.9 \times 10^{-2}$
200	$6.6 \times 10^{-6}$		$1.0 \times 10^{-4}$	$1.9 \times 10^{-4}$
500	$9.6 \times 10^{-7}$		$1.6 \times 10^{-5}$	$2.6 \times 10^{-5}$
(b) Frequency = 100kHz				
b(m)	0.04		1	2
R(m)				
2	2.2		34.8	62
20	$2.2 \times 10^{-2}$		0.35	0.62
200	$2.4 \times 10^{-4}$		$4.0 \times 10^{-3}$	$7.0 \times 10^{-3}$
500	-*		-*	-*
(c) Frequency = 1MHz				
b(m)	0.04		1	2
R(m)				
2	22.4		356	632
20	0.26		4.0	7.0
200	-*		-*	-*
500	-*		-*	-*

Source: Arthur D. Little, Inc.

Entries in the Table are currents in  $\mu$ A for a source strength of  $M = 1$  amp-meter<sup>2</sup> and matched terminations  $Z_1 = Z_2 = Z_0$

\* Dash indicates that inductive field approximations do not apply at these ranges for the indicated frequencies.



In the inductive field region of interest, examination of the reciprocal problem of coupling from a long two-wire line to a small loop reveals that the mutual coupling impedance  $Z_m = V_{loop}/I_{line}$ , is identical for both the coplanar-1a and coaxial (aligned) - 1b configurations. Therefore, for the aligned case (1b) one can simply use the coplanar values computed above, or utilize a value of L equal to R, (as used in Smith's approximate E-field method) in order to compensate for the factor of two introduced by the  $H_r$  field that now links the cable, and which is twice the strength of the  $H_\theta$  loop field in the inductive field region. The approximate flux linkage method of computation is illustrated below for this coaxial (aligned) case 1b in which the r-component,  $H_r$ , of the loop field is the appropriate one to use. (This result has been verified by evaluating the appropriate integrals.)

## 2. Case 1b - Aligned Geometry, Magnetic Field Method

To estimate the voltage induced in the twin lead cable conductors in the aligned case 1b, the  $H_r$  field strength will be assumed constant over a line length  $L = R$ , and zero elsewhere on the line, for computing the effective flux linking the cable as noted above. Therefore the required  $H_r$  field strength is that produced by the loop at a distance R, which again is the shortest distance from the center of the loop to the midpoint between the cable conductors. The effective area being linked by the flux is given by  $Lb = Rb$ . The relevant expressions are:

$$H_r(\theta = 0) = \frac{M}{4\pi} \frac{2}{R^3} \sqrt{(\cos \beta R + \beta R \sin \beta R)^2 + (\beta R \cos \beta R - \sin \beta R)^2} \quad (17)$$

where the symbols have their usual meaning. Now the flux is given by:

$$\phi = Ba \simeq \mu_0 H_r (Rb) \quad (18)$$

and by Lenz's law, the induced series voltage is given by:

$$V \simeq \omega \mu_0 (Rb) H_r \quad (19)$$

Substituting the expression for  $H_r$  and simplifying, leads to the expression:

$$V \simeq \frac{\mu_0 f M b}{R^2} \sqrt{[1 + \beta^2 R^2]} \quad (20)$$

If  $2\pi R \ll \lambda$ , then

$$V = \frac{\mu_0 f M b}{R^2} \quad (21)$$

The corresponding expressions for the coplanar case - 1a, which utilize the loop  $H_\theta$  field component at  $\theta = \pi/2$  are:

$$V \simeq \omega \mu_0 (2Rb) H_\theta \quad (22)$$

and

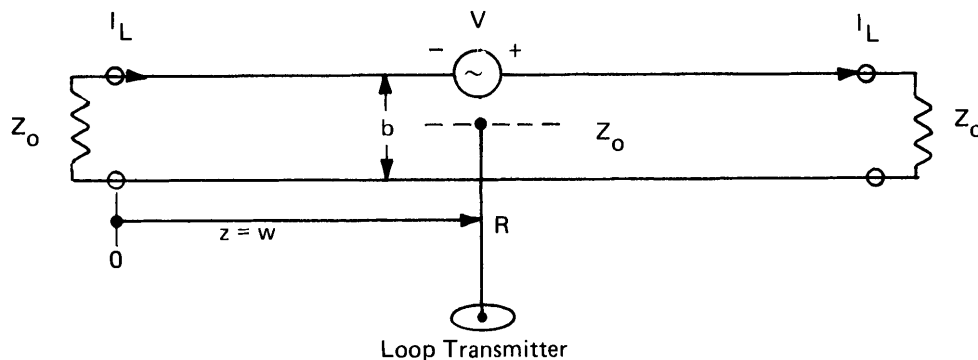
$$V \simeq \frac{\mu_0 f M b}{R^2} \sqrt{1 - \beta^2 R^2 + \beta^4 R^4} \quad (23)$$

which reduces to Equation (21) when  $2\pi R \ll \lambda$ , as it should.

Table 4-5 presents the results of these calculations for  $M = 1$  ampere-meter<sup>2</sup> and the parameters listed. The corresponding currents induced in the load at each end of the matched cable is then given by:

$$I_L = \frac{V}{2Z_0} \quad (24)$$

The equivalent transmission line excitation and terminations are shown in Figure 4-5. As discussed above, the induced voltage is identical for both the aligned and coplanar (shown) geometries. The above technique can also be applied to the cases of arbitrary loads  $Z_1$  and  $Z_2$  terminating the transmission line.



Source: Arthur D. Little, Inc.

FIGURE 4-5 EQUIVALENT TRANSMISSION LINE CIRCUIT FOR INDUCED VOLTAGE AND CURRENT (Case of  $Z_1 = Z_2 = Z_0$ )

### 3. Unfavorable Geometries

Because the plane of the cable conductors is rotated through  $90^\circ$  between the situations of Figures 4-1a and 1c and Figures 4-1b and 1d, the flux linkage in situations approximating those of Figures 4-1c and 1d is substantially reduced below those of the two cases considered above, causing a corresponding major reduction in the magnitude of the induced signals. Alternatively stated, in Figure 4-1c, the values of  $E_\phi$  at the two conductors are equal because they are the same distance from

TABLE 4-5  
 VOLTAGES INDUCED IN CABLE CONDUCTORS  
 IN THE SITUATION OF FIGURE 4-1b  
 (IN AIR)

(a) Frequency = 3kHz			
b (m)	0.04	1	2
R (m)			
2	37.6 $\mu$ V	940 $\mu$ V	1.9mV
20	0.38 $\mu$ V	9.6 $\mu$ V	19.2 $\mu$ V
200	3.8nV	96nV	192nV
500	0.6nV	15nV	30nV
(b) Frequency = 100kHz			
b (m)	0.04	1	2
R (m)			
2	1.3mV	31.4mV	62.6mV
20	12.6 $\mu$ V	320 $\mu$ V	640 $\mu$ V
200	132nV	3.4 $\mu$ V	6.6 $\mu$ V
500	28nV	724nV	1.4 $\mu$ V
			*
(c) Frequency = 1MHz			
b (m)	0.04	1	2
R (m)			
2	12.6mV	0.32V	0.64V
20	136 $\mu$ V	3.4mV	7.0mV
200	5.4 $\mu$ V	138 $\mu$ V	276 $\mu$ V
500	2.2 $\mu$ V	54 $\mu$ V	108 $\mu$ V

Source: Arthur D. Little, Inc.

Voltage values are for a source strength of  $M = 1$  amp-meter<sup>2</sup> and matched terminations  $Z_1 = Z_2 = Z_0$ .

\* Values of voltage above the dashed lines can be compared with the corresponding current values in Table 4-4 by dividing the above voltages by  $2Z_0$ . Values of voltage below the dashed line are coarser estimates for the transition and radiative field regions.

the loop, while in Figure 4-1d the E-field at the conductor is effectively zero. In both cases no lines of magnetic flux link the conductors.

Similarly, the signals induced by the loop antenna in arrangements approximating Figures 4-1e and 4-1f are also significantly less than those of cases 1a and 1b because the net flux linkages are zero as shown, and still insignificant for small deviations from the alignments shown.

#### E. COUPLING TO TWISTED-PAIR CABLE

We have not performed similar calculations for the twisted-pair cases because the paper "Predicting the Magnetic Fields from a Twisted-Pair Cable" by J. R. Moser and R. F. Spencer, IEEE Trans. EMC, EMC-10, 324-329 (1968) states that the field from a twisted pair is reduced by 50dB from the field from a twin-lead at a distance  $d = 1.5p$  from the cable, where  $p$  is the pitch of the twisted pair, assuming both wires are carrying the same current. Assuming reciprocity, this implies a reduction of at least 50dB in the inward coupling parameter for all twisted-pairs with  $p < 1$  m, which is still a conservative relatively large (or loose) pitch in practice.

#### F. LOOP-TO-LOOP COUPLING VIA THE LINE

By the principle of reciprocity it is possible to use the loop-to-line coupling equations to compute the coupling between a transmit and a receive loop via the line. The equations developed above in D.2 for the induced voltage in the line using the magnetic flux linkage approach are particularly convenient in this regard, although the equations using the E-field approach to compute the induced line current can also be utilized by first dividing by  $2Z_0$  to get the voltage.

Proceeding with the induced voltage approach in D.2 we have, by reciprocity,

$$Z_m = \frac{V_{oc-line}}{I_{loop}} = \frac{V_{oc-loop}}{I_{line}} \quad (25)$$

where  $Z_m$  is the mutual coupling impedance, and  $V_{oc-line}$  is given by Equations (20), (21) or (23), with  $M$  in these equations given by

$$M = NA_{loop} \quad (26)$$

Therefore,

$$V_{oc-loop} = Z_m I_{line} = \frac{V_{oc-line}}{I_{loop}} I_{line} \quad (27)$$

so line-to-loop coupling for a given value of  $I_{line}$  can be computed by substituting (20), (21) or (23) and (26) with  $NA = N_r A_r$  into (27), where the subscript  $r$  denotes receive loop; and loop-to-loop coupling via the line can be computed by further substituting (24) for  $I_{line}$  and (26) with  $NA = N_t A_t$  into (27), where the subscript  $t$  denotes transmit loop.

When the ranges from the loops to the line are much smaller than the wavelengths, a commonly encountered practical case in coal mines, Equation (21) can be used for  $V_{oc-line}$ . Then for line-to-loop coupling (27) becomes

$$V_{oc-loop} = \frac{\mu f b N_r A_r}{R_r^2} I_{line} \quad (28)$$

and for loop-to-loop coupling (27) becomes

$$V_{oc-loop-r} = \frac{(\mu f b)^2 N_r A_r N_t A_t}{2Z_o R_r^2 R_t^2} I_{loop-t} \quad (29)$$

Equations (28) and (29) are the formulas which apply for a matched lossless transmission line. For a lossy matched line, (28) and (29) would be multiplied by  $e^{-\alpha \ell}$  where  $\alpha$  is the line attenuation in nepers per meter,  $\ell$  in (28) is the distance in meters along the line from the signal generator to the loop, and  $\ell$  in (29) is the length of line in meters separating the transmit and receive loops. Equations (28) and (29) can be used to calculate numerical results for the coupling factors between line and loop and loop-to-loop via the line, and the absolute signal voltage levels induced in the receive loop, for typical guided wireless configurations in mine haulageways.

## G. SIGNAL-TO-NOISE RATIO ESTIMATES

Estimates of output signal-to-noise ratios can be obtained by comparing the signal levels given by (28) and (29) with the corresponding output noise voltages induced in the receive loop by the ambient H-field noise, or by comparing the measured H-field noise levels in the air with the calculated H-field signal levels in the air given by equations (28) and (29) divided by  $2\pi f \mu N_r A_r$ . Namely, for line-to-loop communications, the received H-field signal level is

$$H_r = \frac{b I_{\text{line}}}{2\pi R_r^2} \quad (30)$$

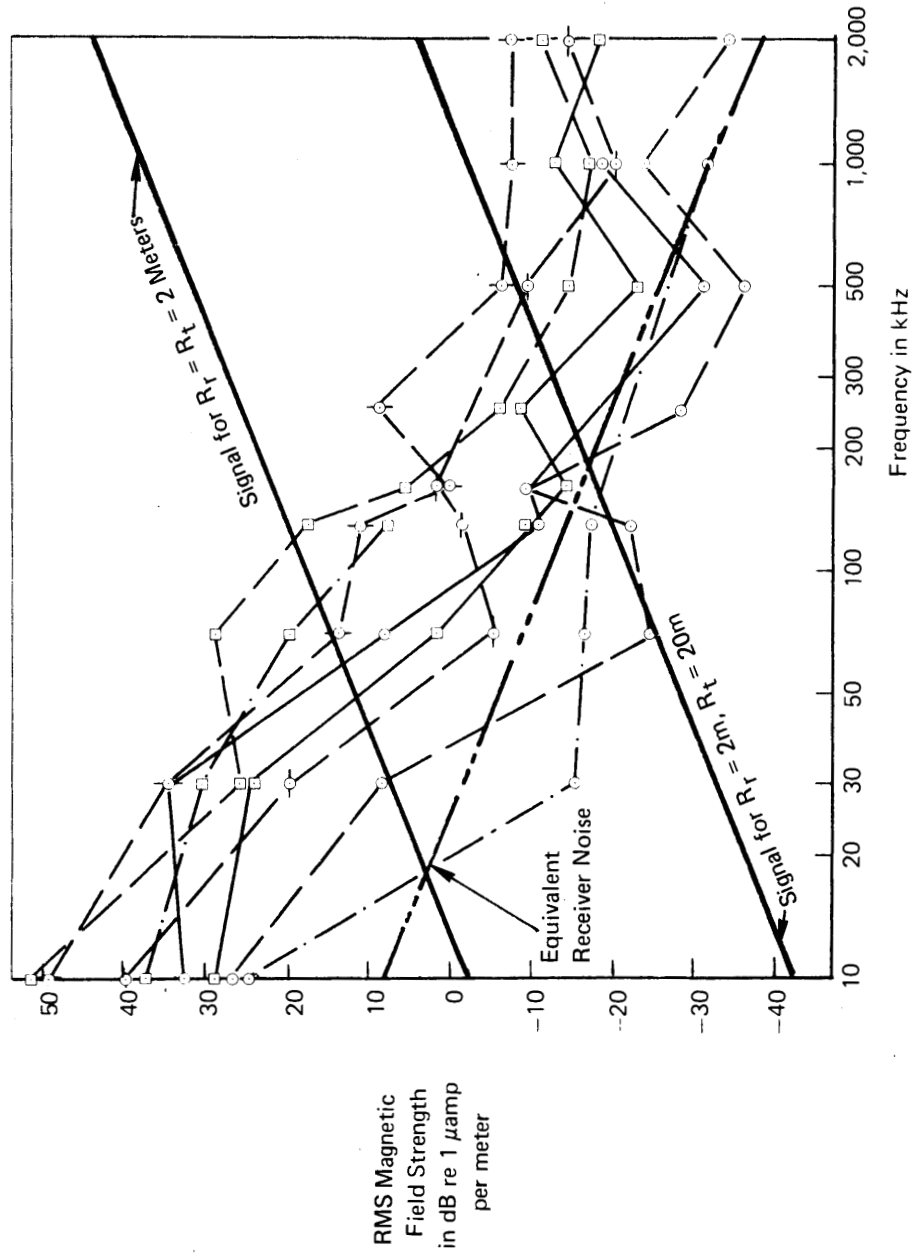
and for loop-to-loop communications, the received H-field signal level is

$$H_r = \frac{\mu f b^2 N_t A_t}{4\pi Z_0 R_r^2 R_t^2} I_{\text{loop-t}} \quad (31)$$

Equations (28) and (30) are convenient to use in cases where the line is direct-driven by a signal source, as in the case of a trolley wire carrier system; whereas (29) and (31) apply to cases where a matched dedicated line or trolley wire is inductively driven by a loop-fed signal source.

Figures 4-6 and 4-7 compare received H-field mine noise levels and calculated signal levels for a loop-to-loop via the line communications link. The curves are plotted versus frequency. A narrow-band FM radio communication system having an IF bandwidth  $B = 12$  kHz, receiver noise figure  $F = 6$  dB, transmit air-core loop magnetic moment  $M_t = I_t N_t A_t = 1$  amp-m<sup>2</sup>, and receive air-core loop effective turns area  $N_r A_r = 1$  m<sup>2</sup>, similar to a system presently being considered for wireless mine communication applications by Collins Radio Group on Bureau of Mines Contract H0346047. The rms noise levels chosen to characterize the mine electromagnetic noise environment were derived from the sample of magnetic

Legend for Mine Noise Curves Shown on Figure 2-7  
 Noise Levels Based on a 12 kHz Receiver Bandwidth  
 Two-Wire Line Conductor Separation -  $b = 2$  Meters  
 Transmit Moment -  $M_t = 1$  amp -  $m^2$   
 Signal Attenuation Along Transmission Line Not Included

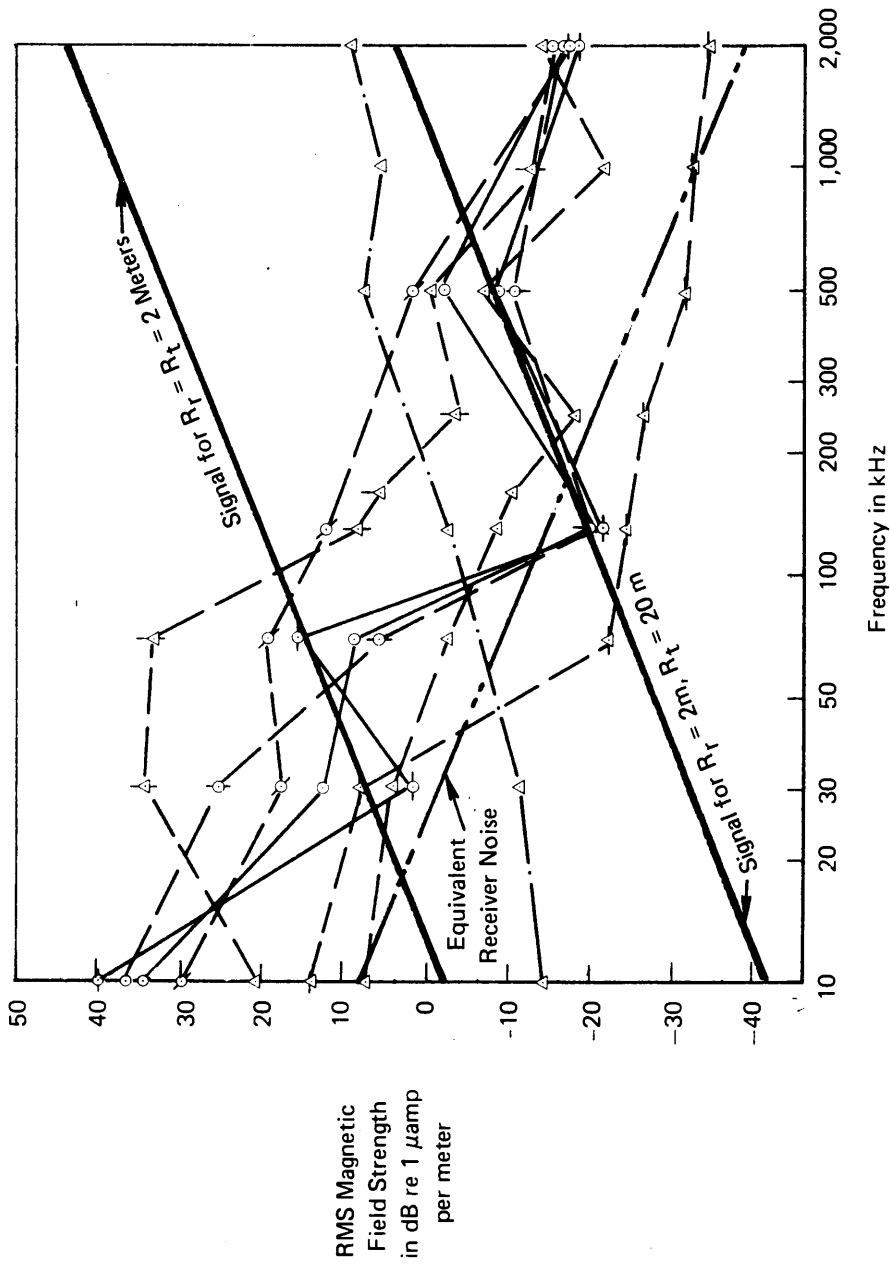


Source: National Bureau of Standards (Report NBSIR 74-389, June 1974) and Arthur D. Little, Inc.

FIGURE 4-6 COMPARISON OF LOOP-TO-LOOP-VIA-THE-LINE SIGNAL LEVELS IN AIR WITH EQUIVALENT RECEIVER NOISE AND REPRESENTATIVE RMS MAGNETIC FIELD NOISE LEVELS MEASURED IN THE McELROY COAL MINE



Legend for Mine Noise Curves Shown on Figure 2-8  
 Noise Levels Based on a 12 kHz Receiver Bandwidth  
 Two - Wire Line Conductor Separation -  $b = 2$  Meters  
 Transmit Moment -  $M_t = 1$  amp -  $m^2$   
 Signal Attenuation Along Transmission Line Not Included



Source: National Bureau of Standards (Reports NBS Technical Note 654, April 1974 Robena; and NBSIR 74-390, June 1974, Itmann) and Arthur D. Little, Inc.

FIGURE 4-7 COMPARISON OF LOOP-TO-LOOP-VIA-THE-LINE SIGNAL LEVELS IN AIR WITH EQUIVALENT RECEIVER NOISE AND REPRESENTATIVE RMS MAGNETIC FIELD NOISE LEVELS MEASURED IN THE ROBENA AND ITMANN COAL MINES

field, time-averaged, rms noise levels measured (with 1 kHz bandwidth instrumentation) at spot frequencies in the frequency range of interest in three coal mines by Bensema, Kanda, and Adams of the National Bureau of Standards. The measurement conditions and locations for these noise levels are the same as those described in the comprehensive legends of Figures 2-8 and 2-9. Also shown is a curve representing equivalent field strength for the intrinsic receiver noise.

In Figures 4-6 and 4-7, signal levels are shown for two transmitter and receiver configurations of interest relative to the location of a matched trolley wire/rail or dedicated wire/rail transmission line in a high-coal haulageway tunnel. The transmission line conductor separation,  $b$ , is 2 meters and the line characteristic impedance,  $Z_0$ , is 300 ohms. The first configuration is for the case when both transmit and receive units are located at different stations along the haulageway, but at the same distance of 2 meters from the transmission line and with the planes of both loops parallel to the plane of the transmission line. The second is for the case when only one unit is located 2 meters from the transmission line and the second unit is located 20 meters away from the line, perhaps in an adjacent entry. These signal curves apply strictly for an air medium, which the 2 meter case in a mine tunnel closely approximates. However, only minor downward corrections are necessary (and only at the highest, most favorable coupling frequencies) to apply the 20 meter results to the case of a homogeneous, moderately conducting medium ( $\sigma = 10^{-2}$  Mho/m). This can be seen by comparing the "30 meter" in-air and conducting medium curves in Figures 2-8 and 2-9.

Figures 4-6 and 4-7 show that the mine noise levels generally diminish with increasing frequency (approximately as  $1/f$ ), and that mine generated noise greatly exceeds receiver noise under most mine operational conditions in haulageways and near section mining machinery and power conversion equipment. These figures also show that signals which have been coupled onto and off transmission lines, such as trolley wire/rails, are high when the portable wireless transmit/receive units are close to these lines (the  $R_T = R_R = 2$  meter case); and that the signal field strength at the receiver increases proportional to frequency if the signal attenuation caused by resistive losses along the cable is neglected.

A reasonable radio circuit grade of performance for a wireless mine communication system is the Circuit Merit Figure #3 classification (occasional message repetitions required). This is the minimum figure normally considered for commercial radio service. It requires that the average rms carrier-to-noise ratio at the receiver be at least 10 dB or better for the mine noise conditions prevailing during the communication intervals. Comparing signal and noise levels according to this criterion, we find that loop-to-loop communications via the line can be established over significantly longer ranges than those obtainable in the absence of the line (Chapter II)

Figures 4-6 and 4-7 also suggest that, the higher the frequency above about 100 kHz, the better performance will be. However, in practice, the attenuation suffered by the signal while travelling along the transmission line (due mainly to resistive losses in the tunnel walls) also increases with frequency. This attenuation loss will cause the plotted signal curves to eventually droop downwards as the frequency is increased, with the number of dB to be subtracted from the signal curves depending on the length of transmission line between the two portable units. Theoretical analyses conducted by J. Wait\* of NOAA indicate that the attenuation rate along unloaded trolley wire/rail transmission lines in mine tunnels can vary from about 1 dB/km at 100 kHz to about 10 dB/km at 1 MHz. Wait\*\* has also shown that similar behavior, but at slightly higher attenuation rates, can be expected with single power cables

---

\* J.R. Wait and D.A. Hill, "Radio Frequency Transmission Via a Trolley Wire in a Tunnel with a Rail Return", to be published in the March, 1977 issue of IEEE Transactions on Antennas and Propagation

D.A. Hill and J.R. Wait, "Analysis of Radio Frequency Transmission Along a Trolley Wire in a Mine Tunnel", IEEE Transactions on Electromagnetic Compatibility, November, 1976.

\*\*J.R. Wait and D.A. Hill, "Low-Frequency Radio Transmission in a Circular Tunnel Containing a Wire Conductor Near the Wall", Electronics Letters, 24 June 1976, Vol. 12, No. 13, pp. 346-347.

and phone lines hanging from the roof of a mine tunnel (in this case the return current path is in the surrounding rock). The method of images can also be a useful tool for gaining understanding of signal behavior for such configurations. Taking these attenuation rates into consideration for a 1 km length of transmission line, the signal level curves can be expected to start decreasing above about 500 kHz, thereby defining a somewhat broad optimum operating region between approximately 200 kHz and 1 MHz. Recent tests conducted by Dushac\* with Plessey Telecommunications SSB portable radios operating at 425 kHz along trolley haulage-ways in several coal mines have shown that loop-to-loop via the line communication ranges in excess of 1/2 to 1 km are attainable with practically-sized portable units, and that such units are well suited for use in haulage loop-around operations for communication between the locomotive operator and the snapper who couples and uncouples coal cars.

When one of the portables is located in an adjacent entry (the  $R_r = 2m$ ,  $R_t = 20 m$  case) signal levels will be substantially reduced (by about 40 dB). However, one can also expect lower noise levels (by about 20 dB), thereby effectively decreasing the noise curves relative to the  $R_r = 2m$ ,  $R_t = 20 m$  signal curves by about 20 dB in the figures. Thus, marginal but adequate radio communication may still be possible at frequencies between about 300 kHz and 1 MHz when one of the units is located in an adjacent entry.

Other analyses, by Arthur D. Little, Inc.,\*\* also indicate that attenuation losses on trolley wire/rail transmission lines can increase by an order of magnitude if the line is heavily shunt loaded, as is the case for many trolley wire/rail lines. In such cases, loop-to-loop-via-the-line system longitudinal range will most likely be limited by the distance between discrete shunt loads such as power rectifiers.

---

\*Dushac, H.M., "Two-Way Wireless Voice Communication System for Under ground Coal Mines", Internal Report, Lee Engineering Division, Consolidation Coal Company, February, 1976.

\*\*Arthur D. Little, Inc., "Improvements for Mine Carrier Phone Systems," Report on Task II, Task Order No. 2, Contract No. HO346045, May 1977.

In conclusion, to better characterize the behavior and determine the limits and the practicality of both loop-to-loop via-the-line and totally wireless loop-to-loop communications in mines, a measurement program has been defined and is being conducted in several coal mines for the Bureau of Mines, PMSRC, by a measurement and analysis team consisting of Spectra Associates/Collins Radio Group on Contract H0366028 and Arthur D. Little, Inc., on Contract H0346045, Task Order No. 4.

(This page intentionally left blank)

## V. HYBRID NOISE CANCELLING DIVERSITY RECEIVING TECHNIQUE

### A. SUMMARY

A hybrid noise cancelling diversity receiving technique has been examined that would try to capitalize on the high levels of both electric and magnetic field noise components present in many parts of a mine at the frequencies of interest below 1 MHz. Namely, if the instantaneous correlation is high enough between the noise E and H field components, it should be possible to improve the output signal-to-noise performance of a mine wireless system by cancelling a major portion of the H-field noise picked up in a loop antenna by properly combining it (manually or automatically) with the E-field noise picked up by a dipole or whip antenna that would be insensitive to both the H-field signals generated by the wireless transmitter and the ambient H-field noise. This selectivity between signal and noise would come about from the fact that the loop signal transmitters generate very little E field and are coupled to the receiver primarily through magnetic induction. Calculations to date indicate that potential signal-to-noise improvements between 10-15 dB may be possible when the E and H noise components are 80% to 90% correlated, a condition which may prevail in the vicinity of severe noise sources. Such a S/N increase could then result in extending the range of a wireless communications system or reducing the power to attain a given range. The next step required in the pursuit of this approach is a set of basic field measurements to determine whether the degree of correlation between the E and H noise field components is high enough to warrant a more rigorous analysis and further development effort.

### B. INTRODUCTION

The review and analysis work treated in the previous chapters lead to the following comments and observations. No matter what equipment is used for mine wireless electromagnetic communications below about 1 MHz, one encounters three difficulties in underground mines.

The first is that at the low and medium frequencies desired, the attenuation and field fall off in a homogeneous conductor-free region are very high because of the surrounding medium losses and the fact that

near zone conditions prevail for the transmitter and receiver. To date, because of power limitations in portable equipment, it has been difficult to provide communications for distances up to a few thousand feet even in ideal ground. Depending upon the investigator, the model he establishes and the assumptions made about system parameters, the signal strength has been calculated to vary somewhere between  $r^{-1/2} e^{-\alpha r}$  and  $r^{-3} e^{-\alpha r}$  over the ranges of interest. This is a formidable barrier to overcome no matter what the specific details of the system are. Even the favorable results obtained from mine wireless propagation tests in Consolidation Coal's Ireland mine indicate that the desired portable unit wireless range of 1350 feet may only be attainable under the most favorable conditions of noise and medium conductivity. These results and a propagation model to fit them are presented in the Task F final report of this Contract\* and have been summarized in Chapter II of the present report.

The second difficulty is that in addition to the weak signal one expects to receive at extreme range, there can be an extremely high background of electromagnetic noise coming in with the signal due to a variety of causes. This noise is generated by DC traction machines, AC to DC converters, a variety of tools, mining equipment, pumps, compressors, etc., all of which are working in an active mine. Measurement of the noise power at various frequencies indicate that it is of significant level up to well above most of the frequencies one would like to use to establish a miner-to-miner voice-modulated EM communication system in the VLF to MF bands.

The third difficulty is that in an operating mine both signals and noise will be carried to most places where miners are located, as a result of the random excitation of trolley wires, pipes, tracks, telephone pairs, and the like.

Because of this chaotic physical environment, the receiving antenna of a wireless induction system receives a number of E and H components and reacts to a complicated vector summation of these. These components are derived from a number of sources, active and parasitic, and have a number of different properties. A few of these components may be listed:

- From nearby trolley wires there is an induction H field due to DC and AC power transients as well as trolley

---

\*Arthur D. Little, Inc., Task F--Final Report--"Propagation of Radio Waves in Coal Mines," Chapter IV, U.S. Bureau of Mines Contract HO346045, Task Order No. 1, October 1975.



phone currents around 100 kHz and its harmonics.

- From distant sources there may be plane waves of natural and man-made interference in which E and H are related by a characteristic impedance.
- From a nearby wireless transmitter there may be induction field components of correlated E and H arriving from an arbitrary direction with an arbitrary polarization.
- From trolley wires there may be strong E fields due to arcs and switching transients not necessarily associated with any H field.
- There can be induced voltages and currents from any of these primary sources inductively coupled to wires, cables and piping which will result in secondary coupling and a repeat and complication of all the factors we have just cited.

Measurements made by the National Bureau of Standards\* in several coal mines substantiate these generalities both with respect to noise power level and its variation with time and location.

Finally, we observe that none of these conditions or any others similar to them are stable. Mining operations progress, wires are changed and removed, power systems are altered, pipes, pumps and trailing cables will be shifted. Last, but not least, the spatial relationship of the transmitter and receiver for a miner-to-miner communication system can vary according to the movement of the men and equipment as well as their particular physical positions.

---

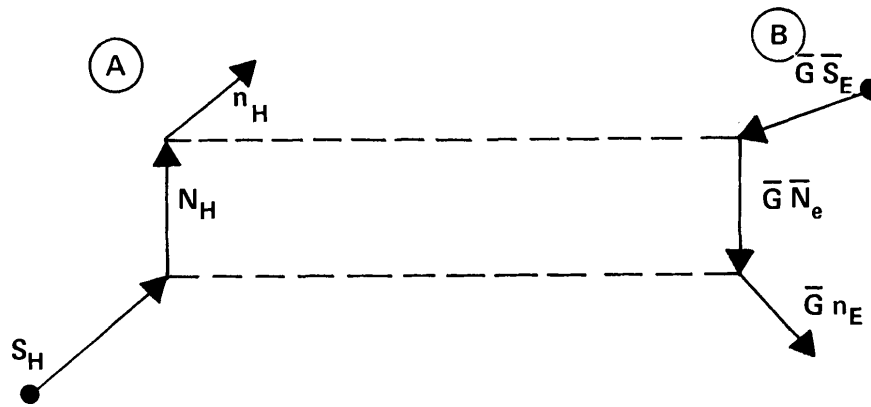
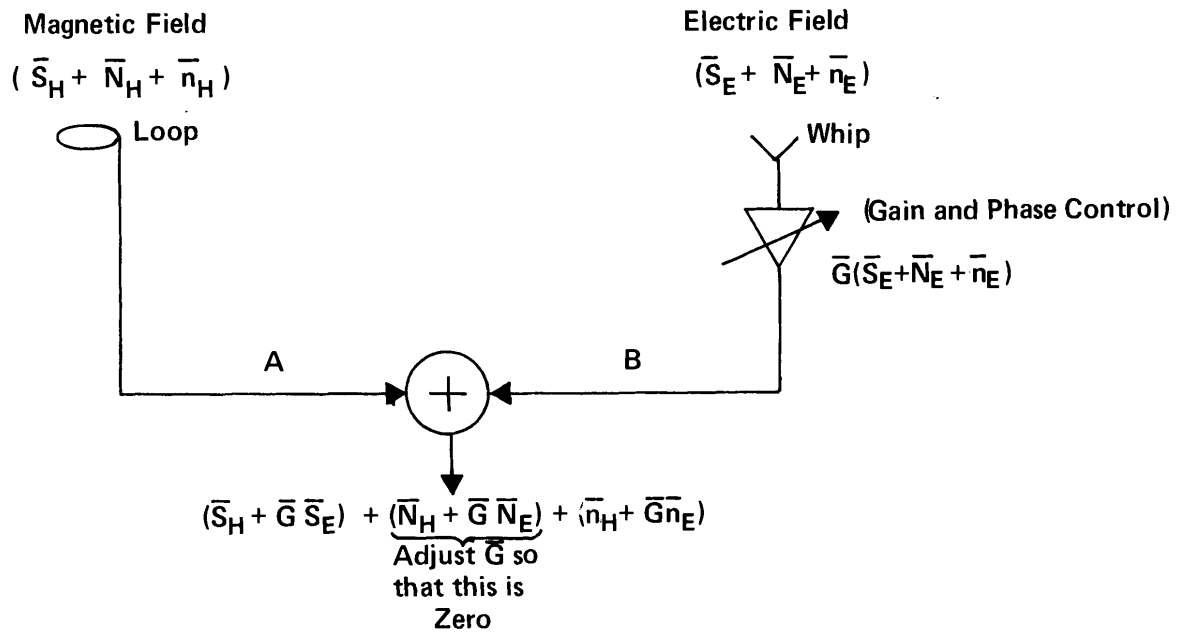
\*Bensema, W.D., M. Kanda, and J.W. Adams (1974a), Electromagnetic Noise in Robena No. 4 Coal Mine, Nat. Bur. Stand. (U.S.), Tech. Note 654, 194 pp., April 1974, SD Cat. No. C13.46:654, Sup. of Doc., U.S. Government Printing Office, Washington, D.C. 20402 (U.S. Bureau of Mines Contract H0133005).

Kanda, M., J.W. Adams, and W.D. Bensema (1974c), Electromagnetic Noise in McElroy Mine, Nat. Bur. Stand. (U.S.), NBSIR 74-389, 170 pp., June 1974, order under SD Cat. No. C13, Sup. of Doc., U.S. Government Printing Office, Washington, D.C. 20402 (U.S. Bureau of Mines Contract H0133005).

Bensema, W.D., M. Kanda, and J.W. Adams (1974b), Electromagnetic Noise in Itmann Mine, Nat. Bur. Stand. (U.S.), NBSIR 74-390, 112 pp., June 1974, order under SD Cat. No. C13, Sup. of Doc., U.S. Government Printing Office, Washington, D.C. 20402 (U.S. Bureau of Mines Contract H0133005).

Up to now methods recommended for combatting mine electromagnetic noise as it affects induction or wireless radio systems have mostly involved: modulation techniques, signal bandwidth reduction, voice processing or signal coding, optimizing carrier frequency selection, achieving maximum power efficiency. These are what one might call "whole signal" techniques and do not make use of the fact that before the total signal is converted to a single current in a receiver, there are noise components of that signal which may be separated from the information carrying portion. Specifically, by the use of separate antennas, sensitive independently to E and H fields, perhaps separately spaced in special configurations, and fed to phasing and balancing networks, a substantial increase in signal-to-noise ratio may be achievable even before the whole signal processing techniques are applied within the receiver.

The rest of this chapter is devoted to the description and analysis of a signal reception technique that should be subjected to test and assessment to determine whether it may be feasible to realize an overall system performance improvement when in the presence of mine electromagnetic noise. The technique involves making use of the possible correlations which may exist between the electric and magnetic field vectors of the mine electromagnetic noise. If these correlations can be demonstrated, there is real possibility of constructing a receiver which, in its simplest form, receives and combines outputs from two separate antennas; one primarily sensitive to the E-field, and the other to the H-field as shown in Figure 5-1. This receiver would combine the antenna outputs of these separate sensors in such a way (vectorially and perhaps adaptively) that the noise picked up by the E-field antenna would be used to cancel the correlated noise component of the total output received by the loop or H-field antenna, thereby enhancing the signal-to-noise ratio of the final output. This should be possible if the signal-to-noise ratio at each antenna is different and the noise components are highly correlated. Thus, by amplitude, phase, and possibly directional adjustments, it may be possible to improve, before any further processing steps, the signal-to-noise ratio at the receiver output terminals. This proposed technique, in its simplest form, is a diversity reception scheme using E- and H-field components which can be received separately and independently by selective E- and H-field sensors.



Source: Arthur D. Little, Inc.

FIGURE 5-1 HYBRID NOISE CANCELLING DIVERSITY RECEIVING TECHNIQUE (Simplified Basic Operation)

## C. SIGNAL-TO-NOISE RATIO IMPROVEMENT ANALYSIS

### 1. Nomenclature

Suppose that an antenna which is only sensitive to the H field picks up a signal voltage  $\bar{S}_H$  combined with noise  $\bar{N}_H$  and suppose that an adjacent E antenna picks up a signal  $\bar{S}_E$  combined with noise  $\bar{N}_E$ . (The bars over the letters denote a vector quantity). If the two noise voltages are partly correlated with each other, we can let  $\bar{n}_H$  = the uncorrelated part of the H noise and  $\bar{n}_E$  = the uncorrelated part of the  $\bar{E}$  noise. Let the parts which are correlated be  $\bar{N}_{HC}$  and  $\bar{N}_{EC}$ , respectively. Since they are correlated, it should be possible to cancel one with the other. One way to achieve this is to pass the output of the E antennas through a variable gain amplifier and a variable phase changer. This enables us to manipulate the magnitude and phase of the voltage received from the E-antenna prior to summation of the E and H inputs to the receiver as depicted in Figure 5-1.

The presence of an  $\bar{S}_E$  electric field signal is not necessary for this technique to be applied. Only the presence of noise is required on the E-field antenna. In fact, the following analysis implicitly assumes that if an E-signal is present, a means must be provided to independently sense and process the E-field noise without interference from the E-field signal. Otherwise, whenever the signal-to-noise ratio on the E-antenna was much greater than about 1, the noise canceller would try to cancel the correlated E and H signal outputs, thereby driving the signal level to a minimum instead of the noise. The remainder of this chapter is concerned with the examination of the feasibility and potential utility of such a noise cancelling technique from an analytic viewpoint, and not on the conceiving of specific manual or automatic means of implementing it in practical hardware. The analysis also assumes a substantial degree of correlation between the magnetic and electric field noise components. This must also be verified by measurements.

### 2. Signal-to-Noise Ratio

We can write the voltage at the E antenna as:

$$\bar{V}_E = (\bar{S}_E + \bar{N}_{EC} + \bar{n}_E). \quad (1)$$

After passing through the amplifier and phase changer this voltage becomes:

$$\bar{V}_E = \bar{G}(\bar{S}_E + \bar{N}_{EC} + \bar{n}_E) \quad (2)$$

where:

$$\bar{G} = g e^{j\psi} \quad (3)$$

$g$  = the adjustable gain (or attenuation) of the amplifier

$\psi$  = the adjustable phase angle of the phase changer.

The voltage from the H antenna can be written:

$$\bar{V}_H = (\bar{S}_H + \bar{N}_{HC} + \bar{n}_H) \quad (4)$$

If we sum the two voltages (2) and (4) above by passing them through a summing network we get the voltage:

$$\bar{V}_\Sigma = (\bar{S}_H + \bar{G}\bar{S}_E) + (\bar{N}_{HC} + \bar{G}\bar{N}_{EC}) + (\bar{n}_H + \bar{G}\bar{n}_E). \quad (5)$$

The correlated noise portion of the voltage is  $(\bar{N}_{HC} + \bar{G}\bar{N}_{EC})$ . From Figure 5-2 it is seen that  $|\bar{N}_{HC} + \bar{G}\bar{N}_{EC}|^2$  can be written as

$$P_N = |\bar{N}_{HC} + \bar{G}\bar{N}_{EC}|^2 = N_{HC}^2 + (gN_{EC})^2 + 2gN_{EC}N_{HC}\cos(\psi + \Delta) \quad (6)$$

where  $\Delta$  = an arbitrary constant phase angle between the correlated portions of the E and H noise vectors

and

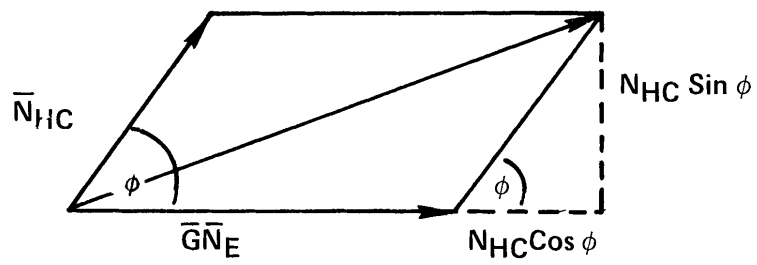
$$\phi = \psi + \Delta. \quad (7)$$

The convention  $|\bar{N}_{HC}| = N_{HC}$  is used to denote vector magnitude. If we assume, as we are perfectly free to assume, that standard impedances apply throughout, (6) represents the correlated noise power,  $P_N$ . Now, assuming it possible to adjust  $g$  so that

$$g = \frac{N_{HC}}{N_{EC}}, \quad (8a)$$

and adjust  $\psi$  so that

$$\phi = \psi + \Delta = \pi, \quad (8b)$$



Source: Arthur D. Little, Inc.

FIGURE 5-2 CORRELATED NOISE VECTOR DIAGRAM

expression (6) becomes zero. Namely, the correlated noise would be perfectly cancelled by making  $\bar{G}$  such that

$$\bar{G} \bar{N}_E = -\bar{N}_H . \quad (9)$$

In practice, the presence of uncorrelated noise components would set a lower limit to the degree of cancellation of even the correlated components. The intent here is to assess whether the potential range improvement obtainable under favorable cancelling situations warrants a more rigorous experimental and analytical investigation.

When the correlated noise is cancelled as defined in (9), the summed voltage (5) becomes:

$$\bar{V}_\Sigma = (\bar{S}_H + \bar{G} \bar{S}_E) + (\bar{n}_H + \bar{G} \bar{n}_E) , \quad (10)$$

where  $\bar{G}$  now has the special value assigned by (8) and (9) above. Suppose that, under these circumstances, the net phase angle remaining between  $\bar{S}_H$  and  $\bar{G} \bar{S}_E$  is  $\theta$ . Then as in (6) above we can write

$$P_S = \left| \bar{S}_H + \bar{G} \bar{S}_E \right|^2 = S_H^2 + (gS_E)^2 + 2gS_E S_H \cos \theta . \quad (11)$$

This is the signal power at the output of the summing network. Since  $\bar{n}_H$  and  $\bar{G} \bar{n}_E$  are uncorrelated, the noise portion of the voltage (1) above has a power  $P_n$  of

$$P_n = n_H^2 + (gn_E)^2 . \quad (12)$$

Therefore the signal-to-noise ratio  $R_\Sigma$  of (10) is given by

$$R_\Sigma = \frac{(S_H)^2 + (gS_E)^2 + 2gS_E S_H \cos \theta}{(n_H)^2 + (gn_E)^2} . \quad (13)$$

If the H antenna is used alone, the signal-to-noise power ratio reduces

to  $R_H$

$$R_H = \frac{S_H^2}{(n_H)^2 + (N_{HC})^2} \quad (14)$$

Dividing (13) by (14) and substituting (8a) for the value of  $g$ , gives a rational measure of the signal-to-noise ratio improvement obtained by this noise cancelling technique. Calling this improvement ratio the Improvement Factor,  $I$ , it can be shown that:

$$I = [1 + (R_{EC}/R_{HC})^2 + 2(R_{EC}/R_{HC})\cos\theta] \left[ \frac{1 + (1/\alpha)^2}{1 + (\beta/\alpha)^2} \right] \quad (15)$$

where:

$$\begin{aligned} R_{EC} &= (S_E/N_{EC}), \text{ E signal to E correlated noise ratio} \\ R_{HC} &= (S_H/N_{HC}), \text{ H signal to H correlated noise ratio} \\ \alpha &= (n_H/N_{HC}), \text{ H uncorrelated to correlated noise ratio} \\ \beta &= (n_E/N_{EC}), \text{ E uncorrelated to correlated noise ratio} \end{aligned} \quad (16a, b, c, d)$$

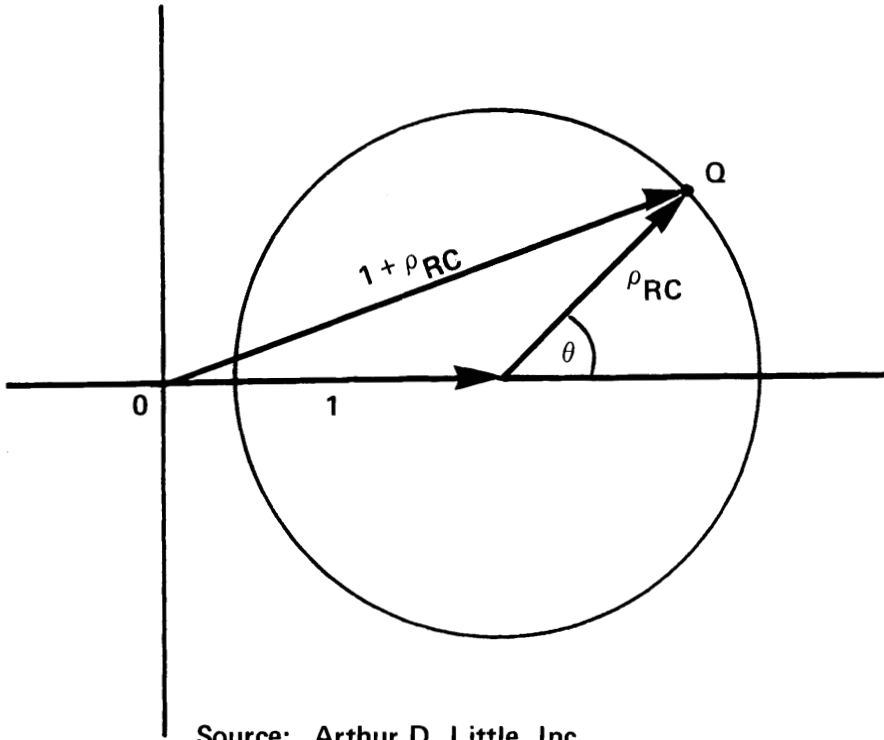
### 3. Circle Diagram Interpretations

An insight into the behavior of the Improvement Factor  $I$  as a function of the relative signal and noise levels and the net phase angle  $\theta$  between the E and H signal outputs can be obtained by using a circle diagram which occurs repeatedly in engineering. If we regard  $\theta$  as the angle between a unit vector  $\bar{1}$  and the vector  $\bar{\rho}_{RC} = \bar{R}_{EC}/\bar{R}_{HC}$ , we draw the diagram of Figure 5-3 in which the length of the vector.  $OQ$ , is seen to be:

$$OQ = |1 + \bar{\rho}_{RC}| = |1 + (\bar{R}_{EC}/\bar{R}_{HC})| = [1 + (R_{EC}/R_{HC})^2 + 2(R_{EC}/R_{HC})\cos\theta]^{1/2} \quad (17)$$

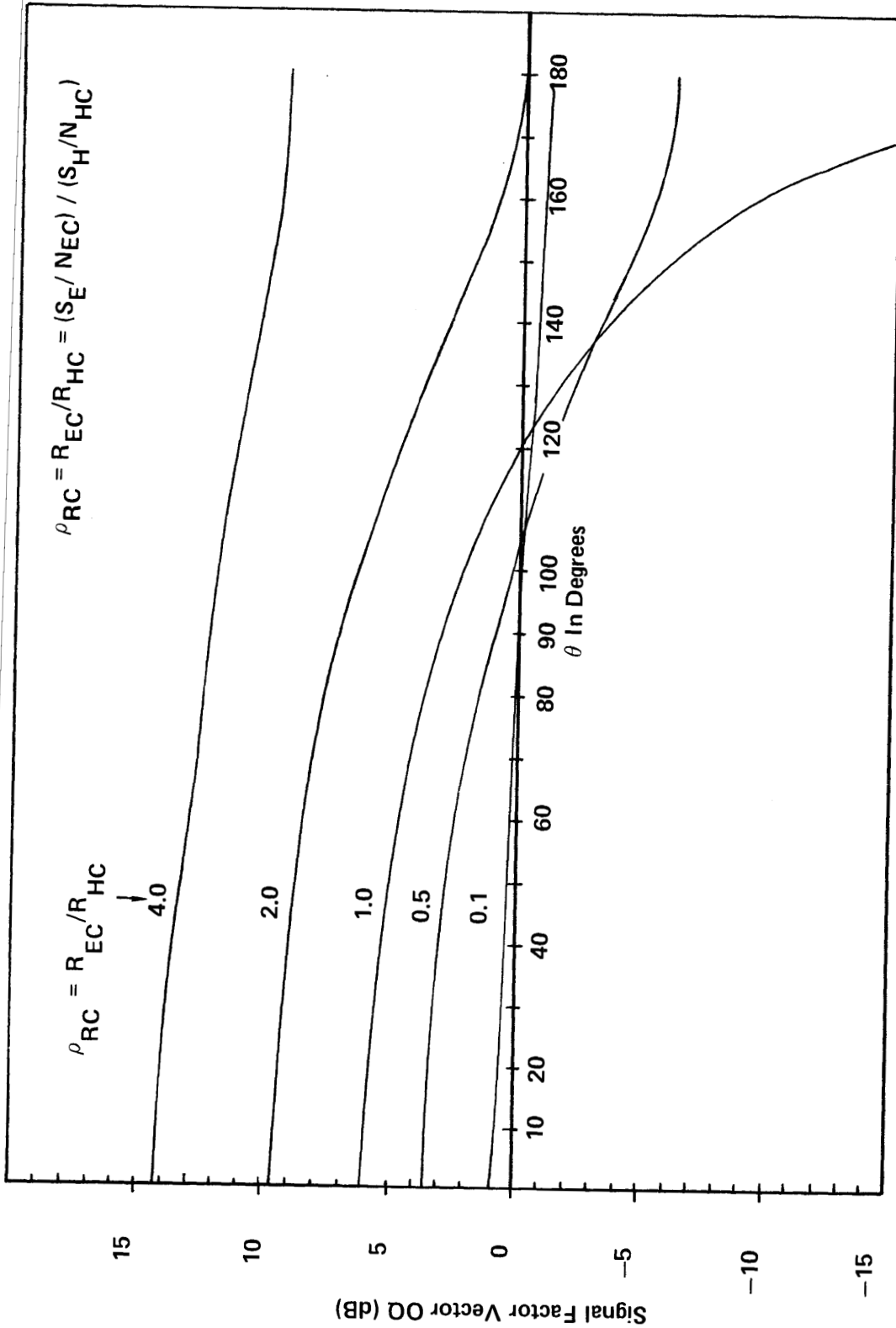
As  $\theta$  varies, the locus of the point  $Q$  is a circle of radius  $\rho_{RC} = |R_{EC}/R_{HC}|$ , centered on  $(1,0)$ . Figure 5-4 illustrates how  $(OQ)^2$  expressed in dB behaves as a function of  $\theta$  and the relative values of  $R_{EC}$  and  $R_{HC}$ . Figure 5-4 shows that if the E-field signal-to-correlated noise ratio  $R_{EC}$  is greater than twice the H-field signal-to-correlated noise ratio  $R_{HC}$ , the Improvement Factor  $I$  will be increased by the presence of the E-signal (assuming that the gain  $g$  is set independently of  $S_E$ ). However, if  $R_{EC}$  is less than twice  $R_{HC}$ , the presence of  $S_E$  can cause a reduced value of  $I$  over that attainable in the absence of  $S_E$ ; namely, whenever the resultant phase angle  $\theta$  falls between  $90^\circ$  and  $270^\circ$ .





Source: Arthur D. Little, Inc.

FIGURE 5-3 SIGNAL FACTOR CIRCLE DIAGRAM



Source: Arthur D. Little, Inc.

FIGURE 5-4 SIGNAL FACTOR OF I VERSUS PHASE ANGLE  $\theta$  IN THE PRESENCE OF AN E-FIELD SIGNAL  $S_E$

Now let another circle of radius  $\rho_{Nn}$  be drawn centered at the origin as in Figure 5-5,

$$\rho_{Nn} = \left[ \frac{1 + (\beta/\alpha)^2}{1 + (1/\alpha)^2} \right]^{1/2} \quad (18)$$

The Improvement Factor, I, now shows directly on the figure as the square of the ratio of OQ to OM.

$$I = \left( \frac{OQ}{OM} \right)^2 = \frac{|1 + \bar{\rho}_{RC}|^2}{\rho_{Nn}^2} \quad (19)$$

Points P in Figure 5-5 have a special interest. As shown in Figure 5-6, these points give the values  $\theta_o$  for which I is unity; i.e., no improvement. If we consider  $\theta$  as an equally distributed random variable, then Figure 5-6 shows that the probability p that  $I \geq 1$ , is given by,  $p = |\theta_o|/\pi$ . Further examination of Figure 5-5 reveals that when an E-signal  $S_E$  is not present,  $\rho_{RC} = 0$  and OQ reduces to unity, so that the Improvement Factor depends only on the degree of noise correlation; namely

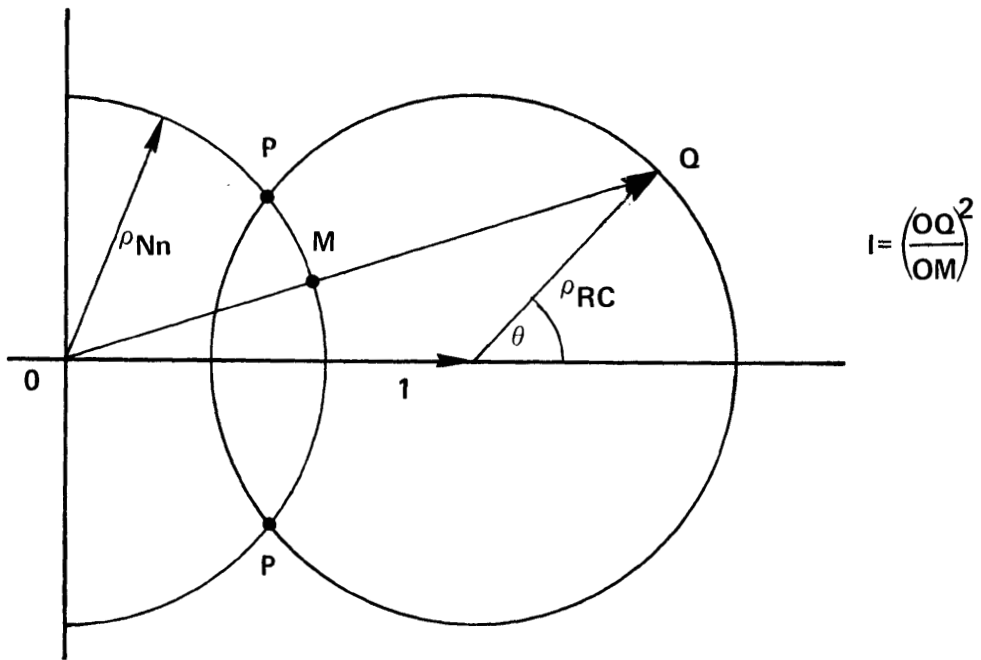
$$I = \frac{1}{\rho_{Nn}^2} \quad (20)$$

When the degree of correlation between the E and H components is very small; i.e., when  $N_H, N_E \rightarrow 0$ , the gain setting g defined by (8a) will be indeterminate. In that case the required gain and phase adjustment reduces mathematically to unity gain with zero phase shift. Thus (20) would reduce to

$$I = \left[ \frac{1}{1 + (n_E/n_H)^2} \right], \quad (21)$$

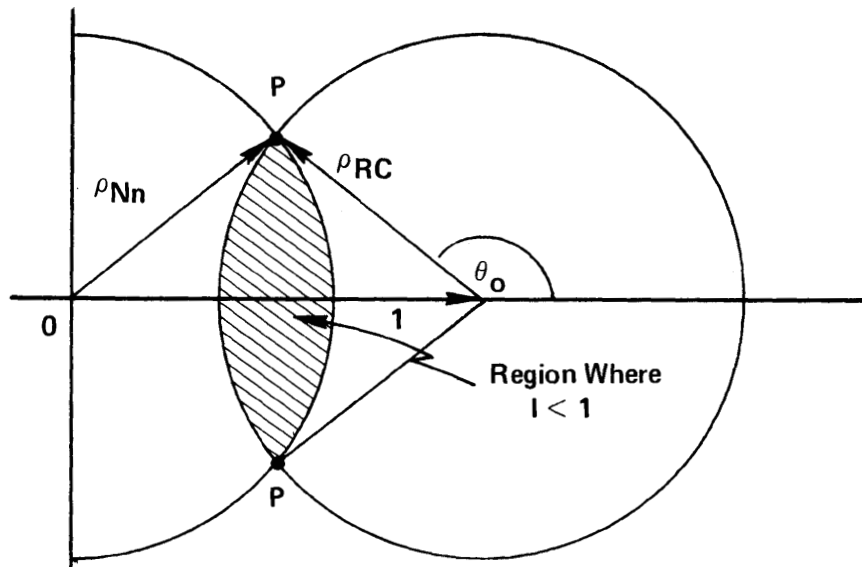
which reveals a decrease in net signal-to-noise ratio compared to reception on only the loop antenna. Conversely, when the degree of correlation between the E and H field noise components is large; i.e.,  $\alpha, \beta$  small, (20) becomes

$$I \cong \frac{(1/\alpha)^2}{1 + (\beta/\alpha)^2} \quad (22)$$



Source: Arthur D. Little, Inc.

FIGURE 5-5 CIRCLE DIAGRAM FOR SIGNAL AND NOISE FACTORS OF I



Source: Arthur D. Little, Inc.

FIGURE 5-6 CIRCLE DIAGRAM INDICATING REGION WHERE  $I \leq 1$

Examination of (22) reveals the following. In the ideal case of completely correlated noise,  $\alpha, \beta = 0$ , the noise cancellation would be perfect, giving infinite improvement. If the H-antenna output contains only correlated noise, then  $\alpha = 0$ , and (22) reduces to

$$I = (1/\beta)^2 \quad , \quad (23)$$

which gives significant improvement whenever  $\beta$  is small. If the E-antenna output contains only correlated noise, then  $\beta = 0$  and (22) reduces to

$$I = (1/\alpha)^2 \quad , \quad (24)$$

leading to significant improvement whenever  $\alpha$  is small. Finally, if the ratio of uncorrelated-to-correlated noise is non-zero but of similar value for both E and H antenna outputs; i.e.,  $\alpha = n_H/N_H \approx n_E/N_E = \beta$ , (22) reduces approximately to

$$I \cong \frac{1}{2} (1/\alpha)^2 \quad , \quad (25)$$

giving half the improvement of the  $\beta = 0$  condition.

#### 4. Expected Values

It should be emphasized that the circle diagrams of Figure 5-3 and 5-5 and the plot of Figure 5-4 have been included here to illustrate the role played by the variable  $\theta$ . Since we lack experimental data, we will deal primarily with the expected value of  $\theta$ . In view of the wide variety of coupling structures and noise sources likely to be encountered in mines, the only rational assumption we can make in regard to  $\theta$  is that it is an equally distributed random variable. Consequently, the expected value of  $\cos \theta$  in (15) is 0, the expected value of  $\theta$  can be taken as  $\pi/2$ , and the expected value of  $I$  is given by

$$\langle I \rangle = [1 + (R_{EC}/R_{HC})^2] \left[ \frac{1 + (1/\alpha)^2}{1 + (\beta/\alpha)^2} \right] \quad . \quad (26)$$

This is the statistical measure of performance averaged over all situations encountered. Expressing (26) in dB we get

$$\langle I \rangle \text{ (dB)} = 10 \log_{10} \langle I \rangle$$

or

(27a, b)

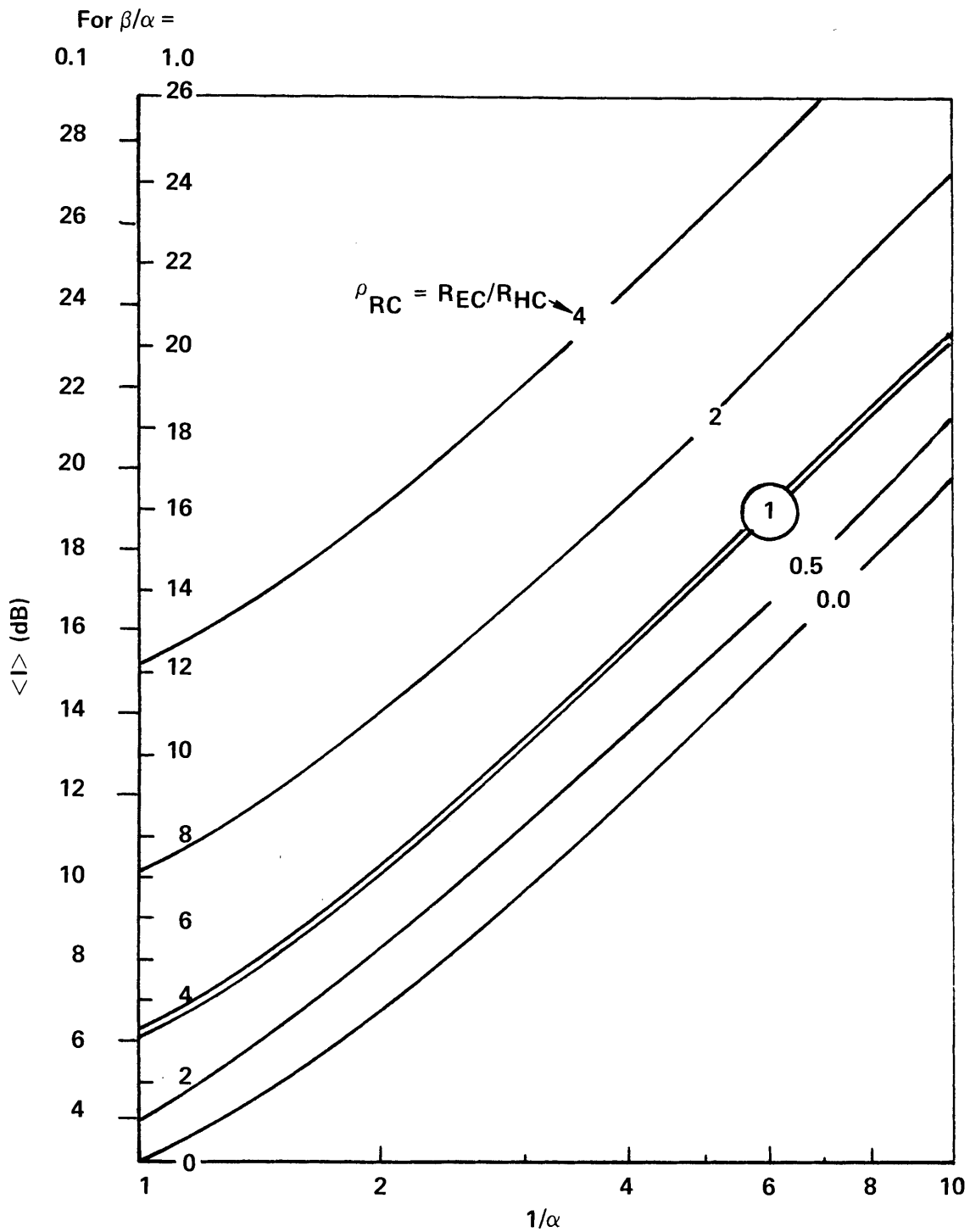
$$\langle I \rangle \text{ (dB)} = 10 \log [1 + (R_{EC}/R_{HC})^2] + 10 \log [1 + (1/\alpha)^2] - 10 \log [1 + (\beta/\alpha)^2]$$

Figure 5-7 presents plots of the "average" improvement factor  $\langle I \rangle$  in dB, as a function of the H-field correlated-to-uncorrelated noise factor,  $1/\alpha$ , for two representative values of the relative correlation ratio  $\beta/\alpha$ , and five values of the ratio of signal-to-noise ratios on the E and H antennas. The figure illustrates that, in the absence of an E-field signal, when the E and H field noises enjoy the same degree of correlation ( $\beta/\alpha = 1$ ), significant improvement occurs as the correlated-to-uncorrelated noise ratio  $1/\alpha$  increases; i.e.,  $\langle I \rangle = 17$  dB for  $\alpha = 0.1$ ,  $1/\alpha = 10$ . Only a marginal 3 dB additional improvement is obtained if the E-field noise is much more correlated than the H-field noise ( $\beta/\alpha = 0.1$ ). It is also seen that the presence of an E-field signal (if it is not allowed to interfere with the noise cancelling process) may also on the average result in a net improvement, depending on the value of the relative signal-to-noise ratio factor ( $R_{EC}/R_{HC}$ ).

The plots of  $\langle I \rangle$  in Figure 5-7 assume an average value of  $\pi/2$  for  $\theta$ . If  $\theta$  has some other value, the expression for  $\langle I \rangle$  given by equations (27) would need a correction term of  $Q$  dB added to it, where  $Q$  is given by

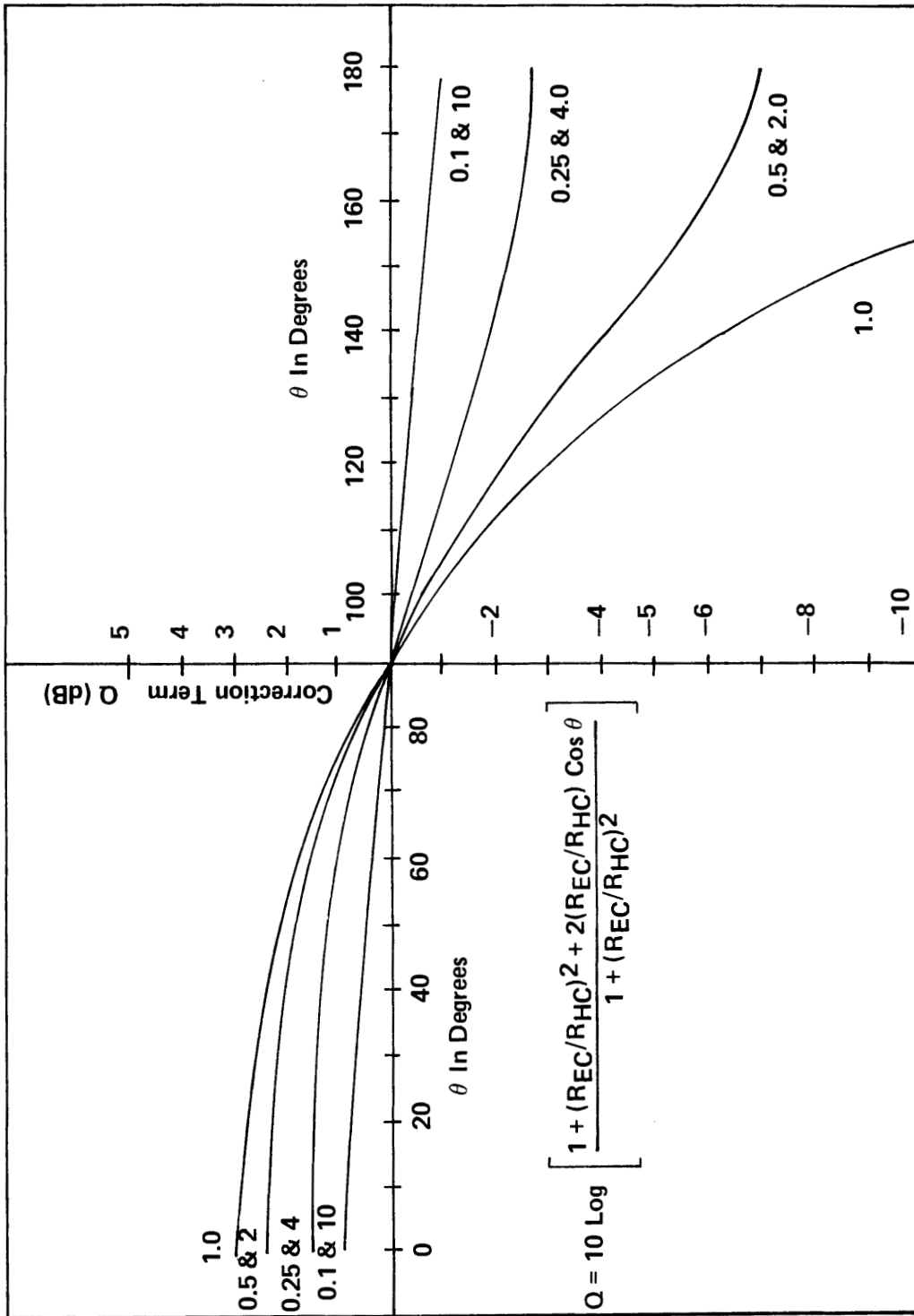
$$Q = 10 \log_{10} \left[ \frac{1 + (R_{EC}/R_{HC})^2 + 2(R_{EC}/R_{HC}) \cos \theta}{1 + (R_{EC}/R_{HC})^2} \right], \quad (28)$$

to represent the improvement  $I$  in dB for a specific angle  $\theta$ . Figure 5-8 plots  $Q$  against  $\theta$  for various values of  $R_{EC}/R_{HC}$ . This figure gives the number of dB which must be added to the values of Figure 5-7 to find  $I$  for a particular value of  $\theta$ , and illustrates that the presence of an E-field signal can be detrimental when the resultant phase angle  $\theta$  obtained from the noise cancelling procedure falls between  $90^\circ$  and  $270^\circ$ .



Source: Arthur D. Little, Inc.

FIGURE 5-7 EXPECTED VALUE OF THE IMPROVEMENT FACTOR  $\langle I \rangle$  IN dB VERSUS  $1/\alpha$  AND  $(R_{EC}/R_{HC})$  FOR TWO VALUES OF  $\beta/\alpha$  (0.1, 1.0) AND  $\langle \theta \rangle = \pi/2$



Source: Arthur D. Little, Inc.

FIGURE 5-8 CORRECTION TERM Q TO  $\langle \theta \rangle$  VERSUS PHASE ANGLE  $\theta$  AND RATIO REC/RHC

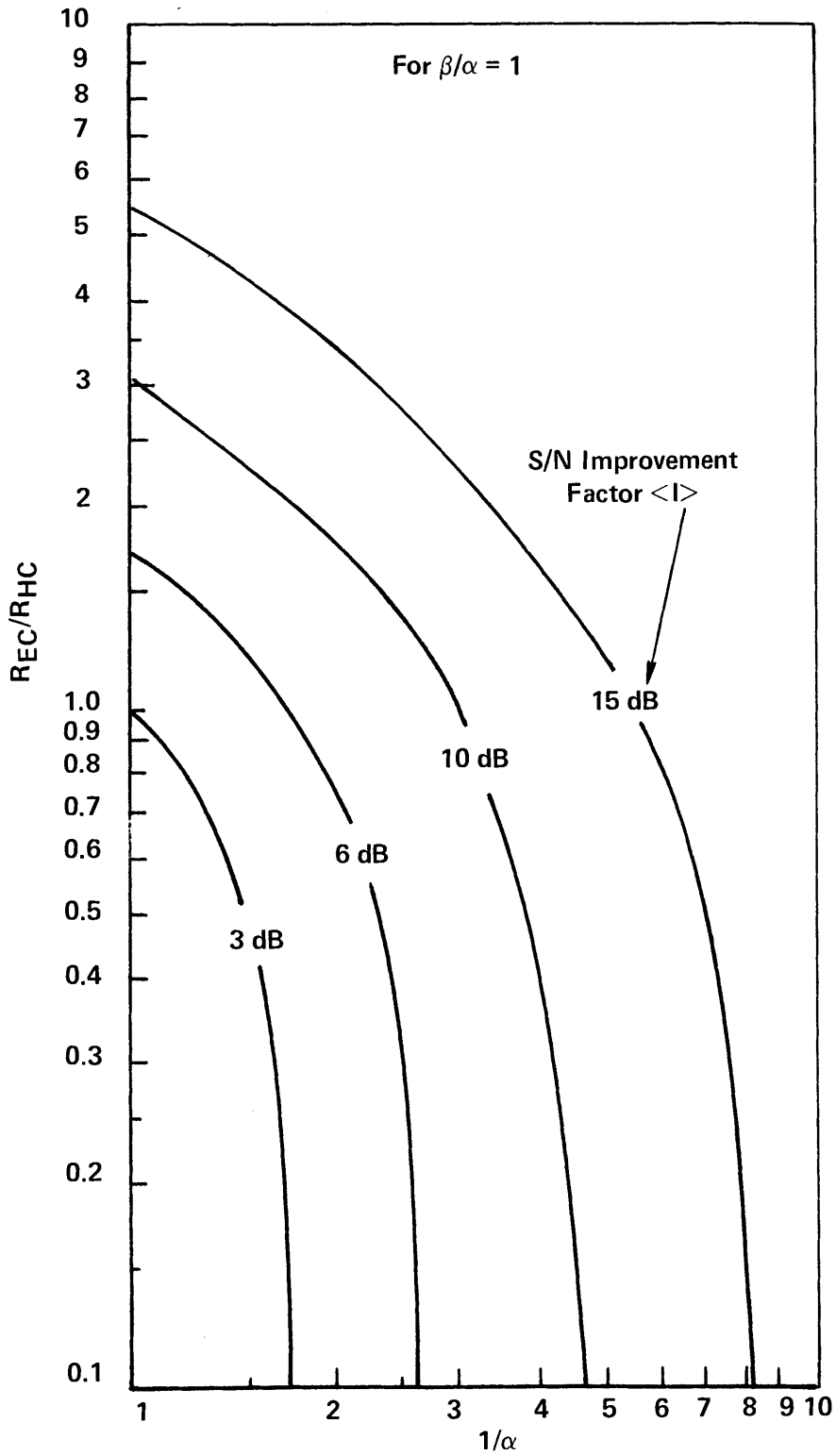


## 5. Boundary Plots and Performance

Another instructive way to plot the dependence of  $\langle I \rangle$  on the degree of noise correlation and the signal-to-correlated noise ratios at the E and H antennas is in the form of boundary plots. Namely, choose desired Improvement Factor values  $\langle I \rangle$  and plot the parameter values need to achieve these Improvement Factors. As an example, Figure 5-9 presents the combination of values of  $(R_{EC}/R_{HC})$  and  $1/\alpha$  to achieve four different degrees of S/N improvement  $\langle I \rangle$  under noise conditions where  $\beta/\alpha = 1$ . Note the key role played by  $1/\alpha$ , which is a measure of the degree of noise correlation. In the absence of an E-signal, if  $1/\alpha$  is larger than about 6 or 7, improvements in excess of 12 dB can be achieved; improvements that could mean the difference between marginal or no communications and satisfactory communication in a high ambient electrical noise environment. To substantially reduce this requirement on the value of  $1/\alpha$ ,  $(R_{EC}/R_{HC})$  must exceed unity, a condition that presently appears improbable for inductively coupled wireless communication systems in a mine environment. The above analysis indicates that the degree of noise correlation in mine environments is of critical importance, and therefore needs to be established for the frequency band of interest.

For the sake of simplicity in the above analysis, we have used a simple phase shifter and variable gain stage to illustrate the noise cancellation process. The noise measurements should examine not only the variables of gain and phase to accomplish cancellation, but also the spacing and relative orientation between antennas, since it is anticipated that these geometrical factors may also play an important role in achieving discrimination against the adverse effects of mine noise.

It is not yet clear exactly how such an adaptive noise cancelling process to maximize output signal-to-noise ratio will be implemented. Completely automatic methods to quite rudimentary manual methods that can be switched in and out at will, can be conceived. If the method is simple but incapable of distinguishing between signals and noise, the presence of an appreciable E-signal will clearly be a liability. However, when a strong E-signal is present, adequate system performance should be obtainable simply by switching the canceller out of the receive circuits, and choosing



Source: Arthur D. Little, Inc.

FIGURE 5-9 BOUNDARY PLOT OF  $R_{EC}/R_{HC}$  VERSUS  $1/\alpha$  FOR SPECIFIED IMPROVEMENT FACTORS  $\langle I \rangle$  WITH  $\beta/\alpha = 1$

the channel with the best perceived signal-to-noise ratio. An automatic system capable of distinguishing between signals and noise, and then operating only on the noise, may prove to be too complex for the intended portable application for use in mines unless the noise is found to exhibit some highly favorable distinguishing features that can be easily utilized.

The conditions which appear most favorable for using a simple means to achieve significant improvements through noise cancelling are those in which both E and H field noise components are present and highly correlated with each other, and in which the E-field signal-to-correlated noise is negligible compared to the H-field signal-to-correlated noise ratio. Without measurements of the degree of correlation between the E and H field components of mine electromagnetic noise, further analysis is probably a waste of time. The next section outlines a modest series of field measurements for quickly estimating the degree of correlation between in-mine E- and H-field noise.

#### D. RECOMMENDED FIELD MEASUREMENTS

To see if some form of noise cancelling diversity reception involving instantaneous correlation between E and H fields as well as direction of arrival is possible, we recommend that a modest number of basic measurements be made in an environment which simulates to a first order the type of industrial RFI environment which one encounters in operating mines. The first and simplest is to obtain a measure of the normalized cross-correlation between the E and H vectors of the noise field.

If this correlation is found to be high, then in a magnetic induction wireless link, we can hope to cancel the H-noise picked up on a loop antenna by using the E-noise picked up on a dipole or whip antenna which would be insensitive to the H-field generated by the signal transmitting device. This selectivity comes about from the fact that the transmitter will utilize a loop antenna which generates very little E field, and which is "connected" to the receiver through magnetic induction. A further extension of the use of separate E and H sensitive antennas is the testing of the potential benefits of signal and noise differentiation based on sensitivity to antenna orientation.

To assess the feasibility of the above discussed noise cancelling technique we recommend the following set of field measurements:

- From existing laboratory components and equipment, assemble an experimental test receiving system operating in the 15 to 300 kHz range which will simultaneously display on an oscilloscope face a measure of the instantaneous cross-correlation of the normalized voltages received by independent E-field and H-field sensitive antennas. This portable equipment should be checked and calibrated in the laboratory and simple procedures for operation and adjustment established.
- Make arrangements to allow access to a non-mine industrial site which uses heavy electrical equipment, in order to measure the E- and H-fields produced by traction motors, welders, etc. A trolley car barn or subway switch yard typifies such an environment and should provide an adequate representation of a mine environment. If desired, these measurements could be followed by in-mine measurements to confirm the findings for the above industrial site.
- Take the measurements at the site with different equipment sensitivities and antenna orientations in various locations to determine some empirical rules as to the degree and constancy of the correlation between E- and H-field noise components in real time.
- If a strong correlation effect is discovered, perform additional measurements with the same test equipment and a signal source to demonstrate that a signal-to-noise improvement is possible. This critical experiment should involve the temporary establishment at some distance from the measuring

equipment of a simple CW transmitting loop to provide the test signal.

- Upon the completion of these tests, prepare a test report describing the results of this work. including a series of conclusions and recommendations relating to the next steps to be taken.

The purpose of this modest program is to perform in the simplest and most rapid manner a series of basic measurements to explain the physics of the situation. If these tests and measurements prove successful, a follow-on effort aimed at prototype equipment design and development can be pursued.



CAMBRIDGE,  
MASSACHUSETTS

SAN FRANCISCO  
WASHINGTON  
ATHENS  
BRUSSELS  
LONDON  
PARIS  
RIO DE JANEIRO  
TORONTO  
WIESBADEN